Metagenomics-driven predictions in Archaea from hydrocarbon-rich Arctic hydrothermal systems:

Phylogenetic and metabolic analyses of methane and short-chain alkane-degrading lineages

Francesca Vulcano

Thesis for the degree of Philosophiae Doctor (PhD)
University of Bergen, Norway
2023

UNIVERSITY OF BERGEN

Metagenomics-driven predictions in Archaea from hydrocarbon-rich Arctic hydrothermal systems:

Phylogenetic and metabolic analyses of methane and short-chain alkane-degrading lineages

Francesca Vulcano

Thesis for the degree of Philosophiae Doctor (PhD)
at the University of Bergen

Date of defense: 14.04.2023

Year: 2023

Title: Metagenomics-driven predictions in Archaea from hydrocarbon-rich Arctic hydrothermal systems:

Name: Francesca Vulcano

Print: Skipnes Kommunikasjon / University of Bergen

Table of content

Acknowledgements

First, I want to thank my main supervisor Prof. Ida Helene Steen. You have seen qualities in me I did not know I had and helped me use them. You taught me a lot about science and research, and I will always carry your advice with me. I thank my supervisor Dr. Runar Stokke for helping me with bioinformatics and listening to my theories. My co-supervisors, Prof. Håkon Dahle for very interesting discussions, Prof. Eoghan Reeves, and Prof. Desiree Roerdink for introducing me to the wonders of geochemistry. I thank Dr. Gunter Wegener for welcoming me into his lab and his research group. Dr. Anita-Elin Fedøy that thought me a lot in the lab, all researchers at the Center for Deep Sea Research, Dr. Thibaut Barreyre and Prof. Steffen Leth Jørgensen whose enthusiasm always inspired me.

I thank all the people I have met in my Norwegian years. My colleagues and office mates in Realfabygget, and at BIO. My flatmates Carmelo, Marco, and Katerina, you've been like a family to me. People I met on research cruises. I enjoyed every mud sample we have collected, every meal we have shared, every box we have loaded. Thank you, Giuliana, Dimitri, Claudio, Pier, for all the fun and the scientific support.

I want to thank Emily for your support over these last months, you are a strong, brilliant, and curious researcher and I hope we will work more together in the future. I want to thank Hasan, and Victoria. You have welcomed me in your family and taken care of me. You've shown me so many things I didn't know I liked and that now I love. Thank you for the dnd sessions, the dinners, the videogames, the vinyls and for teaching me the importance of embracing my creative mind and have fun with it. I want to thank Petra for being by my side, literally, for our political debates, the cozy dinners and movie nights, the 6pm popcorn stash, the UNO tournaments, the question-lamp, for the times we have been both so tired but supportive. Your creativity and determination will bring you far even when things seem unreachable. Angi, you've been my role model, I have always been amazed by your strength and independence. Thank you for all the bouldering, all the Sammen stuff, the pool, the steam bath, the dinners, the cabins. You've been like a sister to me, and you helped me go thought the toughest time. Thank you for telling me that I was strong when I felt so weak. Without you guys I would never be the person I am today. You've helped me grow and find who I am.

I want to thank all the people that followed me from home. All the friends from SEC and Amici di San Pietro. I know I will always have a home with all of you in our mountain. My friends Seri and Cri, I am so happy and proud to see you becoming wonderful teachers and wonderful moms. I want to thank Ste, Tia, Dav, always there to share feelings, thoughts, books, games, and adventures. I want to thank my dear Chicca. We have been walking parallel paths in these long years and we've only grown closer even though we were far apart. I cannot thank you enough for all the long vocal messages. Together we always manage to understand the riddles in our lives with analytical precision and solve them. You've always made me feel understood and this freedom of expressing my concerns gave me strength and relief.

I want to thank my brother, who I am so proud of. I thank you for all the deep discussions, for never being afraid of dissecting reality to its core, for teaching me to dare to follow my dreams, to express what is enclosed in my mind and make that part of my work. You've grown into a great man, do not forget it and do not give up.

I want to thank my parents who always supported me, listen to my frustration even after long days at work, and gave me advice every single time, even though I am a stubborn girl that always wants to be right. I want to thank them for letting me find myself. You taught me to help everyone in need, you taught me love, kindness, self-consciousness, and freedom and for that I thank you with my brain and with my heart.

Finally, I want to acknowledge this city. Bergen put me through challenging times, made me feel more alone than ever, but proved to me that I can be strong, and that things above all wonders can happen, like walking on an ocean of ice at the top of the world or finding a special unicorn.

Francesca, January 2023

Scientific environment

The work presented in this thesis was carried out at the Centre for Deep Sea Research and the Deep-Sea Biology research group at the University of Bergen, Norway. It was funded by the Department of Biological Sciences of the University of Bergen, the Norwegian Research Council, through the Center for Geobiology, and the DeepSeaQuence project. The project has been funded by Center for Deep Sea Research, the Trond Mohn Foundation (grant # TMS2020TMT13), and the Norway Financial Mechanism through the National Science Centre, (Poland) GRIEG1 grant: UMO-2019/34/H/NZ2/00584.

Abstract

Methane and short chain alkanes are potent greenhouse gases generated and degraded mainly biotically. In the ocean, methane and hydrocarbons accumulate in sediments and hydrothermal vents. Recent metagenomic studies have dramatically expanded the diversity of archaeal lineages involved in methane and hydrocarbon cycling. They also have revealed that metabolic modules at the basis of hydrocarbon cycling are relatively conserved and common in Archaea and can occur in heterotrophic lineages determining a mixotrophic lifestyle. Further metagenomic studies can contribute to expand such diversity and describe the environmental role of microorganisms involved in cycling of hydrocarbons. In the last decade, hydrocarbon-enriched hydrothermal vents have been discovered along the Arctic Mid Ocean Ridges (AMOR). This project aimed at identifying lineages of anaerobic hydrocarbon-degraders in these vents and describe their phylogenetic and metabolic diversity, mainly by reconstructing and analyzing metagenome-assembled genomes (MAGs) from various anoxic and actively venting hydrothermal locations. Potential for methane oxidation was also evaluated in MAGs of Korarchaeia since they have been previously proposed as methane oxidizers in terrestrial environments. Overall, several new lineages of anaerobic methanotrophic archaea ANME-1 were identified, including one new family. Two lineages of short-chain alkane oxidizers were found, one an ethane oxidizer and the other a butane/propane oxidizer. All encoded canonical routes for syntrophic anaerobic oxidation of methane and short-chain alkanes. Previously undescribed functional differences were found between ANME-1 lineages. Marine hydrothermal Korarchaeia did not encode genes for anaerobic oxidation of methane. They were instead identified as sugars and amino acids fermenters. Deep-branching lineages of Korarchaeia encoded a complete Wood-Ljungdahl pathway that is likely used reductively as electron sink during fermentation resulting in a homoacetogenic metabolism. Overall, this study confirms that hydrocarbon-rich hydrothermal vents at AMOR host microbial lineages with the potential for degradation of hydrocarbons and contributes to expanding the known phylogenetic and functional diversity of hydrocarbon-degrading lineages in marine hydrothermal systems.

Abstract in Norwegian

Metan og hydrokarboner er potente klimagasser som produseres og nedbrytes hovedsakelig biotisk. I havet akkumuleres metan og hydrokarboner i sedimenter og hydrotermiske systemer. Nylige metagenomstudier har utvidet mangfoldet av slektslinjer av arker involvert i metan- og hydrokarbonsyklus. De har vist at metabolske moduler for omsetningsreaksjoner i hydrokarbonsyklus er vanlige i arker og kan forekomme i heterotrofe slektslinjer som bestemmer en mixotrofisk livsstil. Ytterligere metagenomstudier kan bidra til å øke forståelsen av den miljømessige rollen mikroorganismer involvert i omsetning av hydrokarboner har. I løpet av det siste tiåret har hydrokarbon-anrikede hydrotermiske systemer blitt oppdaget langs de arktiske midthavsryggene. I dette studiet har fokuset vært å beskrive det fylogenetiske og metabolske mangfoldet av anaerobe hydrokarbonnedbrytende slektslinjer i disse systemene, hovedsakelig ved å analysere genomer rekonstruert fra metagenomdata. Flere nye slektslinjer av anaerobe metanotrofe arker av typen ANME-1, ble identifisert, inkludert en ny familie. To slektslinjer som kunne oksidere kortkjedede hydrokarboner, henholdsvis etan og propan/butan ble også identifisert. Samtlige av slektslinjene benyttet etablerte metabolismeveier for syntrof anaerob oksidasjon av metan og hydrokarboner. Tidligere ubeskrevne funksjonelle forskjeller ble imidlertid identifisert mellom ulike ANME-1. Basert på tidligere funn i terrestriske hydrotermiske systemer, ble potensialet for metanoksidasjon også evaluert i rekonstruerte genomer av Korarchaeia. Korarchaeia fra marine hydrotermiske system, ble funnet å mangle gen for anaerob oksidasjon av metan. De ble i stedet identifisert som fermenterende mikroorganismer med evne til å benytte sukker og aminosyrer. En komplett Wood-Ljungdahl metabolismevei ble identifisert i dypforgrenede slektslinjer av Korarchaeia og gir sannsynligvis grunnlag for homoacetogenese. Totalt sett har denne studien bekreftet at hydrokarbonrike hydrotermiske systemer ved de arktiske midthavsryggene er tilholdssted for slektslinjer med potensial for hydrokarbonnedbrytning og bidrar til å utvide det fylogenetiske og funksjonelle mangfoldet av slektslinjer som bryter ned hydrokarboner i marine hydrotermiske systemer.

Abbreviations

AMOR: Arctic Mid Ocean Ridges

MAG: metagenome-assembled genome

ANME: anaerobic methanotrophic archaea

LCVF: Loki's Castle Vent Field

JMVF: Jan Mayen Vent Field

SDMO: sulfate-dependent methane oxidation

SRB: sulfate-reducing bacteria

MCR: methyl-CoM reductase

AOM: anaerobic oxidation of methane

H_4MPT: tetrahydromethanopterin

MTR: tetrahydromethanopterin S-methyltransferase

WLP: Wood-Ljungdahl pathway

F_{420}: factor 420

$F_{420}H_2$: reduced factor 420

Hdr: heterodisulfide reductase

Fd: ferredoxin

Fqo: $F_{420}H_2$:quinone oxidoreductase

DET: direct electron transfer

ACR: alkyl-CoM reductase

CODH/ACS: carbon monoxide dehydrogenase/acetyl-CoA synthase

ECR: ethyl-CoM reductase

TACK: Thaumarchaeota, Aigarchaeota, Crenarchaeota, Korarchaeota

McrA: subunit A of the MCR

HGT: horizontal gene transfer

Dsr: dissimilatory sulfite reductase

GTDB: Genome Taxonomy Database

ANI: average nucleotide identity

AAI: average amino acid identity

CARD-FISH: catalyzed reported deposition fluorescence *in situ* hybridization

HMM: hidden Markov model profile

Pfam: protein families database

KO: KEGG Orthology database

List of Publications

I. Vulcano, F., Hahn, C.J., Roerdink, D., Dahle, H., Reeves, E.P., Wegener, G., et al. (2022) Phylogenetic and functional diverse ANME-1 thrive in Arctic hydrothermal vents. *FEMS Microbiol Ecol* **98**: 1–11.

II. Hahn, C.J., Laso-Pérez, R., Vulcano, F., Vaziourakis, K.-M., Stokke, R., Steen, I.H., et al. (2020) "*Candidatus* Ethanoperedens," a Thermophilic Genus of *Archaea* Mediating the Anaerobic Oxidation of Ethane. *MBio* **11**: e00600-20.

III. Vulcano, F., Hribovšek, P., Olesin Denny, E., Steen, I.H., Stokke, R., (2022) Potential for homoacetogenesis via the Wood-Ljungdahl pathway in Korarchaeia lineages from marine hydrothermal vents. (In review: Environmental Microbiology Reports).

1. Introduction

1.1 Background

Ever since the first observation of microorganisms (Leeuwenhoek, 1677), our interpretation of their role in the environment has changed substantially. Initially, microorganisms were described as little animals (Leeuwenhoek, 1677) and known to be responsible for some chemical reactions or linked to infectious diseases. Microorganisms are now acknowledged as a major component of Earth's biomass (Bar-On et al., 2018) and fundamental drivers in biogeochemical cycles (Falkowski et al., 2008). At the beginning of the 20th century, Winogradsky and Beijerinck successfully isolated various soil and aquatic microorganisms (Winogradsky, 1887; Winogradsky, 1890; Beijerinck, 1901). Their work was critical to comprehend the relationship between microorganisms and their environment. In fact, they accomplished some fundamental breakthroughs in microbial ecology, such as the discovery of chemolithotrophy (Winogradsky, 1887). Furthermore, cultivation efforts resulted in the isolation and characterization of several strains of methane-producing microorganisms (Stephenson & Stickland 1933, Bryant et al., 1968; Edwards & McBride, 1975; Balch et al., 1979 and reference therein). The advent of molecular biology and PCR-based gene amplification (Mullis et al., 1992) in the second half of the 20th century further revolutionized the field of microbial ecology. In the late 1970s, Woese and Pace used ribosomal genes for the phylogenetic analysis of microorganisms (Stahl et al., 1985; Pace et al., 1986). This approach revealed three distinct clusters of rRNA sequences, corresponding to the three domains of life and Archaea were described for the first time (Woese & Fox, 1977; Woese et al., 1978; Woese et al., 1990). This molecular method was a first crucial step in the representation of the microbial diversity inhabiting natural environments. In the following years, the improvement of DNA sequencing techniques replenished the tree of life with numerous rRNA genes amplified from various habitats, like soils, ocean waters, and extreme environments, revealing a much wider taxonomic diversity than originally thought (Schmidt et al., 1991; Tsai & Olson, 1992; Moyer et al., 1994; Stephen et al., 1996; Eder et al., 1999; Dunbar et al., 1999; Baker et al., 2006; Lloyd et al., 2006).

Nevertheless, during the 1980s, it became clear that most of the newly identified taxa could not be isolated in the laboratory (Staley & Konopka, 1985) and that cultivation-based studies could only target a minimal fraction of the microbial diversity found in the environment (Mosser et al., 1974; Torsvik et al., 1990). This challenging obstacle called for new strategies that could attribute physiological properties to uncultivable microorganisms. Such endeavors led to the emergence of metagenomics, the study of the structure and function of the genetic material recovered directly from the environment (Handelsman, 2004). Metagenomics has now become the prime technology for phylogenetic and functional study of uncultivable lineages from various environments, from human and animal guts to terrestrial and marine habitats (Tyson et al., 2004; Qin et al., 2010; Sunagawa et al., 2015; Wallace et al., 2015; Anantharaman et al., 2016; Hug et al., 2016; Parks et al., 2017; Dombrowski et al., 2018). Moreover, it has been critical to improve our current understanding of the diversity and functions of microorganisms involved in the biogeochemical cycling of important greenhouse gases such as methane and hydrocarbons (Hallam et al., 2003; Beck et al., 2013; Sierra-Garcia et al., 2017; Woodcroft et al., 2018), which is the topic of this project.

1.2 Global cycle of methane and alkanes

Methane is a central intermediate in the global carbon cycle, a potent greenhouse gas, and the most abundant hydrocarbon in the atmosphere (Reeburg, 2007a; Thauer et al., 2008). The global methane budget is estimated to be in the order of ~600 Tg CH_4 yr^{-1} (Saunois et al., 2020). Approximately 70% of the methane released in the atmosphere has a biotic origin and corresponds to the final product of microbial degradation of organic matter (Conrad, 2009; Saunois et al., 2020). On land, this process occurs in anoxic organic-rich systems (Thauer, 1998). Wetlands represent the widest methane-producing areas, however, animal guts, rice fields, and waste treatment facilities also discharge significant amounts of microbially derived methane into the atmosphere (Conrad, 2009). Oceanic and freshwater masses contribute only to a minimum extent (~10 Tg CH_4 yr^{-1}) to the global methane budget (Reeburgh, 2007a). Nonetheless, numerous biotic and abiotic sources of methane and other alkanes exist in marine and

freshwater environments (Rosentreter et al., 2021). Like on land, remineralization of organic matter is the most significant source of biogenic methane in anoxic marine environments (Reeburgh, 2007b). Detrital organic matter, sinking from the surface, is decomposed, and ultimately fermented to hydrogen, carbon dioxide, and acetate (Thauer et al., 2008; Arndt et al., 2013). Strictly anaerobic methanogenic microorganisms finally transform carbon dioxide, hydrogen, acetate, or methylated compounds into methane (Liu & Whitman, 2008 and references therein; Borrel et al., 2016; Nobu et al., 2016; Vanwonterghem et al., 2016; Sorokin et al., 2017). Some shallow and abyssal marine habitats are fully fueled by the uprising of microbially derived methane, accumulated in subsurface deposits in form of gas hydrates (Foucher et al., 2009; Suess, 2020). Gas hydrates are unstable and release fractions of buoyant gaseous methane (Koh et al., 2002; Dickens et al., 2003). Methane emissions at the seabed level give rise to pockmarks, gas chimneys, mud volcanoes, and cold seeps, often characterized by visible bubbling (Jørgensen & Boetius, 2007; Foucher et al., 2009).

In addition, organic matter can be thermally degraded to hydrocarbons in anoxic deep hot layers of the crust in environments affected by subduction or tectonic activity (Roberts & Aharon, 1994; Jørgensen & Boetius, 2007). The thermal degradation of organic matter can produce, besides methane, hydrocarbons of various lengths and complexity, including the alkanes ethane, propane, and butane (Sephton & Hazen, 2013). The resulting hydrocarbon reservoirs are mobilized by the water circulation to the sediment surface, forming hydrocarbon seeps (Roberts, 2001; Jørgensen & Boetius, 2007). At hydrothermal vents, hydrocarbons can be generated by thermal degradation of buried organic deposits (Welhan & Lupton, 1987; Simoneit et al., 1988). In the sediment-hosted Guaymas Basin, magma dikes percolate through thick layers of organic deposits resulting in extraordinarily hydrocarbon-rich fluids and oil-impregnated sediments (Simoneit et al., 1979; Bazylinski et al., 1988). Methane and short-chain alkanes can be produced abiotically at hydrothermal vents by mineral-catalyzed reactions at high-temperature and pressures (Foustoukos & Seyfried, 2004). Purely abiotic methane is also chemically produced in areas of exposed mantle (Hyndman & Peacock, 2003; Schrenk et al., 2013). When mantle olivine mixes with

water, it metamorphoses into serpentinite, generating hydrogen that reacts with dissolved inorganic carbon to make methane (McCollom, 2016). This exothermic reaction can fuel massive hydrothermal vents, like the Lost City Hydrothermal Field, an off-axis system characterized by high pH, carbonate towers up to 60m tall, and methane-rich hydrothermal fluids at a temperature of about 40-90°C (Kelley et al., 2001; Früh-Green et al., 2003; Kelley et al., 2005). Alternatively, volcanism-derived abiotic methane can be synthesized from carbon monoxide and carbon dioxide at high temperatures in the mantle or magma intrusion in the crust (Etiope & Sherwood, 2013). Examples of hydrothermal systems rich in biogenic and abiotically produced hydrocarbons are found along the Arctic Mid Ocean Ridges (AMOR), i.e., the Loki's Castle Vent Field (LCVF) and the Jan Mayen Vent Field (JMVF) (Pedersen et al., 2010a), respectively. Their geology and geochemistry are described in detail in section 3.1.

Terrestrial hydrothermal systems, i.e., hot springs, are found in proximity of volcanic calderas, and they are powered by heat and freshwater circulation (Des Marais & Walter, 2019). Like marine vents, hot springs can bear thermogenic biotic methane or abiotic methane derived from serpentinization and volcanism (Suda et al., 2022).

In water bodies, methane is readily removed directly at the emission sites and within the water column (Reeburgh, 2007a). This phenomenon explains the minimal contribution of water bodies to the global methane budget (Reeburgh, 2007b). In the water column, methane is consumed by methane-oxidizing bacteria that oxidize methane with oxygen (Murrell, 2010). In anoxic sediments, cold seeps, hydrothermal vents, and freshwater sediments, methane oxidation is carried out by microbial consortia that use sulfate or nitrate as electron acceptors (Knittel & Boetius, 2009; Timmers et al., 2017). Prokaryotes are also responsible for the degradation of short-chain alkanes in the water column (Leahy & Colwell, 1990; Redmond & Valentine, 2012; Olajire & Essien, 2014) or anaerobically in hydrocarbon seeps and sediment-hosted hydrothermal vents (Rabus et al., 2016; Laso-Pérez et al., 2016; Chen et al., 2019; **Paper II**).

Among prokaryotes, cultivated and uncultivated Archaea from anoxic environments can be considered the primary sink of hydrocarbons (Offre et al, 2013; Knittel &

Boetius, 2009). Understanding the taxonomy and physiology of Archaea involved in the cycling of hydrocarbons is crucial to model and predict the emissions of greenhouse gases into the atmosphere. For this reason, anaerobic methane and alkane oxidizers have been the target of microbial ecology since the beginning of the 20th century, as described in the next paragraphs.

1.3 Anaerobic oxidation of methane

The existence of microbial pathways for sulfate-dependent methane oxidation (SDMO) was inferred for the first time in the late 1970s from geochemical profiles in anoxic sediments (Reeburgh, 1976; Barnes & Goldberg, 1976; Martens & Berner, 1977). These profiles showed a sediment horizon where the ascending methane and descending sulfate gradients overlapped and where methane and sulfate were consumed, the sulfate-methane transition zone (SMTZ). Hoehler was the first to hypothesize the existence of a consortium of syntrophic methanogen-related archaea and sulfate-reducing bacteria (SRB) that could revert the methanogenesis pathway using hydrogen as soluble electron carrier and sulfate as terminal electron acceptor (Hoehler et al., 1994). The key actors involved in the SDMO were finally identified only a few years later (Hinrichs et al., 1999; Boetius et al., 2000). By analyzing the 16S rRNA gene sequences from methane seeps sediments rich in archaeal biomarkers, a dominant group of anaerobic methanotrophic archaea (ANME) related to the methanogenic order Methanosarcinales was revealed (Hinrichs et al., 1999). In the following years, several 16S rRNA gene sequences were collected from various anoxic aquatic environments, including deep-sea hydrothermal vents, cold seeps, and lake sediments (Knittel & Boetius, 2009 and references therein). The 16S rRNA phylogeny of ANME identified three main groups: ANME-1a/b, ANME-2a/b/c/d, and ANME-3 that affiliated with methanogens within the phylum Euryarchaeota (Knittel & Boetius, 2009). While ANME-1 appeared to be closely related to Methanomicrobiales, ANME-2 and ANME-3 were related to Methanosarcinales. More recent phylogenomic-based taxonomic classification assigned ANME-1 to the class Syntrophoarchaeia, within phylum Halobacteriota (Rinke et al., 2021) and ANME-1 were ultimately renamed

Candidatus (*Ca.*) Methanophagales (Wegener et al., 2022). Fluorescence *in situ* hybridization targeting the 16S rRNA gene revealed that ANME often occurred in physical association with SRBs of lineage *Desulfosarcina*/*Desulfococcus*-related groups Seep-SRB1 and Seep-SRB2 and *Desulfobulbus*-related species (Boetius et al., 2000; Orphan et al., 2001; Michaelis et al., 2002; Knittel et al., 2005; Niemann et al., 2006; Lösekann et al., 2007; Pernthaler et al., 2008; Wegener et al., 2008; Kleindienst et al., 2012; Ruff et al., 2013; Green-Saxena et al., 2014; Ruff et al., 2016). In 2003, the first direct evidence that ANME use part of the methanogenesis pathway for methane oxidation was collected (Hallam et al., 2003). By then, cultivation and biochemical experiments had already revealed three pathways for methanogenesis in methanogenic Archaea, hydrogen-mediated carbon dioxide reduction, the reduction of methyl groups of methylated compounds, and the disproportionation of acetate (Thauer, 1998 and reference therein). These pathways are known as hydrogenotrophic, methylotrophic, and acetoclastic methanogenesis and share a core set of conserved enzymes. Fosmid libraries of ANME-1 and ANME-2 carried the subunit A of the key methanogenic enzyme methyl-CoM reductase (MCR) (Hallam et al., 2003). Finally, one crucial survey of ANME-1 and ANME-2 fosmids confirmed that ANME encoded all the genes of the methanogenesis pathway (Figure 1), confirming that anaerobic oxidation of methane (AOM) is performed by reverting the methanogenesis pathway (Hallam et al., 2004). In the reverse methanogenesis pathway (Hallam et al., 2004), the MCR oxidizes methane and binds the methyl group to the coenzyme M to form methyl-CoM (Ermler et al., 1997). The methyl group is transferred to tetrahydromethanopterin (H_4MPT) by the tetrahydromethanopterin S-methyltransferase (MTR). The resulting methyl-H_4MPT is oxidized to carbon dioxide by the enzymes of the methyl branch of the Wood-Ljungdahl pathway (WLP). These are the reduced factor 420 ($F_{420}H_2$)-dependent N_5,N_{10}-methylenetetrahydromethanopterin reductase (Mer), the $F_{420}H_2$-dependent methylenetetrahydromethanopterin dehydrogenase (Mtd), the N_5,N_{10}-methenyltetrahydromethanopterin cyclohydrolase (Mch), the formylmethanofuran:tetrahydromethanopterin formyltransferase (Ftr), and the formyl-methanofuran dehydrogenase complex (Fwd). In ANME-1, Mer is replaced by the methylenetetrahydrofolate reductase (Met) (Meyerdierks et al., 2010; Stokke et al.,

2012). Several metagenomic studies have further described genomes from all known ANME groups (Wang et al., 2014; Borrel et al., 2019; Chadwick et al., 2022), revealing an utter conservation of the SDMO pathway. All ANME have a cytoplasmic heterodisulfide reductase (Hdr) complex composed of three subunits (HdrABC) and a formate dehydrogenase-like subunit (FdhB). This complex could oxidize ferredoxin (Fd) and coenzyme M (CoM-SH) + coenzyme B (CoB-SH) and concurrently reduce F_{420}. $F_{420}H_2$ might transfer electrons to hydrophobic electron carriers in the membrane via the $F_{420}H_2$:quinone oxidoreductase (Fqo) or the $F_{420}H_2$ dehydrogenase (Fpo), generating a proton gradient exploited by the conserved ATP synthase (ATPase). Differences between ANME-1 and ANME-2 can be observed in the membrane complexes. While ANME-2a and 2c encode an H+/Na+-translocating ferredoxin:NAD+ oxidoreductase (Rnf) and the HdrDE, ANME-1 seems to rely only on the Fqo to generate the proton motive force.

The possibility that ANME transfer electrons to the partner using soluble carriers, like H_2, acetate, formate or propionate was not supported by experimental evidence, even though theoretically visible (Wegener et al., 2016). The mechanism of electron transfer between archaeal and bacterial syntrophic partners remained unknown for a long time, also owing to the difficulty of cultivating SDMO-cultures. The SDMO reaction has a low energy yield ($\Delta G° = -16.3$ kJ/mol; Timmers et al., 2017) that can only support slow growth rates, with duplication times of a minimum of sixty days (Holler et al., 2011). The development of *ad hoc* cultivation methods for isolating sulfate-dependent anaerobic methane oxidizers was critical to confirm metagenomic predictions (Laso-Pérez et al., 2018). In 2015, a thermophilic ANME-1 was isolated in co-culture (Wegener et al., 2015) with the SRB *Ca*. Desulfofervidus auxilii (Krukenberg et al., 2016) of the lineage HotSeep-1 (Holler et al., 2011). Scanning electron microscopy showed a dense network of nanowires connecting ANME cells to their syntrophic partners, and transcriptomic analysis revealed that the consortia overexpressed extracellular cytochromes when growing under SDMO conditions (Wegener et al., 2015). ANME-1 perform direct electron transfer (DET) to their syntrophic SRB partners via extracellular *c*-type cytochromes and nanowires. Similar results were obtained for ANME-2 by McGlynn et al., 2015. Therefore, the reduced menaquinone

that receives electrons from the Fqo complex can likely discharge them to the membrane and to extracellular cytochromes for DET. ANME-1 were shown to be able to grow via DET-mediated SDMO in a wide range of temperatures. ANME-1 strains have been isolated in coculture with syntrophic SRBs at 37°C (G37ANME1), 60°C (G60ANME1), and 70°C (AOM70) from sediments of the Guaymas Basin (Wegener et al., 2015; Krukenberg et al., 2018; Benito Merino et al., 2022). Interestingly, in 2006, a culture of ANME-2d was obtained on nitrate (Raghoebarsing et al., 2006), proving that some ANME lineages can couple methane oxidation to the more thermodynamically favorable reduction of nitrate ($\Delta G° = -517.2$ kJ/mol; Timmers et al., 2017). Metagenomics confirmed that these ANME, identified as family *Ca.* Methanoperedenaceae, encoded terminal nitrate and nitrite reductases (Haroon et al., 2013; Arshad et al., 2015). In addition, several studies have recently revealed a wide metabolic versatility of ANME, and particularly ANME-2 (Glodowska et al., 2022). In fact, besides sulfate and nitrate, ANME can couple AOM to the reduction of iron, manganese, and other metals (Beal et al., 2009; Ettwig et al., 2016; Weber et al., 2017; Leu et al., 2020; Luo et al., 2017; Luo et al., 2018; Luo et al., 2019; Cai et al., 2018; Shi et al., 2020) and quinone groups (Bai et al., 2019; Zhang et al., 2019). ANME were also shown to be able to generate current in an anoxic bioelectrochemical system while oxidizing methane (Ouboter et al., 2022).

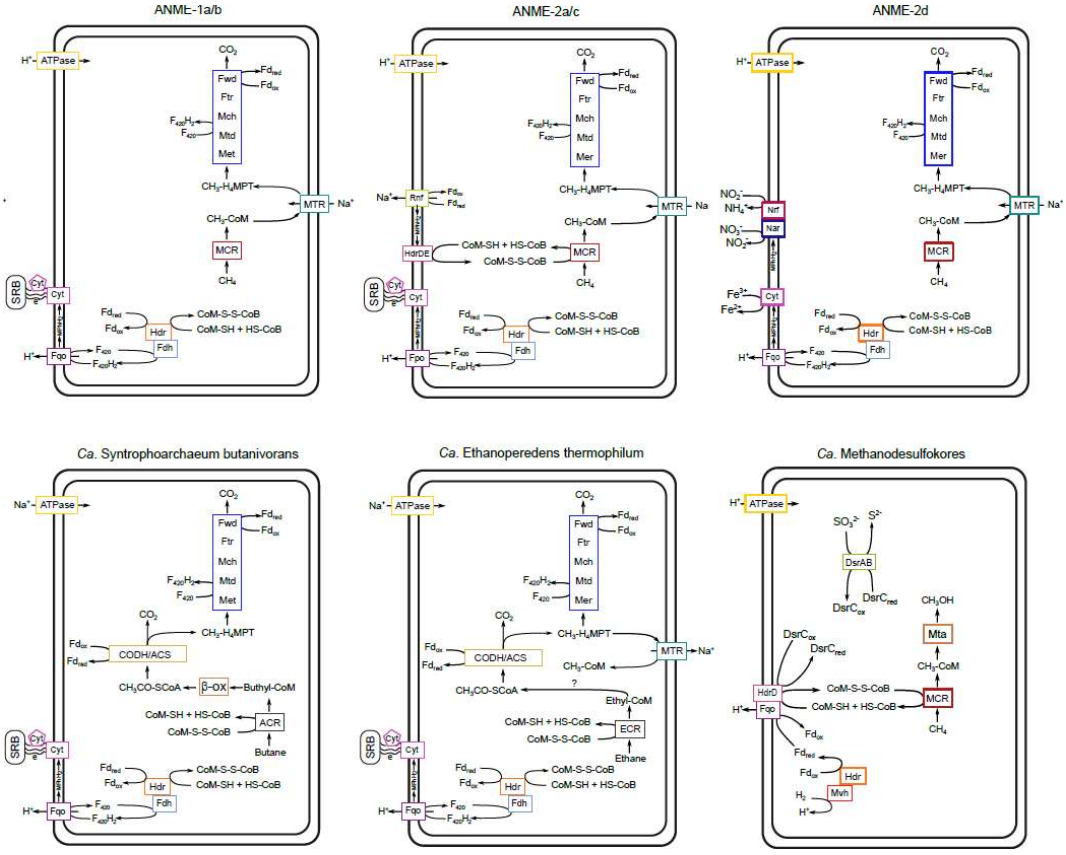

Figure 1. Metabolic model representing anaerobic oxidation of methane and alkane in archaeal lineages. Modified from Borrel et al., 2019 and McKay et al., 2019. Fd_{red}/Fd_{ox} and $DsrC_{red}/Dsr_{ox}$ indicate the reduced and oxidized form of Fd and Dsr, respectively.

1.4 Anaerobic oxidation of non-methane alkanes

In 2016, Archaea capable of oxidizing butane anaerobically were isolated from oily sediments of the Guaymas Basin and described by Laso-Pérez et al., 2016. These microorganisms oxidize butane in syntrophy with the SRB *Ca.* Desulfofervidus auxilii (Krukenberg et al., 2016). Phylogenetic and phylogenomic analyses revealed that these Archaea were related to ANME-1. The two lineages identified were named *Ca.* Syntrophoarchaeum butanivorans and *Ca.* Syntrophoarchaeum caldarius. Microscopy revealed that, like ANME, they interact with the SRB by forming aggregates. The ability of *Ca.* Syntrophoarchaeum to degrade short-chain alkanes depends on its MCR. This is a divergent MCR, named alkyl-CoM reductase (ACR), that likely accommodate larger molecules in its active site. Butane-degrading cultures were capable of degrading propane but not the shorter molecules methane and ethane. The product of the ACR is the intermediate alkyl-CoM. A combination of mass-spectrometry and genome reconstruction revealed that *Ca*. Syntrophoarchaeum utilizes the β-oxidation pathway to convert alkyl-CoM-derived alkyryl-CoA to acetyl-CoA (Figure 1). It remains unknown, however, how alkyl-CoM is converted to alkyryl-CoA. *Ca*. Syntrophoarchaeum encodes the carbon monoxide dehydrogenase/acetyl-CoA synthase (CODH/ACS), which can convert the acetyl-CoA into carbon dioxide and methyl-H_4MPT. Methyl-H_4MPT is fully oxidized to carbon dioxide by running the methyl branch of the WLP in reverse and maintaining redox balance with Fqo. The MTR complex is absent in *Ca*. Syntrophoarchaeum. The enzyme Mer is replaced by Met, as in ANME-1. The electrons released in the membrane via Fqo are channeled to the SRB partner via membrane cytochromes and nanowires.

A few years later, the potential for anaerobic oxidation of ethane was found in ANME-2-related Archaea (Chen et al., 2019; **Paper II**). Two distinct species were enriched. The first, from a cold seep in the Gulf of Mexico, was enriched for over ten years at 12°C and was named *Ca.* Argoarchaeum ethanivorans (Chen et al., 2019). A thermophilic lineage was later enriched from the Guaymas Basin in only 6-7 months at slightly acidic pH and named *Ca.* Ethanoperedens thermophilum (**Paper II**). Both lineages encode the divergent MCR ethyl-CoM reductase (ECR) related to the ACR of *Ca*. Syntrophoarchaeum. As detailly described by **Paper II** and shown in Figure 1, the

ECR converts ethane into ethyl-CoM. The ethyl-CoM is converted to acetyl-CoA by a still unknown pathway. Finally, the CODH/ACS converts acetyl-CoA to methyl-H_4MPT. As ANME and *Ca.* Syntrophoarchaeum, *Ca*. Ethanoperedens are physically associated via nanowires to a syntrophic SRB that acts as an electron acceptor (**Paper II**). A Fqo is likely responsible for recycling $F_{420}H_2$ and transferring electrons to membrane cytochromes. On the contrary, *Ca.* Argoarchaeum was not observed in physical contact with SRBs and a syntrophic interaction via diffusible species was proposed instead (Chen et al., 2019).

Around the same time, the first evidence of archaeal degradation of long-chain alkanes was gathered in a genome reconstructed from oily sediments in the Gulf of Mexico and Santa Barbara oil seep (Laso-Pérez et al., 2019; Borrel et al., 2019). The genome corresponded to a novel lineage, *Ca*. Methanoliparia, with a deep-branching position to ANME-1 and *Ca*. Syntrophoarchaeum. This organism appeared as a single cell attached to oil droplets. Interestingly, *Ca*. Methanoliparia encode an MCR and an ACR and several long-chain acyl-CoA synthetases. As described by Laso-Pérez et al., 2019, the ACR could activate the alkyl units of long-chain alkanes and then oxidize them to acetyl-CoA via the β-oxidation pathway. Acetyl-CoA could be broken up into carbon dioxide and methyl-H_4MPT by CODH/ACS. Methyl-H_4MPT could then be turned into methyl-CoM by MTR and become the substrate of the canonical MCR resulting in methane production. In such a scenario, the methyl branch of the WLP would be used as an electron sink for the cofactors used for the oxidation of alkanes, producing additional methane. If the WLP was run in the oxidative direction to oxidize the methyl-H_4MPT to carbon dioxide, a terminal electron acceptor or a syntrophic partner would be required to oxidize the Fd. However, even though an Rnf for Fd oxidoreduction was identified, no terminal reductases or cytochromes could be found in the *Ca.* Methanoliparia genomes. The non-syntrophic degradation of long-chain alkanes to methane via β-oxidation and a reductive WLP was finally confirmed by cultivation (Zhou et al., 2022).

1.5 Conservation of methane-related pathways in the domain Archaea

The increasing availability of metagenome-assembled genomes (MAGs) of uncultivated microorganisms and the use of genome-based taxonomies has increased the resolution of recent phylogenetic analyses of Archaea. This determined the discovery of a wide diversity of lineages encoding a potential for methylotrophic methanogenesis. New lineages were revealed within the phylum Euryarchaeota, and they were Methanomassiliicoccales[a] (Dridi et al., 2012), the halophilic Methanonatronoarchaeia[b] (Sorokin et al., 2017) and the deep branching Methanofastidiosales[c] (Borrel et al., 2019)[1]. Remarkably, genes for methylotrophic methanogenesis were also identified in the TACK (Thaumarchaeota, Aigarchaeota, Crenarchaeota, Korarchaeota) superphylum[2], i.e., Bathyarchaeia (Evans et al., 2015), Vestraetearchaeota[d] (Vanwonterghem et al., 2016), and Korarchaeia (McKay et al., 2019). The phylogeny of the subunit A of the MCR (McrA) combined with phylogenomic analysis of the recently discovered methanogenic lineages revealed that ANME-1 likely descended from the non-methane alkane-oxidizing Syntropharchaeia (Figure 2; Wang et al., 2021; Wang et al., 2022). While the McrA of ANME-2 is highly related to the McrA of Methanosarcinales, the McrA sequences of ANME-1 cluster with McrA of *Ca.* Methanofastidiosa/*Ca*. Nuwarchaeia suggesting that ANME-1 acquired the MCR via an event of horizontal gene transfer (HGT) (Borrel et al., 2019; Wang et al., 2021).

The potential for AOM was identified in MAGs of Korarchaeia (McKay et al., 2019). Currently, only one Korarchaeia enrichment is available, obtained from the Obsidian Pool in Yellowstone National Park. This represents an organism that can grow anaerobically on peptides, in slightly acidic pH and thermophilic conditions (Elkins et al., 2008). Following metagenomic analysis revealed that Korarchaeia are primarily fermenters as they encode glycolysis/gluconeogenesis pathway, pentose phosphate

[1] The GTDB has recently reclassified the phylum Euryarchaeota replacing traditional 16S rRNA-based phylogeny with a phylogeny based on concatenated markers. Abovementioned methanogenic lineages have been reassigned to phylum Thermoplasmatota[a], Halobacteriota[b] and Methanobacteriota_B[c].

[2] The TACK superphylum was reclassified in GTDB as phylum Thermoproteota. Lineages previously defined as phyla in TACK superphylum have been reclassified as class Methanomethylicia[d], Bathyarchaeia, and Korarchaeia.

pathway and several metabolic routes for assimilation and fermentation of amino acids (McKay et al., 2019). MCR-encoding Korarchaeia corresponding to species *Ca.* Methanodesulfokores washburniensis was recovered from Washburn hot spring in Yellowstone (McKay et al., 2019). *Ca.* Methanodesulfokores MAGs encode for MCR and the dissimilatory sulfite reductase (DsrAB). The korarchaeotal McrA branches with McrA sequences of Vestraetearchaeota and Methanomassiliicoccales and is adjacent to ANME-1 McrA sequences (Figure 2). The DsrAB sequences cluster with sequences of Aigarchaeota and cultivated sulfate-reducing Clostridia and are adjacent to sequences of *Desulfobacca* and Deltaproteobacteria, suggesting that Korarchaeia might be capable of reduction of sulfur species rather than oxidation. The coexistence of MCR and methyltransferases, the HdrD and HdrAC in association with a F_{420}-non-reducing hydrogenase (Mvh), and DsrAB, DsrC/D, DsrMKJOP in the same organism could result in three possible pathways for energy conservation (McKay et al., 2019). First, Korarchaeia could perform methylotrophic methanogenesis with hydrogen as electron donor. Second, they could respire sulfite with hydrogen. Third, they could perform a new type of methane oxidation, in which methane is oxidized to methanol via MCR and a methyltransferase operating in reverse.

Syntropharchaeia-related ACRs were identified in *Ca.* Bathyarchaeia from deep aquifers (Laso-Pérez et al., 2016), Archaeoglobi from deep-subseafloor and hot springs (Boyd et al., 2019; Wang et al., 2019), *Ca.* Helarchaeales from hydrocarbon-rich hydrothermal sediments (Seitz et al., 2019) and *Ca.* Hadarchaeia from hot springs (Wang et al., 2019; Hua et al., 2019). This wide distribution suggests that the ACR has been subjected to events of HGT that might have resulted in the repeated emergence of pathways for anaerobic oxidation of alkanes (Garcia et al., 2022; Wegener et al., 2022). Overall, metagenomic studies have revealed that pathways for anaerobic oxidation of alkanes are widely distributed and ancient in Archaea (Wegener et al., 2022). The modules that constitute these metabolic networks are relatively conserved and their different arrangements generate a wide diversity of pathways for hydrocarbon production and degradation (Garcia et al., 2022). The study of novel marine locations rich in methane and short-chain alkane is pivotal to expand the current knowledge on the phylogenetic diversity of archaeal hydrocarbon-degraders and uncover the full

diversity of metabolic routes at the basis of the removal of the potent greenhouse gases stored in marine anoxic environments.

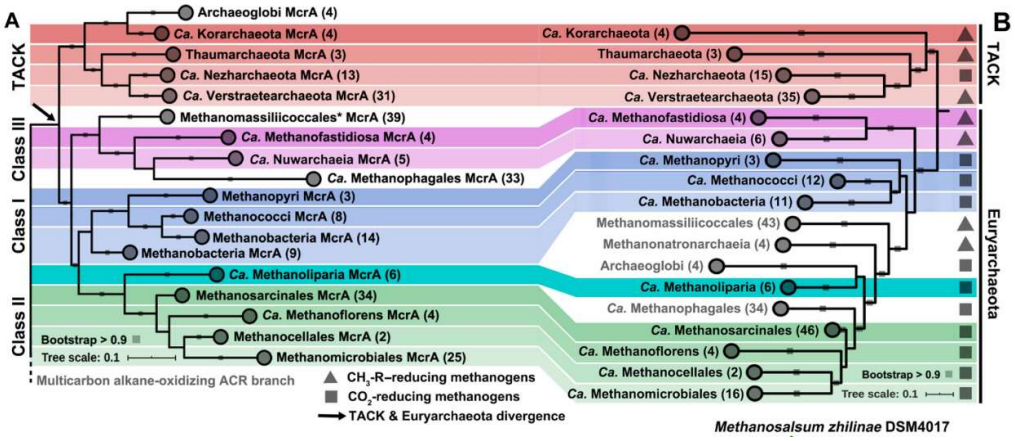

Figure 2. (A) Phylogenetic diversity of archaeal McrA sequences, compared to (B) phylogenomic relationships between Euryarchaeal and TACK lineages. Reprinted from Wang et al., 2021 © The Authors, some rights reserved; exclusive licensee American Association for the Advancement of Science. Distributed under a Creative Commons Attribution NonCommercial License 4.0 (CC BY-NC) http://creativecommons.org/licenses/by-nc/4.0/.

2. Aims of the study

The main aim of this project was to identify archaeal lineages of hydrocarbon-degraders in hydrothermal vents of the AMOR, by using a genome-centric approach, and predict their full metabolic potential based on comparative genomics.

Additional sub-goals were:

- To described phylogenetically, morphologically, and functionally MAGs of anaerobic methane oxidizers at the methane rich LCVF and JMVF and inspect their gene content (**Paper I**)
- To describe phylogenetically, morphologically, and functionally MAGs of anaerobic ethane oxidizers at the sediment hosted LCVF (**Paper II**)
- To assess the full metabolic potential including capacity for methane-oxidation of MAGs of marine Korarchaeia from various hydrothermal systems along AMOR (**Paper III**).

3. Materials and Methods

3.1 The study sites

Samples for this study (**Paper I, II, and III**) were collected from hydrothermal vent systems located along the AMOR. Two vents were investigated in detail, the LCVF and the JMVF. LCVF is located at 73°30′N and 8°E, at the intersection between the Mohns and Knipovich ridges (Pedersen et al., 2010b), at a depth of ca. 2300 m. The venting area consists of two 20-30 m high sulfide mounds (Pedersen et al., 2010a), hosting four chimneys that emit high-temperature fluids (305 to 317°C) (Baumberger et al., 2016). An area of diffuse venting is located on the eastern side of the mounds (Pedersen et al., 2010b). It is characterized by low-temperature (20°C) diluted end-members fluids discharged from sediments and small barite chimneys (Eickmann et al., 2014; Steen et al., 2016). The JMVF (71°17.9'N, 05°42.2'W) is located at the southwestern end of the Mohns Ridge, at a depth of ca. 560 m. It is characterized by focused and diffused hydrothermalism and endmember fluids with a temperature of approximately 242°C. The LCVF and JMVF endmember fluids are enriched in methane (12.5 – 15.6 mmol/kg and 5.4 - 6 mmol/kg, respectively; Baumberger et al., 2016; Stokke et al., 2020). LCVF's endmember fluids are rich in ammonia (4.5 to 6.1 mmol/L) and short-chain alkanes, ethane (150 – 180 µmol/kg), propane (interspersed with C_3H_6 for a total up to 13.9 – 17.6 µmol/kg), butane (0.54 – 0.71 µmol/kg), suggesting that the vent system is sediment hosted (Baumberger et al., 2016). The endmember fluids of JMVF show low concentrations of NH_4^+, suggesting a volcanic origin of the emitted methane (Stokke et al., 2020). ANME-1 MAGs (**Paper I**) were reconstructed from the LCVF and JMVF from high-temperature smokers, high-temperature hydrothermal sediments, low-temperature hydrothermal sediments, and low-temperature barite chimneys. A MAG of a putative ethane oxidizer (**Paper II**) was reconstructed from a low-temperature barite chimney at LCVF. Finally, to compile a comprehensive analysis of the metabolic potential of Korarchaeia lineages across AMOR, Korarchaeia MAGs (**Paper III)** were searched in high-temperature hydrothermal sediments and smokers at LCVF and JMVF and from high-temperature smokers at the Ægir Vent Field and the Fåvne Vent Field (Boonnawa et al., 2022).

Publicly available MAGs from several marine cold seeps, terrestrial hydrothermal systems, hydrocarbon-rich and serpentinite-hosted vents were included as a comparison in all studies, as detailed in **Paper I**, **II** and **III**. Details on the different methods used in this project are given in the respective papers, however, below a selection of the used methods is highlighted.

3.2 Next-generation sequencing of environmental DNA

Environmental DNA from sediments (**Paper I, II**, and **III**) was extracted using an extraction kit optimized for soil and sediment samples used in a large number of studies on various types of samples (e.g., Knittel et al., 2005; Redmond & Valentine, 2012; Haroon et al., 2013; Nobu et al., 2016; Shi et al., 2020; Bowers et al., 2022; Yu et al., 2022). The standard protocol includes a bead-beating step for physical separation of cells from the sediments. Besides sediments samples, this extraction protocol allowed the recovery of MAGs of methane and short-chain alkane degraders from chimney material, even though the kit is not optimized for mineral rich substrates. Environmental DNA was sequenced with the Illumina short-read technology. In **Paper I and II**, the Illumina platform with MiSeq 300 paired-end read chemistry was used, whereas in **Paper III** MAGs were generated from Illumina NovaSeq 6000 (S4 flowcell using 150 bp paired-end reads). Among Illumina platforms, MiSeq 300 provides the longest reads (2 x 300 bp) with up to 15 Gb (Gigabases) of data. NovaSeq can provide up to 3000 Gb of data (2 x 150 bp long reads) with reduced run times (13-44 hours). Illumina is the most base-by-base accurate method available and is currently preferable to long-read technologies for sequencing environmental DNA due to its low error rate (0.1%) (Hu et al., 2021). Due to the high read output of Illumina NovaSeq, samples could be barcoded and multiplexed, adding an individual tag to each sample metagenome and pooling of samples prior to sequencing. Hence, increasing the overall output from each sample with a concomitant reduction in sequencing costs. Furthermore, due to the high read output, Illumina platforms is also likely to target a high fraction of the taxonomic diversity in highly diverse samples (Slatko et al., 2018). The high coverage reduces difficulties in the *de novo* assembly caused by the limited

size of the output reads (50-300 bp). Illumina was also preferred to long-read platforms because of its reduced costs and the availability of several computational tools developed for short-read data. However, the genome of *Ca*. Ethanoperedens was sequenced with the PacBio (Pacific Bioscience) long-read technology. The DNA of the sediment-free *Ca*. Ethanoperedens co-cultures (**Paper II**) was extracted with a freeze/thaw method to reduce DNA fragmentation. This long-read technology does not rely on DNA amplification and can sequence long DNA fragments (30-50 kb), yielding 10-15 kb long reads and 7.6 Gb of data. The long reads generated improve the quality of the genome assembly resulting in highly complete or closed genomes with minimum contamination. To minimize the high error rates of PacBio technology (14%; Hu et al., 2021), ethane-oxidizing cultures were also sequenced as a long-read gDNA library.

3.3 Assembly of MAGs and quality check

Tools for assembly and binning of sequenced reads were selected based on performance and time of the analysis. The licensed Qiagen CLC Genomic Workbench software was initially used for assembly of MAGs from active LCVF low-temperature barite chimneys and JMVF high-temperature sediments (**Paper I and II**). MetaBAT, specifically developed for recovery of high-quality genomes from complex microbial communities (Kang et al., 2015), was chosen for binning of LCVF low-temperature barite chimneys and JMVF high-temperature sediments. MetaBAT was later replaced by a combination of the open-source binning tools (MetaBAT 2.15 – MaxBin v.2.2.7 – CONCOCT 1.1.0) for sequencing of the LCVF low-temperature sediments. Since each binning tool perform differently on different types of samples (Sieber et al., 2018), a combinatorial approach was applied to combine advantages and minimized weaknesses of individual binning approaches. This combinatorial effect was complemented with a final refinement step using DAS Tool. DAS Tool showed to be efficient in reconstructing a high number of high-quality genomes and resolving highly similar genomes, in both low- and high- complexity datasets compared to MetaBAT alone (Sieber et al., 2018). More recently collected samples, like the high-temperature smoker samples from Ægir Vent Field **(Paper III)**, were assembled with the open-

source MEGAHIT that showed a high-throughput performance on large and complex metagenomic datasets (Li et al., 2015). Genome reconstruction from the most recent assembled metagenomes was accomplished using MetaWRAP (Uritskiy et al., 2018), such as the high-temperature smokers in **Paper III**. MetaWRAP outperforms DAS Tool in producing high number of bins with high completion and low contamination, in low- and high- complexity datasets (Uritskiy et al., 2018).

The relative abundance of ANME-1 MAGs (**Paper I**) in metagenomes from LCVF and JMVF was estimated by mapping the sequenced reads against binned MAGs for coverage estimation.

MAGs were further checked for completeness and contamination. To obtain comparable completeness and contamination values, all MAGs from the three studies and the references were evaluated with CheckM by screening for the presence/absence of lineage-specific marker genes (Parks et al., 2015). MAGs with >10% contamination were excluded from all analyses. The threshold for completeness was adjusted depending on the purpose and requirements of each analysis. For phylogenomics in **Paper I and III,** the threshold of >50% completeness was applied as phylogenomic is computed on a conserved but limited fraction of the genomes of interest. Furthermore, the estimation of completeness based on universal markers might undervalue the real genome completeness. Even though CheckM is based on selection of lineage specific marker sets, poorly characterized lineages might suffer from absence of close relatives in the CheckM reference tree. This might result in selection of unspecific marker sets that can cause underestimation of completeness values (Chklovski et al., 2022). Genomes with reduced genome size are affected by a similar bias, and require *ad hoc* compiled marker sets from completeness calculation (Dombrowski et al., 2020). For pangenomic analysis in **Paper I**, MAGs with higher completeness (70%) were selected to limit biases in interpreting the distribution of gene clusters across genomes. For comparative genomics of ANME-1 in **Paper I**, all MAGs (50-100% completeness) were considered. Later, only MAGs >80% complete were included in the large-scale comparative genomic analysis for a more complete description of Korarchaeia metabolic pathways (**Paper III**).

3.4 Taxonomic classification

ANME-1 and Korarchaeia (**Paper I** and **III**) MAGs were initially classified with the Genome Taxonomy Database Toolkit (GTDB-tk), by comparing to references in the Genome Taxonomy Database (GTDB), based on their relative evolutionary divergence and average nucleotide identity (ANI) indices (Parks et al., 2018). GTDB's genome-centered approach provides an updated and systematic classification of largely uncultivated microorganisms that has recently redefined the taxonomy of Archaea (Rinke et al., 2021). Hence, for ANME-1 and Korarchaeia, GTDB's nomenclature was preferred to the taxonomic affiliation provided by the National Center for Biotechnology Information (NCBI).

Family-level lineages identified by GTDB-tk were supported by estimating average amino acid identity (AAI) values. MAGs with an AAI threshold of >65% were considered part of the same genus-level lineage according to the suggested standards for description of uncultivated taxa (Konstantinidis et al., 2017). The threshold of 65% AAI was shown to describe best genomic discreteness at genus-level (Goris et al., 2007).

Species-level lineages identified by GTDB-tk were confirmed with ANI pairwise comparison (**Paper I)** and ANI was used to define species-level groups when GTDB classification was lacking. MAGs with >95% ANI were grouped in the same species, according to Rodriguez-R & Konstantinidis, 2014. ANI value was deemed reliable when the aligned fraction of the query MAGs with >95% ANI was at least 20% based on Richter & Rosselló-Móra, 2009. In **Paper II**, ANI and AAI values were also used to determine the similarity between thermophilic and mesophilic *Ca*. Ethanoperedens cultures, MAGs and single-amplified genomes SAGs.

In parallel to genome-based taxonomic classification, the taxonomy of ANME-1 and GoM-Arc1 was directly assessed in environmental samples from the LCVF low-temperature barite chimneys and sediments with catalyzed reported deposition fluorescence *in situ* hybridization (CARD-FISH). CARD-FISH was used to examine the aggregation status and physical interaction between cells of alkane oxidizers and SRB partners in sediment samples. Since CARD-FISH relies on the activation of multiple tyramides molecules by a horse radish peroxidase-labelled probes against the

16S rRNA rather than fluorescently labeled probes (Amann & Fuchs, 2008), it produces a robust fluorescent signal that allows the visualization of cells in low cell-densities and sediment-rich samples.

3.5 Phylogenomic and phylogenetic classification

Phylogeny of ANME-1, Korarchaeia and ethane oxidizers was evaluated with phylogenomics of concatenated single copy marker genes (**Paper I, II and III**) and supported by 16S rRNA and McrA phylogenies (**Paper I and II)**.

For the separate phylogenomic analyses, lineage-specific marker sets were selected *ad hoc* when highly conserved throughout the lineages of interest. Single marker phylogenies were compiled for each marker to secure that only markers that described the lineages of interest as monophyletic were selected. These strategies reduce the number of markers considered but improves phylogenetic congruence (Dombrowski et al., 2020). The lineage-specific marker sets need to be reevaluated as new genomes are added to the lineages.

For phylogenomic analysis of anaerobic ethane oxidizers in **Paper II,** 32 markers were selected from a list of known archaeal marker genes (Rinke et al., 2013). Of these, 24 markers were used for ANME-1 phylogenomics (**Paper I**) in addition to 11 markers from the Archaea_76 hidden Markov model profile (HMM) (Lee, 2019) provided by Anvi'o (Eren et al., 2021), for a total of 35 markers. Markers were selected when shared by more than 70% of the MAGs and present in less than three copies, to exclude genes affected by duplication events as they do not share common ancestors with parental nodes and do not correctly reflect evolutionary trajectory. For the phylogeny of Korarchaeia in **Paper III**, markers were selected among the 122 archaeal single copy markers used by the GTDB (Parks et al., 2022) when present in at least 75% of the Korarchaeia MAGs and in a maximum of two copies per MAG. Only bests hit were selected. This resulted in 42 marker genes. All were used for the alignment to improve tree resolution. For **Paper I**, long 16S rRNA fragments (1346-690 bp) recovered from ANME-1 MAGs were compared to reference 16S rRNA sequences from the Guaymas Basin (Holler et al., 2011) and the Black Sea (Knittel et al., 2005). In **Paper II**, the 16S

rRNA sequences from the ethane-oxidizing cultures, MAGs and SAGs were compared to 16S rRNA sequences of other Archaea available at SILVA ribosomal RNA gene database (Quast et al., 2012). In **Paper III**, it was opted for a high-resolution phylogeny rather than a large-scale 16S rRNA-based one. Single-gene approaches do not provide the same accuracy in defining phylogenetic relationships at a low taxonomical level because they use a limited fraction of the genome compared to concatenated phylogenies.

Phylogeny of the McrA was compiled for **Paper I** and **Paper II** for comparison of functionally related genomes. The McrA phylogeny was shown to be highly similar to 16S rRNA phylogeny (Luton et al., 2002) and it has been used for taxonomic classification of methanogens and anaerobic methanotrophs (Knittel and Boetius, 2009). The recent expansion of the number of genomes of methane-related microorganisms has revealed that MCR can be affected by HGT events (Borrel et al., 2019; Wang et al., 2021). Therefore, it can be argued that the McrA does not reflect vertical evolution in all alkane-metabolizing lineages. Hence, in this study the use of the McrA phylogeny was limited to the identification of the type of substrate. The McrA clustering with *Ca.* Syntrophoarchaeia sequences were considered specific for short-chain alkanes rather than methane. McrA sequences were extracted from ANME-1 MAGs and aligned, producing a 534 amino acids long alignment. Forty sequences out of 223 were shorter than 400 amino acids but were included because belonging to MAGs from the selected study sites. Phylogenetic markers were identified by screening MAGs against dedicated HMMs profiles from Boyd et al., 2019. For **Paper II**, longer sequences were considered (1060 amino acids).

Prior to tree computation, ANME-1 and Korarchaeia marker sequences were aligned with an iterative refinement method in MAFFT (Katoh et al., 2002) and trimmed. The trimming has proved beneficial for the accuracy of phylogenies of highly divergent sequences without removing crucial phylogenetic information, even when relaxed conditions are applied (gaps present in half of the sequences) (Talavera & Castresana, 2007). For our study, the software TrimAl for automated trimming was used because suitable for large alignments (Capella-Gutiérrez et al., 2009). IQTREE was used for all phylogenies, with an automatically selected model that combines a general amino acid

replacement matrix method (LG, Le & Gascuel, 2008), empirical state frequency (F), and free rate model with relaxed Gamma-distributed heterogeneity rates (R6 was automatically selected for single gene phylogenies, R10 for concatenated phylogenies). As shown by Shaiber et al., 2020, phylogenetic relationships are not always reflected by similarities in genetic content. To test this hypothesis in the metabolically similar ANME-1, the phylogeny of ANME-1 and related Syntrophoarchaeia (**Paper I**) was compared to the hierarchical clustering of MAGs based on the pattern of gene cluster distribution. Gene clusters are defined as "homologous genes grouped on the basis of their amino acid similarity across genomes as judged by translated DNA sequences" (Shaiber et al., 2020). It remains to be assessed whether such a comparison holds for high taxonomic ranks and medium-quality MAGs (only 70% complete and <10% contaminated).

3.6 Comparative genomics of MAGs

Functional annotation of genomes is challenging as it primarily relies on sequence comparison and can therefore only identify proteins with significant sequence similarity to known protein sequences stored in curated databases. The identification of a certain protein is dependent on the database of reference and the aligning approach used, i.e., local comparison or HMMs. To identify the highest number of proteins and combine different searching algorithms, various annotation pipelines were used for MAGs functional annotation. ANME-1 and related MAGs (**Paper I**) were annotated against the protein families database (Pfam) (Mistry et al., 2021), and the KEGG Orthology (KO) database (Kanehisa et al., 2016a) from the Kyoto Encyclopedia of Genes and Genomes (KEGG). Functional predictions were manually curated based on presence of KO identifiers for functional orthologs. Since cytochromes are not assigned identifiers in the KO database, and HMMs from the Pfam were used instead, as in Wegener et al., 2015. The KO database was preferred over the Clusters of Orthologous Genes (COG) database because COG database was not updated recently (Galperin et al., 2015) and because KO functional orthologs are defined in the context of KEGG molecular networks. Furthermore, the reverse methanogenesis pathway includes

conserved enzymes well-characterized in the KO database. MAGs were screened with two automatic annotation servers, GhostKOALA and KofamKOALA (Kanehisa et al., 2016b). GhostKOALA was preferred over BlastKOALA to reduce the running time of the analysis, significative longer when performed using the Basic Local Alignment Search Tool (BLAST). KofamKOALA relies on HMMs corresponding to functional orthologs, resulting in a more compressed database and a faster screening (Aramaki et al., 2020). Based on results in **Paper I**, both annotation tools showed a similar efficiency in detecting the genes and redox complexes involved in the reverse methanogenesis, but only KofamKOALA could identify the Fqo, with default settings. The software tool Prokka (Seemann, 2014) was used for annotation of *Ca*. Ethanoperedens (**Paper II)**. Prokka performs a multistep annotation that includes BLAST-based searches against UniProt and RefSeq databases, followed by screening against the Pfam. For a more accurate, high-throughput, and highly comparative annotation, the over 90 Korarchaeia MAGs (**Paper III**) were annotated using a pipeline developed by Dombrowski et al., 2020. This pipeline concatenates several annotations resulting in concomitant annotation of each genes against several databases, e.g., UniProtKB (SwissProt) ("UniProt: The Universal Protein Knowledgebase in 2023," 2023), KO, COG, arCOGs (Makarova et al., 2007; Makarova et al., 2015), Pfam, the Carbohydrate-Active enZYmes Database CAZy (Drula et al., 2022), InterPro (Paysan-Lafosse et al., 2023), TIGRFAM (Haft et al., 2012) and with the tool HydDB for hydrogenase classification (Søndergaard et al., 2016). This combined approach resulted in several protein signatures assigned to each query sequence. This pipeline allows the analysis of several MAGs at once and offers the possibility to generate heatmaps based on the presence/absence of genes of interest. The ORFs are also screened against function-specific databases. These classes are described by specific structural, biochemical, and physiological information. Finally, the pipeline developed by Dombrowski and colleagues is suitable for high-throughput detection of known metabolic enzymes but can also be used to identify uncharacterized modular complexes, like membrane terminal reductases, because it integrates domain-specific annotations.

4. Results and discussion

4.1 Phylogeny, functions, and syntrophic interactions

Overall, this study showed that hydrocarbon-rich hydrothermal vents at AMOR host several lineages capable of alkane cycling. Altogether, all reconstructed ANME-1 MAGs (19) were identified as methane oxidizers (**Paper I**), the single MAG of GoM-Arc1 as ethane oxidizer (**Paper II**), whereas none of the 50 MAGs of Korarchaeia (**Paper III**) encoded a capacity to perform oxidation of methane or short-chain alkanes. Within **Paper I** it was shown that ANME-1 at AMOR have an encoded capacity to degrade methane and hence mitigate methane emission in all ranges of temperatures and geochemical conditions in the studied locations. The methane oxidation rate of 110 nmol d^{-1} in the LCVF low-temperature sediments is within the range as previously determined in seeps SMTZs (Knittel & Boetius, 2009 and references therein).

A total of seven species-level ANME-1 lineages were identified, one of which represented a novel deep-branching ANME-1 family, *Ca*. Veteromethanophagaceae. The relative abundances of MAGs described in **Paper I** suggest that methane availability and temperature are likely drivers for the distribution of ANME-1 lineages, as predicted by energy landscape modeling (Dahle et al., 2015). Arguably, the ANME-1 population at LCVF and JMVF have diversified into phylogenetically diverse lineages adapted to high and low-temperatures, in line with previous observation at Guaymas Basin (Holler et al., 2011).

For the first time vent-specific and generalist groups of ANME-1 were defined (**Paper I**). All examined ANME-1 encoded the canonical set of enzymes necessary to perform SDMO, i.e., the MCR, the MTR, the WLP, and the typical redox complexes for energy conservation (**Paper I**), including predicted *c*-type cytochromes for DET to a sulfate-reducing partner bacterium. Besides being phylogenetically divergent, these generalist and vent-specific ANME-1 show a distinct assortment of accessory gene clusters. All generalist ANME-1 are enriched in nucleases, proteases, restriction enzymes, and genes of the toxin-antitoxin system. These features might grant tolerance to environmental stressors and could represent a tool set to survive or spread in

unfavorable and variable habitats. However, information about the role and expression of these genetic systems under certain environmental conditions is missing.

ANME-1 establish DET with different SRB at different temperatures (Knittel & Boetius, 2009; Krukenberg et al., 2018). Multiple partner SRB were identified and co-occurred with ANME-1 in all sites studied, as described in **Paper I**. Cold-adapted Seep-SRB1 and Seep-SRB2 (Knittel et al., 2005) were found in the LCVF low-temperature barite chimneys. *Ca*. Desulfofervidales, related to the thermophilic *Ca.* Desulfofervidus auxilii (Krukenberg et al., 2016) were instead found in locations with higher temperatures at both LCVF and JMVF. The observed presence of *Ca*. Desulfofervidus also in low-temperature sediments at LCVF indicates cold-adapted lineages of *Ca*. Desulfofervidales. Alternatively, there may be temperature fluctuations in the sediments caused by transient transit of warmer fluids from deeper subsurface locations. Uniquely, high 16S rRNA relative abundances of Thermodesulfobacteria were observed in the wall of the high-temperature smoker at LCVF where the ANME-1 lineage of the new family *Ca.* Veteromethanophagaceae dominated (**Paper I**). This observation was not discussed in **Paper I**. However, the recent finding that a thermophilic cultivate representatives of family *Ca.* Veteromethanophagaceae can perform SDMO in consortia with Thermodesulfobacteria (Benito Merino et al., 2022) argues in favor that Thermodesulfobacteria are the syntrophic partners of *Ca.* Veteromethanophagaceae in the LCVF high-temperature smoker. Even though multiple partnerships between ANME-1 and known sulfate reducing partner bacteria seem possible in the studied locations, it remains to be experimentally verified if specific syntrophic relationships exist and/or if these partnerships are interchangeable.

In **Paper II**, the GoM-Arc1 population previously identified in LCVF low-temperature barite chimneys based on 16S rRNA surveys (Steen et al., 2016) was phylogenetically and morphologically compared to other recently discovered GoM-Arc1 lineages. The MAG GoM-Arc1-LC reconstructed from LCVF low-temperature barite chimneys was identified as a putative ethane oxidizer by phylogenetic analysis of concatenated markers and McrA phylogeny. As corollary to **Paper II**, the metabolic potential of GoM-Arc1-LC was assessed with the annotation pipeline adopted in **Paper III.** GoM-

Arc1-LC was found to encode a capacity to perform SDMO (Figure 3). GoM-Arc1-LC was more closely related to the cold-adapted ethane oxidizer, *Ca*. Argoarchaeum ethanivorans (Chen et al., 2019), than its thermophilic relative *Ca*. Ethanoperedens thermophilum (presented in **Paper II**).

CARD-FISH analysis revealed that in contrast to the other described GoM-Arc1 lineages, GoM-Arc1 from LCVF low-temperature barite chimneys did not form tight

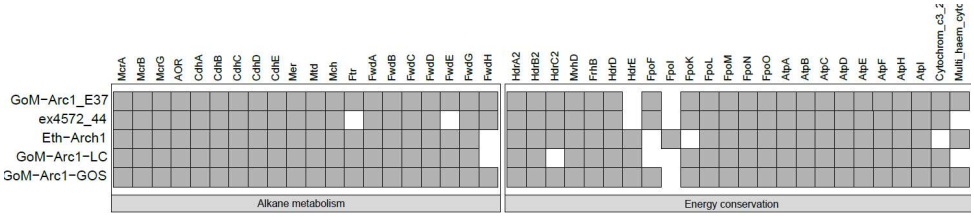

Figure 3. Comparative genomic analysis of GoM-Arc1 MAGs with >90% completeness described in **Paper II**. Proteins of the alkane metabolism and for energy conservation are reported.

aggregates with putative syntrophic SRB. The results obtained agrees with previous morphological analysis of cold-adapted GoM-Arc1 lineages that showed GoM-Arc1 in loose association with syntrophic partners (Chen et al., 2019). Only a few GoM-Arc1 cells could be identified in the 5-10 cmbsf horizon of the low-temperature sediments (data not shown). This observation agrees with 16S rRNA data given in **Paper I** which showed no GoM-Arc1-related 16S rRNA sequences in LCVF low-temperature sediments. In addition, also in **Paper I**, rates of anaerobic oxidation of ethane were not detectable in the sediments. This could be explained by a subsurface biotic degradation of ethane as previously proposed (Viflot, 2019). Putative partners of GoM-Arc1-LC in low-temperature barite chimneys were not discussed in detail in **Paper II**, but results collected in **Paper I** could provide a preliminary outlook on the matter. In the low-temperature barite chimneys, the canonical partners of *Ca.* Argoarchaeum, Eth-SRB1 and Eth-SRB2 (Chen et al., 2019), were not found, neither *Ca.* Desulfofervidus auxilii which was identified as partner of *Ca.* Ethanoperedens thermophilum (**Paper II)**. Whether cold-adapted Seep-SRB1 and Seep-SRB2 found in low-temperature barite chimneys can act as a partner for GoM-Arc1-LC, remains unresolved. ANME-1 cells in the low-temperature barite chimneys were not tightly associated to SRB, while they did form tight aggregates in LCVF low-temperature sediments (**Paper II**). This

indicates that a so-far-unknown geochemical/geophysical environment in the low-temperature barite chimneys may influence ANME-1 and GoM-Arc1 interactions with SRBs. Nonetheless, direct evidence that free-living ANME-1 and GoM-Arc1-LC are metabolically active *in situ* is missing.

Beside methane and ethane, potential for microbial degradation of propane/butane was found at LCVF, and briefly reported in **Paper I**. The high-temperature smoker hosted a group of *Ca.* Alkanophagaceae (AAlk_8), a putatively anaerobic short-chain alkane degrader, related to Syntrophoarchaeia (Zehnle et al., 2022).

Altogether, these observations suggest that the AMOR vent fields represent a remarkable location for further physiological studies of microorganisms performing anaerobic degradation of alkanes.

Results collected in **Paper III,** suggest that Korarchaeia from AMOR do not encode the potential for methane oxidation. **Paper III** also shows that, overall, methane metabolism is a rare trait in Korarchaeia, seemingly confined to terrestrial habitats. Among the 14 genera of Korarchaeia identified none of the marine hydrothermal genomes encodes MCR. They encode a conserved set of metabolic enzymes for fermenting peptides and sugars (Elkins et al., 2008; McKay et al., 2019) combined with hydrogen evolving [FeFe]-hydrogenases. The comparative genomic analysis of the entire class of Korarchaeia suggests the potential for growth on a limited range of substrates, i.e., proteins, and simple sugars. This implies that Korarchaeia in marine hydrothermal systems are heterotrophs and are involved in the degradation of organic matter, as proposed for terrestrial Korarchaeia (Elkins et al., 2008) and other lineages in the TACK superphylum (Baker et al., 2020). Remarkably, some deep branching lineages of Korarchaeia encoded the potential for homoacetogenic metabolism, i.e., a complete WLP and genes for the exergonic synthesis of acetate from acetyl-CoA. The pathway is not used for carbon fixation but rather as an electron sink for reoxidation of the Fd, followed by a final step of ATP synthesis via substrate-level phosphorylation and acetate production. Even though not discussed in **Paper III**, the putative metabolic end products, acetate, and hydrogen, could support a syntrophic interaction with methanogens, thus influencing methane budget at vents and in hot springs.

Furthermore, MtoAC genes coding for methyltransferases and previously found in one genome of Korarchaeia from Guaymas Basin sediments (Welte et al., 2017) were conserved in Korarchaeia with the WLP pathway. As shown for *Archaeoglobus fulgidus*, the WLP could be involved in the degradation of methoxylated aromatic compounds aromatic compounds when run oxidatively (Welte et al., 2017). Interestingly, based on domain-based sequence annotation, one of the WLP-encoding lineages comprised genes that could correspond to a putative terminal electron acceptor. This complex could potentially be involved in discharging electrons derived from an oxidative WLP. Overall, the genome-inferred metabolic potential of Korarchaeia remains to be verified.

Korarchaeia distribution in hydrothermal environments was not deeply investigated in **Paper III**. Nevertheless, our collection of Korarchaeia MAGs from marine hydrothermal systems can give some preliminary insights into the environmental drivers of Korarchaeia distribution. Contrary to what was observed for ANME-1 and ethane oxidizers, Korarchaeia do not seem to differentiate in thermophilic and cold-adapted lineages as Korarchaeia MAGs were only recovered from high-temperature sediments and smokers (personal communication Dr. Runar Stokke). Results from **Paper III** suggest that Korarchaeia might prefer high-temperature niches in marine hydrothermal systems, differently from other TACK lineages. In fact, even though Korarchaeia and Bathyarchaeia share an analogous metabolism, Bathyarchaeia are globally distributed generalists (Zhou et al., 2018) that carry thermal adaptation (Qi et al., 2021) and, at AMOR, they have been reconstructed from high-temperature smokers and low-temperature sediments.

4.2 Methane-metabolizing modules in ANME-1, ethane oxidizers, and Korarchaeia

The WLP, MCR and MTR modules were conserved in MAGs of ANME-1 (**Paper I**) and GoM-Arc1 (**Paper II**), and, in both lineages, they are at the basis of the anaerobic oxidation of methane and short-chain alkanes, as described for other hydrocarbon-degrading lineages (Borrel et al., 2019 and references therein). This study revealed that, beside the previously observed MCR (McKay et al., 2019), the WLP is also encoded

in some lineages of Korarchaeia (**Paper III**). The two modules, however, never cooccur in the same lineages. This discovery expands the number of heterotrophic TACK that encode modules of methane-related metabolisms (He et al., 2016).

The presence of the WLP in Korarchaeia has not been extensively discussed in evolutionary terms in **Paper III**, but it can be interpreted in the light of novel theories about the evolution of methane-related pathways (Wang et al., 2021; Adam et al., 2022). The search for methane-related metabolisms in novel uncharacterized Archaea has revealed that traces of the pathways for methanogenesis remain in all archaeal phyla besides DPANN (Wang et al., 2021). When the WLP is maintained, it likely determines mixotrophic metabolisms (Adam et al., 2022). The metabolic analysis performed in **Paper III** is in line with Adam's theory as the WLP in marine Korarchaeia might have been repurposed for homoacetogenic metabolism after being likely inherited vertically. Vertical inheritance is suggested by the high sequence similarity to Bathyarchaeia WLP enzymes. Nevertheless, phylogenetic comparisons performed so far are still insufficient to fully support this hypothesis as they do not describe in detail how the WLP was acquired.

The MCR has had a convoluted evolutionary history as well, dramatically affected by events of HGT and mutations (Borrel et al., 2019; Wang et al., 2021). These events were critical for the emergence of all three archaeal lineages that have been the object of this project. As discussed, the capacity to degrade methane appeared in ANME-1 only after horizontally transfer of the MCR (Borrel et al., 2019). Duplication events of the ancestral MCR led to the emergence of the ethane specific ECR (Wang et al., 2021) that granted Methanosarcinia the capacity to metabolize ethane. The comprehensive study presented in **Paper III,** covering most of Korarchaeia genomes currently available, provided new elements for evaluating the evolutionary history of MCR in Korarchaeia. McrA phylogenies revealed that the McrA of *Ca.* Methanodesulfokores cluster with the McrA of other members of the TACK (McKay et al., 2019; Wang et al., 2021, Figure 2), advocating a vertical inheritance from the last methane-metabolizing ancestor. Nonetheless, according to phylogenomic reconstruction presented in **Paper III**, it appears the MCR has been retained only in a recently evolved branch. Hence, the MCR must have been lost multiple times throughout Korarchaeia

evolution in favor of fermentative metabolism or horizontally acquired from related TACK.

5. Future work

To verify genome-inferred metabolisms and fully understand the ecological role of the studied lineages, metagenomics should be combined with laboratory-based experimental approaches.

The knowledge gained during this project on abundancies of lineages, functional subgroups and of syntrophic partners can guide future sampling for establishment of enrichments of ANME-1 and GoM-Arc1-LC. Cultivation should be primarily aimed at defining growth temperature ranges and describe the diversity of inter-species syntrophic relationships. Traditional cultivation protocols can be applied (Laso-Pérez et al., 2018; Chen et al., 2019; **Paper II**). In addition, several alternative protocols have been tested on ANME and could be successful in samples from AMOR. These can include the use of electrodes for DET-active lineages (Zhang et al., 2020; Ouboter et al., 2022) or continuous-flow reactors (Aoki et al., 2014). Exposing enrichments to high pressure and high fluid-flow rates might enhance ANME-1 growth based on Timmers et al., 2015 and Girguis et al., 2005, respectively. For Korarchaeia lineages, cultivation could be attempted following protocols presented in Elkins et al., 2008. Growth on various sugars and amino acids, and at various temperatures should be attempted to confirm the metagenomics-driven metabolic predictions and the thermophilic behavior of Korarchaeia. The capacity of WLP-coding lineages to grow on methylated compounds (Welte et al., 2017) or autotrophically should also be verified experimentally.

Next-generation physiology approaches (Hatzenpichler et al., 2020), i.e., FISH-nanoSIMS (Green-Saxena et al., 2014; Dekas et al., 2016; Scheller et al., 2016), SIP DNA/RNA (Orsi et al., 2020) and BONCAT-FISH (Hatzenpichler & Orphan, 2016; Hatzenpichler et al., 2016) are necessary for *in situ* experimental verification of metagenomics-based functional inferences. These methods could also represent a valid strategy to verify whether free-living ANME-1 and GoM-Arc1 are active *in situ* and assess the effect of artificial electron acceptors addition in slurries rich in free-living ANME-1 and GoM-Arc1.

Collection of metatranscriptomics and metaproteomics datasets would be beneficial for the identification of terminal reductases that could support a free-living lifestyle in ANME-1/GoM-Arc1 an oxidative use of the WLP in Korarchaeia. For example, meta-omics datasets could be screened for terminal reductases known to be involved in reduction of metals (Glodowska et al., 2022). Uncharacterized terminal reductases could be instead identified by sequence analysis using domain-based databases (i.e., Pfam, TIGR, InterPro) as in **Paper III**. Identified candidates could then be confirmed experimentally by gene expression and purification (Handelsman, 2004).

The continuous discovery of new hydrocarbon-degrading lineages (Benito Merino et al., 2022; Laso-Pérez et al., 2023) indicates that further metagenomic analysis and genome reconstruction from more anoxic environments can further expand the knowledge on phylogenetic and functional diversity of the lineages studied in this project. Future sequencing efforts and MAG reconstruction of uncultivated microorganisms should be combined with a systematic taxonomic classification based on GTDB standardized phylogeny (Parks et al., 2022; Rinke et al., 2021) and the guidelines proposed by the SeqCode project for quality standards and nomenclature (Hedlund et al., 2022). For a better phylogenetic characterization, alternative phylogenetic approaches could be used to complement phylogenomic analysis, i.e., multigene supertrees (Williams et al., 2017). Various combinations of alternative marker sets should also be tested (Dombrowski et al., 2020; Palmer et al., 2019).

Several ecological questions about ANME-1, ethane oxidizers, and Korarchaeia can be answered with metagenomic data if better metadata are collected. Sampling strategies could be improved with the use of electrode-based probes (https://unisense.com/), temperature probes (Fornari et al., 1998) and less invasive coring devices. Metagenomes could be used to track the dispersal patterns of microbial species. For example, mapping the LCVF MAGs against ocean (e.g., TARA Oceans metagenomes, at NCBI: PRJEB1787) and terrestrial metagenomes could illuminate the connectivity between geographically distant environments.

6. Conclusions

Altogether, the work presented in this project revealed the presence of archaeal lineages with potential for anaerobic oxidation of methane, ethane, and other short chain alkanes at hydrothermal vents along the AMOR. The aims set for this doctoral work have been met as metagenomics and genome-centric approaches have been successful in characterizing these lineages phylogenetically and functionally. First, the metagenomic survey allowed a general assessment of the environmental distribution of these alkane-degrading lineages and their partners showing that hydrocarbon-degraders occur in a wide range of temperatures and locations. Second, MAG reconstruction has allowed the application of modern phylogenomics methods for high-resolution phylogenetic analysis. It has also allowed the use of large-scale comparative genomics analysis, i.e., pangenomics, that revealed overlooked genetic features possibly at the basis of survival strategies. The combined use of a variety of annotation tools has allowed metabolic predictions in all lineages analyzed. It supported an active role of ANME-1 and GoM-Arc1 in cycling of hydrocarbons. It excluded a role of Korarchaeia in anaerobic oxidation of methane and revealed that they likely perform sugars and amino acids fermentation to hydrogen or to acetate via a WLP. On a smaller scale, detailed domain-based analysis of coding sequences allowed the detection of novel candidates for respiratory enzymes.

Despite metagenomics was effective for studying uncultivable lineages from AMOR, it should ultimately be combined with cultivation and *in situ* analysis for verification of predicted physiological features.

References

Adam, P. S., Kolyfetis, G. E., Bornemann, T. L., Vorgias, C. E., & Probst, A. J. (2022). Genomic remnants of ancestral methanogenesis and hydrogenotrophy in Archaea drive anaerobic carbon cycling. *Science Advances*, *8*(44), eabm9651.

Amann, R., & Fuchs, B. M. (2008). Single-cell identification in microbial communities by improved fluorescence in situ hybridization techniques. *Nature Reviews Microbiology*, *6*(5), 339-348.

Anantharaman, K., Brown, C. T., Hug, L. A., Sharon, I., Castelle, C. J., Probst, A. J., ... & Banfield, J. F. (2016). Thousands of microbial genomes shed light on interconnected biogeochemical processes in an aquifer system. *Nature communications*, *7*(1), 13219.

Aoki, M., Ehara, M., Saito, Y., Yoshioka, H., Miyazaki, M., Saito, Y., ... & Imachi, H. (2014). A long-term cultivation of an anaerobic methane-oxidizing microbial community from deep-sea methane-seep sediment using a continuous-flow bioreactor. *PLoS One*, *9*(8), e105356.

Aramaki, T., Blanc-Mathieu, R., Endo, H., Ohkubo, K., Kanehisa, M., Goto, S., & Ogata, H. (2020). KofamKOALA: KEGG Ortholog assignment based on profile HMM and adaptive score threshold. *Bioinformatics*, *36*(7), 2251-2252.

Arndt, S., Jørgensen, B. B., LaRowe, D. E., Middelburg, J. J., Pancost, R. D., & Regnier, P. (2013). Quantifying the degradation of organic matter in marine sediments: A review and synthesis. *Earth-science reviews*, *123*, 53-86.

Arshad, A., Speth, D. R., De Graaf, R. M., Op den Camp, H. J., Jetten, M. S., & Welte, C. U. (2015). A metagenomics-based metabolic model of nitrate-dependent anaerobic oxidation of methane by Methanoperedens-like archaea. *Frontiers in microbiology*, *6*, 1423.

Bai, Y. N., Wang, X. N., Wu, J., Lu, Y. Z., Fu, L., Zhang, F., ... & Zeng, R. J. (2019). Humic substances as electron acceptors for anaerobic oxidation of methane driven by ANME-2d. *Water Research*, *164*, 114935.

Baker, B. J., Tyson, G. W., Webb, R. I., Flanagan, J., Hugenholtz, P., Allen, E. E., & Banfield, J. F. (2006). Lineages of acidophilic archaea revealed by community genomic analysis. *Science*, *314*(5807), 1933-1935.

Baker, B. J., De Anda, V., Seitz, K. W., Dombrowski, N., Santoro, A. E., & Lloyd, K. G. (2020). Diversity, ecology and evolution of Archaea. *Nature microbiology*, *5*(7), 887-900.

Balch, W. E., Fox, G. E., Magrum, L. J., Woese, C. R., & Wolfe, R. (1979). Methanogens: reevaluation of a unique biological group. *Microbiological reviews*, *43*(2), 260-296.

Bar-On, Y. M., Phillips, R., & Milo, R. (2018). The biomass distribution on Earth. *Proceedings of the National Academy of Sciences*, *115*(25), 6506-6511.

Barnes, R. O., & Goldberg, E. D. (1976). Methane production and consumption in anoxic marine sediments. *Geology*, *4*(5), 297-300.

Baumberger, T., Früh-Green, G. L., Thorseth, I. H., Lilley, M. D., Hamelin, C., Bernasconi, S. M., ... & Pedersen, R. B. (2016). Fluid composition of the sediment-influenced Loki's Castle vent field at the ultra-slow spreading Arctic Mid-Ocean Ridge. *Geochimica et Cosmochimica Acta*, *187*, 156-178.

Bazylinski, D. A., Farrington, J. W., & Jannasch, H. W. (1988). Hydrocarbons in surface sediments from a Guaymas Basin hydrothermal vent site. *Organic Geochemistry*, *12*(6), 547-558.

Beal, E. J., House, C. H., & Orphan, V. J. (2009). Manganese-and iron-dependent marine methane oxidation. *Science*, *325*(5937), 184-187.

Beck, D. A., Kalyuzhnaya, M. G., Malfatti, S., Tringe, S. G., Del Rio, T. G., Ivanova, N., ... & Chistoserdova, L. (2013). A metagenomic insight into freshwater methane-utilizing communities and evidence for cooperation between the Methylococcaceae and the Methylophilaceae. *PeerJ*, *1*, e23.

Beijerinck, M. W. (1901). Uber oligonitrophile mikroben. *Zentralbl. Bakterol. Parasitenkd. Infektionskr. Hyg. Abt. II.*, *7*, 561-582.

Benito Merino, D., Zehnle, H., Teske, A., & Wegener, G. (2022). Deep-branching ANME-1c archaea grow at the upper temperature limit of anaerobic oxidation of methane. *Frontiers in Microbiology*, *13*.

Boetius, A., Ravenschlag, K., Schubert, C. J., Rickert, D., Widdel, F., Gieseke, A., ... & Pfannkuche, O. (2000). A marine microbial consortium apparently mediating anaerobic oxidation of methane. *Nature*, *407*(6804), 623-626.

Boonnawa, C., Viflot, T., Pereira, S., Barreyre, T., Jamieson, J. W., Stokke, R., ... & Reeves, E. P. (2022, December). Diverse styles of hydrothermal chemistry on the ultraslow Arctic Mohns Ridge: the Fåvne, Ægir and Loki's Castle vent fields. In *Fall Meeting 2022*. AGU.

Borrel, G., Adam, P. S., & Gribaldo, S. (2016). Methanogenesis and the Wood–Ljungdahl pathway: an ancient, versatile, and fragile association. *Genome biology and evolution*, *8*(6), 1706-1711.

Borrel, G., Adam, P. S., McKay, L. J., Chen, L. X., Sierra-Garcia, I. N., Sieber, C. M., ... & Gribaldo, S. (2019). Wide diversity of methane and short-chain alkane metabolisms in uncultured archaea. *Nature microbiology*, *4*(4), 603-613.

Bowers, R. M., Nayfach, S., Schulz, F., Jungbluth, S. P., Ruhl, I. A., Sheremet, A., ... & Woyke, T. (2022). Dissecting the dominant hot spring microbial populations based on community-wide sampling at single-cell genomic resolution. *The ISME Journal*, *16*(5), 1337-1347.

Boyd, J. A., Jungbluth, S. P., Leu, A. O., Evans, P. N., Woodcroft, B. J., Chadwick, G. L., ... & Tyson, G. W. (2019). Divergent methyl-coenzyme M reductase genes in a deep-subseafloor Archaeoglobi. *The ISME journal*, *13*(5), 1269-1279.

Bryant, M. P., McBride, B. C., & Wolfe, R. S. (1968). Hydrogen-oxidizing methane bacteria I. Cultivation and methanogenesis. *Journal of Bacteriology*, *95*(3), 1118-1123.

Cai, C., Leu, A. O., Xie, G. J., Guo, J., Feng, Y., Zhao, J. X., ... & Hu, S. (2018). A methanotrophic archaeon couples anaerobic oxidation of methane to Fe (III) reduction. *The ISME journal*, *12*(8), 1929-1939.

Capella-Gutiérrez, S., Silla-Martínez, J. M., & Gabaldón, T. (2009). trimAl: a tool for automated alignment trimming in large-scale phylogenetic analyses. *Bioinformatics*, *25*(15), 1972-1973.

Chadwick, G. L., Skennerton, C. T., Laso-Pérez, R., Leu, A. O., Speth, D. R., Yu, H., ... & Orphan, V. J. (2022). Comparative genomics reveals electron transfer and syntrophic mechanisms differentiating methanotrophic and methanogenic archaea. *PLoS biology*, *20*(1), e3001508.

Chen, S. C., Musat, N., Lechtenfeld, O. J., Paschke, H., Schmidt, M., Said, N., ... & Musat, F. (2019). Anaerobic oxidation of ethane by archaea from a marine hydrocarbon seep. *Nature*, *568*(7750), 108-111.

Chklovski, A., Parks, D. H., Woodcroft, B. J., & Tyson, G. W. (2022). CheckM2: a rapid, scalable and accurate tool for assessing microbial genome quality using machine learning. *bioRxiv*, 2022-07.

Conrad, R. (2009). The global methane cycle: recent advances in understanding the microbial processes involved. *Environmental microbiology reports*, *1*(5), 285-292.

Dahle, H., Økland, I., Thorseth, I. H., Pederesen, R. B., & Steen, I. H. (2015). Energy landscapes shape microbial communities in hydrothermal systems on the Arctic Mid-Ocean Ridge. *The ISME journal*, *9*(7), 1593-1606.

Dekas, A. E., Connon, S. A., Chadwick, G. L., Trembath-Reichert, E., & Orphan, V. J. (2016). Activity and interactions of methane seep microorganisms assessed by parallel transcription and FISH-NanoSIMS analyses. *The ISME Journal*, *10*(3), 678-692.

Des Marais, D. J., & Walter, M. R. (2019). Terrestrial hot spring systems: Introduction. *Astrobiology*, *19*(12), 1419-1432.

Dickens, G. R. (2003). Rethinking the global carbon cycle with a large, dynamic and microbially mediated gas hydrate capacitor. *Earth and Planetary Science Letters*, *213*(3-4), 169-183.

Dombrowski, N., Teske, A. P., & Baker, B. J. (2018). Expansive microbial metabolic versatility and biodiversity in dynamic Guaymas Basin hydrothermal sediments. *Nature communications*, *9*(1), 4999.

Dombrowski, N., Williams, T. A., Sun, J., Woodcroft, B. J., Lee, J. H., Minh, B. Q., ... & Spang, A. (2020). Undinarchaeota illuminate DPANN phylogeny and the impact of gene transfer on archaeal evolution. *Nature Communications*, *11*(1), 3939.

Dridi, B., Fardeau, M. L., Ollivier, B., Raoult, D., & Drancourt, M. (2012). Methanomassiliicoccus luminyensis gen. nov., sp. nov., a methanogenic archaeon isolated from human faeces. *International journal of systematic and evolutionary microbiology*, *62*(Pt_8), 1902-1907.

Drula, E., Garron, M. L., Dogan, S., Lombard, V., Henrissat, B., & Terrapon, N. (2022). The carbohydrate-active enzyme database: functions and literature. *Nucleic acids research*, *50*(D1), D571-D577.

Dunbar, J., Takala, S., Barns, S. M., Davis, J. A., & Kuske, C. R. (1999). Levels of bacterial community diversity in four arid soils compared by cultivation and 16S rRNA gene cloning. *Applied and environmental microbiology*, *65*(4), 1662-1669.

Eder, W., Ludwig, W., & Huber, R. (1999). Novel 16S rRNA gene sequences retrieved from highly saline brine sediments of Kebrit Deep, Red Sea. *Archives of microbiology*, *172*, 213-218.

Edwards, T., & McBride, B. C. (1975). New method for the isolation and identification of methanogenic bacteria. *Applied microbiology*, *29*(4), 540-545.

Eickmann, B., Thorseth, I. H., Peters, M., Strauss, H., Bröcker, M., & Pedersen, R. B. (2014). Barite in hydrothermal environments as a recorder of subseafloor processes: a multiple-isotope study from the Loki's Castle vent field. *Geobiology*, *12*(4), 308-321.

Elkins, J. G., Podar, M., Graham, D. E., Makarova, K. S., Wolf, Y., Randau, L., ... & Stetter, K. O. (2008). A korarchaeal genome reveals insights into the evolution of the Archaea. *Proceedings of the National Academy of Sciences*, *105*(23), 8102-8107.

Eren, A. M., Kiefl, E., Shaiber, A., Veseli, I., Miller, S. E., Schechter, M. S., ... & Willis, A. D. (2021). Community-led, integrated, reproducible multi-omics with anvi'o. *Nature microbiology*, *6*(1), 3-6.

Ermler, U., Grabarse, W., Shima, S., Goubeaud, M., & Thauer, R. K. (1997). Crystal structure of methyl-coenzyme M reductase: the key enzyme of biological methane formation. *Science*, *278*(5342), 1457-1462.

Etiope, G., & Sherwood Lollar, B. (2013). Abiotic methane on Earth. *Reviews of Geophysics*, *51*(2), 276-299.

Ettwig, K. F., Zhu, B., Speth, D., Keltjens, J. T., Jetten, M. S., & Kartal, B. (2016). Archaea catalyze iron-dependent anaerobic oxidation of methane. *Proceedings of the National Academy of Sciences*, *113*(45), 12792-12796.

Evans, P. N., Parks, D. H., Chadwick, G. L., Robbins, S. J., Orphan, V. J., Golding, S. D., & Tyson, G. W. (2015). Methane metabolism in the archaeal phylum Bathyarchaeota revealed by genome-centric metagenomics. *Science*, *350*(6259), 434-438.

Falkowski, P. G., Fenchel, T., & Delong, E. F. (2008). The microbial engines that drive Earth's biogeochemical cycles. *science*, *320*(5879), 1034-1039.

Fornari, D. J., Shank, T., Von Damm, K. L., Gregg, T. K. P., Lilley, M., Levai, G., ... & Lutz, R. (1998). Time-series temperature measurements at high-temperature hydrothermal vents, East Pacific Rise 9 49′–51′ N: Evidence for monitoring a crustal cracking event. *Earth and Planetary Science Letters*, *160*(3-4), 419-431.

Foucher, J. P., Westbrook, G. K., Boetius, A., Ceramicola, S. I. L. V. I. A., Dupré, S., Mascle, J., ... & Praeg, D. (2009). Structure and drivers of cold seep ecosystems. *Oceanography*, *22*(1), 92-109.

Foustoukos, D. I., & Seyfried Jr, W. E. (2004). Hydrocarbons in hydrothermal vent fluids: the role of chromium-bearing catalysts. *Science*, *304*(5673), 1002-1005.

Früh-Green, G. L., Kelley, D. S., Bernasconi, S. M., Karson, J. A., Ludwig, K. A., Butterfield, D. A., ... & Proskurowski, G. (2003). 30,000 years of hydrothermal activity at the Lost City vent field. *Science*, *301*(5632), 495-498.

Galperin, M. Y., Makarova, K. S., Wolf, Y. I., & Koonin, E. V. (2015). Expanded microbial genome coverage and improved protein family annotation in the COG database. *Nucleic acids research*, *43*(D1), D261-D269.

Garcia, P. S., Gribaldo, S., & Borrel, G. (2022). Diversity and evolution of methane-related pathways in archaea. *Annual Review of Microbiology*, *76*, 727-755.

Girguis, P. R., Cozen, A. E., & DeLong, E. F. (2005). Growth and population dynamics of anaerobic methane-oxidizing archaea and sulfate-reducing bacteria in a continuous-flow bioreactor. *Applied and environmental microbiology*, *71*(7), 3725-3733.

Glodowska, M., Welte, C. U., & Kurth, J. M. (2022). Metabolic potential of anaerobic methane oxidizing archaea for a broad spectrum of electron acceptors. *Advances in Microbial Physiology*, *80*, 157-201.

Goris, J., Konstantinidis, K. T., Klappenbach, J. A., Coenye, T., Vandamme, P., & Tiedje, J. M. (2007). DNA–DNA hybridization values and their relationship to whole-genome sequence similarities. *International journal of systematic and evolutionary microbiology*, *57*(1), 81-91

Green-Saxena, A., Dekas, A. E., Dalleska, N. F., & Orphan, V. J. (2014). Nitrate-based niche differentiation by distinct sulfate-reducing bacteria involved in the anaerobic oxidation of methane. *The ISME journal*, *8*(1), 150-163.

Haft, D. H., Selengut, J. D., Richter, R. A., Harkins, D., Basu, M. K., & Beck, E. (2012). TIGRFAMs and genome properties in 2013. *Nucleic acids research*, *41*(D1), D387-D395.

Hahn, C. J., Laso-Pérez, R., Vulcano, F., Vaziourakis, K. M., Stokke, R., Steen, I. H., ... & Wegener, G. (2020). "Candidatus Ethanoperedens," a thermophilic genus of archaea mediating the anaerobic oxidation of ethane. *MBio*, *11*(2), e00600-20.

Hallam, S. J., Girguis, P. R., Preston, C. M., Richardson, P. M., & DeLong, E. F. (2003). Identification of methyl coenzyme M reductase A (mcrA) genes associated with methane-oxidizing archaea. *Applied and environmental microbiology*, *69*(9), 5483-5491.

Hallam, S. J., Putnam, N., Preston, C. M., Detter, J. C., Rokhsar, D., Richardson, P. M., & DeLong, E. F. (2004). Reverse methanogenesis: testing the hypothesis with environmental genomics. *Science*, *305*(5689), 1457-1462.

Handelsman, J. (2004). Metagenomics: application of genomics to uncultured microorganisms. *Microbiology and molecular biology reviews*, *68*(4), 669-685.

Haroon, M. F., Hu, S., Shi, Y., Imelfort, M., Keller, J., Hugenholtz, P., ... & Tyson, G. W. (2013). Anaerobic oxidation of methane coupled to nitrate reduction in a novel archaeal lineage. *Nature*, *500*(7464), 567-570.

Hatzenpichler, R., & Orphan, V. J. (2016). Detection of protein-synthesizing microorganisms in the environment via bioorthogonal noncanonical amino acid tagging (BONCAT). *Hydrocarbon and lipid microbiology protocols: Single-cell and single-molecule methods*, 145-157.

Hatzenpichler, R., Connon, S. A., Goudeau, D., Malmstrom, R. R., Woyke, T., & Orphan, V. J. (2016). Visualizing in situ translational activity for identifying and sorting slow-growing archaeal–bacterial consortia. *Proceedings of the National Academy of Sciences*, *113*(28), E4069-E4078.

Hatzenpichler, R., Krukenberg, V., Spietz, R. L., & Jay, Z. J. (2020). Next-generation physiology approaches to study microbiome function at single cell level. *Nature Reviews Microbiology*, *18*(4), 241-256.

He, Y., Li, M., Perumal, V., Feng, X., Fang, J., Xie, J., ... & Wang, F. (2016). Genomic and enzymatic evidence for acetogenesis among multiple lineages of the archaeal phylum Bathyarchaeota widespread in marine sediments. *Nature microbiology*, *1*(6), 1-9.

Hedlund, B. P., Chuvochina, M., Hugenholtz, P., Konstantinidis, K. T., Murray, A. E., Palmer, M., ... & Whitman, W. B. (2022). SeqCode: a nomenclatural code for prokaryotes described from sequence data. *Nature Microbiology*, *7*(10), 1702-1708.

Hinrichs, K. U., Hayes, J. M., Sylva, S. P., Brewer, P. G., & DeLong, E. F. (1999). Methane-consuming archaebacteria in marine sediments. *Nature*, *398*(6730), 802-805.

Hoehler, T. M., Alperin, M. J., Albert, D. B., & Martens, C. S. (1994). Field and laboratory studies of methane oxidation in an anoxic marine sediment: Evidence for a methanogen-sulfate reducer consortium. *Global biogeochemical cycles*, *8*(4), 451-463.

Holler, T., Widdel, F., Knittel, K., Amann, R., Kellermann, M. Y., Hinrichs, K. U., ... & Wegener, G. (2011). Thermophilic anaerobic oxidation of methane by marine microbial consortia. *The ISME journal*, *5*(12), 1946-1956.

Hu, T., Chitnis, N., Monos, D., & Dinh, A. (2021). Next-generation sequencing technologies: An overview. *Human Immunology*, *82*(11), 801-811.

Hua, Z. S., Wang, Y. L., Evans, P. N., Qu, Y. N., Goh, K. M., Rao, Y. Z., ... & Li, W. J. (2019). Insights into the ecological roles and evolution of methyl-coenzyme M reductase-containing hot spring Archaea. *Nature communications*, *10*(1), 4574.

Huang, W. C., Liu, Y., Zhang, X., Zhang, C. J., Zou, D., Zheng, S., ... & Li, M. (2021). Comparative genomic analysis reveals metabolic flexibility of Woesearchaeota. *Nature Communications*, *12*(1), 5281.

Hug, L. A., Baker, B. J., Anantharaman, K., Brown, C. T., Probst, A. J., Castelle, C. J., ... & Banfield, J. F. (2016). A new view of the tree of life. *Nature microbiology*, *1*(5), 1-6.

Hyndman, R. D., & Peacock, S. M. (2003). Serpentinization of the forearc mantle. *Earth and Planetary Science Letters*, *212*(3-4), 417-432.

Jørgensen, B. B., & Boetius, A. (2007). Feast and famine—microbial life in the deep-sea bed. *Nature Reviews Microbiology*, *5*(10), 770-781.

Kanehisa, M., Sato, Y., Kawashima, M., Furumichi, M., & Tanabe, M. (2016a). KEGG as a reference resource for gene and protein annotation. *Nucleic acids research*, *44*(D1), D457-D462.

Kanehisa, M., Sato, Y., & Morishima, K. (2016b). BlastKOALA and GhostKOALA: KEGG tools for functional characterization of genome and metagenome sequences. *Journal of molecular biology*, *428*(4), 726-731.

Kang, D. D., Froula, J., Egan, R., & Wang, Z. (2015). MetaBAT, an efficient tool for accurately reconstructing single genomes from complex microbial communities. *PeerJ*, *3*, e1165.

Katoh, K., Misawa, K., Kuma, K. I., & Miyata, T. (2002). MAFFT: a novel method for rapid multiple sequence alignment based on fast Fourier transform. *Nucleic acids research*, *30*(14), 3059-3066.

Kelley, D. S., Karson, J. A., Blackman, D. K., FruÈh-Green, G. L., Butterfield, D. A., Lilley, M. D., ... & AT3-60 Shipboard Party. (2001). An off-axis hydrothermal vent field near the Mid-Atlantic Ridge at 30 N. *Nature*, *412*(6843), 145-149.

Kelley, D. S., Karson, J. A., Fruh-Green, G. L., Yoerger, D. R., Shank, T. M., Butterfield, D. A., ... & Sylva, S. P. (2005). A serpentinite-hosted ecosystem: the Lost City hydrothermal field. *Science*, *307*(5714), 1428-1434.

Kleindienst, S., Ramette, A., Amann, R., & Knittel, K. (2012). Distribution and in situ abundance of sulfate-reducing bacteria in diverse marine hydrocarbon seep sediments. *Environmental microbiology*, *14*(10), 2689-2710.

Knittel, K., Lösekann, T., Boetius, A., Kort, R., & Amann, R. (2005). Diversity and distribution of methanotrophic archaea at cold seeps. *Applied and environmental microbiology*, *71*(1), 467-479.

Knittel, K., & Boetius, A. (2009). Anaerobic oxidation of methane: progress with an unknown process. *Annual review of microbiology*, *63*, 311-334.

Koh, C. A., Westacott, R. E., Zhang, W., Hirachand, K., Creek, J. L., & Soper, A. K. (2002). Mechanisms of gas hydrate formation and inhibition. *Fluid Phase Equilibria*, *194*, 143-151.

Konstantinidis, K. T., Rosselló-Móra, R., & Amann, R. (2017). Uncultivated microbes in need of their own taxonomy. *The ISME journal*, *11*(11), 2399-2406.

Krukenberg, V., Harding, K., Richter, M., Glöckner, F. O., Gruber-Vodicka, H. R., Adam, B., ... & Wegener, G. (2016). Candidatus Desulfofervidus auxilii, a hydrogenotrophic sulfate-reducing bacterium involved in the thermophilic anaerobic oxidation of methane. *Environmental microbiology*, *18*(9), 3073-3091.

Krukenberg, V., Riedel, D., Gruber-Vodicka, H. R., Buttigieg, P. L., Tegetmeyer, H. E., Boetius, A., & Wegener, G. (2018). Gene expression and ultrastructure of meso-and thermophilic methanotrophic consortia. *Environmental microbiology*, *20*(5), 1651-1666.

Laso-Pérez, R., Wegener, G., Knittel, K., Widdel, F., Harding, K. J., Krukenberg, V., ... & Musat, F. (2016). Thermophilic archaea activate butane via alkyl-coenzyme M formation. *Nature*, *539*(7629), 396-401.

Laso-Pérez, R., Krukenberg, V., Musat, F., & Wegener, G. (2018). Establishing anaerobic hydrocarbon-degrading enrichment cultures of microorganisms under strictly anoxic conditions. *Nature protocols*, *13*(6), 1310-1330.

Laso-Pérez, R., Hahn, C., van Vliet, D. M., Tegetmeyer, H. E., Schubotz, F., Smit, N. T., ... & Wegener, G. (2019). Anaerobic degradation of non-methane alkanes by "Candidatus Methanoliparia" in hydrocarbon seeps of the Gulf of Mexico. *MBio*, *10*(4), e01814-19.

Laso-Pérez, R., Wu, F., Crémière, A., Speth, D. R., Magyar, J. S., Zhao, K., Krupovic, M., & Orphan, V. J. (2023). Evolutionary diversification of methanotrophic ANME-1 archaea and their expansive virome. Nature microbiology, 10.1038/s41564-022-01297-4.

Le, S. Q., & Gascuel, O. (2008). An improved general amino acid replacement matrix. *Molecular biology and evolution*, *25*(7), 1307-1320.

Leahy, J. G., & Colwell, R. R. (1990). Microbial degradation of hydrocarbons in the environment. *Microbiological reviews*, *54*(3), 305-315.

Lee, M. D. (2019). GToTree: a user-friendly workflow for phylogenomics. *Bioinformatics*, *35*(20), 4162-4164.

Leeuwenhoek, A. V. Observations, communicated to the publisher by Mr. Antony van Leewenhoeck, in a dutch letter of the 9th Octob. 1676. here English'd: concerning little animals by him observed in rain-well-sea-and snow water; as also in water wherein pepper had lain infused. *Philosophical Transactions of the Royal Society of London*, *12*(133), 821-831.

Leu, A. O., Cai, C., McIlroy, S. J., Southam, G., Orphan, V. J., Yuan, Z., ... & Tyson, G. W. (2020). Anaerobic methane oxidation coupled to manganese reduction by members of the Methanoperedenaceae. *The ISME Journal*, *14*(4), 1030-1041.

Li, D., Liu, C. M., Luo, R., Sadakane, K., & Lam, T. W. (2015). MEGAHIT: an ultra-fast single-node solution for large and complex metagenomics assembly via succinct de Bruijn graph. *Bioinformatics*, *31*(10), 1674-1676.

Liu, Y., & Whitman, W. B. (2008). Metabolic, phylogenetic, and ecological diversity of the methanogenic archaea. *Annals of the New York Academy of Sciences*, *1125*(1), 171-189.

Lloyd, K. G., Lapham, L., & Teske, A. (2006). An anaerobic methane-oxidizing community of ANME-1b archaea in hypersaline Gulf of Mexico sediments. *Applied and Environmental Microbiology*, *72*(11), 7218-7230.

Luo, J. H., Wu, M., Yuan, Z., & Guo, J. (2017). Biological bromate reduction driven by methane in a membrane biofilm reactor. *Environmental Science & Technology Letters*, *4*(12), 562-566.

Luo, J. H., Chen, H., Hu, S., Cai, C., Yuan, Z., & Guo, J. (2018). Microbial selenate reduction driven by a denitrifying anaerobic methane oxidation biofilm. *Environmental science & technology*, *52*(7), 4006-4012.

Luo, J. H., Wu, M., Liu, J., Qian, G., Yuan, Z., & Guo, J. (2019). Microbial chromate reduction coupled with anaerobic oxidation of methane in a membrane biofilm reactor. *Environment international*, *130*, 104926.

Luton, P. E., Wayne, J. M., Sharp, R. J., & Riley, P. W. (2002). The mcrA gene as an alternative to 16S rRNA in the phylogenetic analysis of methanogen populations in landfill. *Microbiology*, *148*(11), 3521-3530.

Lösekann, T., Knittel, K., Nadalig, T., Fuchs, B., Niemann, H., Boetius, A., & Amann, R. (2007). Diversity and abundance of aerobic and anaerobic methane oxidizers at the Haakon Mosby Mud Volcano, Barents Sea. *Applied and environmental microbiology*, *73*(10), 3348-3362.

Makarova, K. S., Sorokin, A. V., Novichkov, P. S., Wolf, Y. I., & Koonin, E. V. (2007). Clusters of orthologous genes for 41 archaeal genomes and implications for evolutionary genomics of archaea. *Biology direct*, *2*, 1-20.

Makarova, K. S., Wolf, Y. I., & Koonin, E. V. (2015). Archaeal clusters of orthologous genes (arCOGs): an update and application for analysis of shared features between Thermococcales, Methanococcales, and Methanobacteriales. *Life*, *5*(1), 818-840.

Martens, C. S., & Berner, R. A. (1977). Interstitial water chemistry of anoxic Long Island Sound sediments. 1. Dissolved gases 1. *Limnology and Oceanography*, *22*(1), 10-25.

McCollom, T. M. (2016). Abiotic methane formation during experimental serpentinization of olivine. *Proceedings of the National Academy of Sciences*, *113*(49), 13965-13970.

McGlynn, S. E., Chadwick, G. L., Kempes, C. P., & Orphan, V. J. (2015). Single cell activity reveals direct electron transfer in methanotrophic consortia. *Nature*, *526*(7574), 531-535.

McKay, L. J., Dlakić, M., Fields, M. W., Delmont, T. O., Eren, A. M., Jay, Z. J., ... & Inskeep, W. P. (2019). Co-occurring genomic capacity for anaerobic methane and dissimilatory sulfur metabolisms discovered in the Korarchaeota. *Nature microbiology*, *4*(4), 614-622.

Meyerdierks, A., Kube, M., Kostadinov, I., Teeling, H., Glöckner, F. O., Reinhardt, R., & Amann, R. (2010). Metagenome and mRNA expression analyses of anaerobic methanotrophic archaea of the ANME-1 group. *Environmental microbiology*, *12*(2), 422-439.

Michaelis, W., Seifert, R., Nauhaus, K., Treude, T., Thiel, V., Blumenberg, M., ... & Gulin, M. B. (2002). Microbial reefs in the Black Sea fueled by anaerobic oxidation of methane. *Science*, *297*(5583), 1013-1015.

Mistry, J., Chuguransky, S., Williams, L., Qureshi, M., Salazar, G. A., Sonnhammer, E. L., ... & Bateman, A. (2021). Pfam: The protein families database in 2021. *Nucleic acids research*, *49*(D1), D412-D419.

Mosser, J. L., Bohlool, B. B., & Brock, T. D. (1974). Growth rates of Sulfolobus acidocaldarius in nature. *Journal of Bacteriology*, *118*(3), 1075-1081.

Moyer, C. L., Dobbs, F. C., & Karl, D. M. (1994). Estimation of diversity and community structure through restriction fragment length polymorphism distribution analysis of bacterial 16S rRNA genes from a microbial mat at an active, hydrothermal vent system, Loihi Seamount, Hawaii. *Applied and Environmental Microbiology*, *60*(3), 871-879.

Mullis, K., Faloona, F., Scharf, S., Saiki, R., Horn, G., & Erlich, H. (1992). Specific enzymatic amplification of DNA in vitro: the polymerase chain reaction. *Biotechnology Series*, 17-17.

Murrell, J. C. (2010). The aerobic methane oxidizing bacteria (methanotrophs). In *Handbook of hydrocarbon and lipid microbiology*.

Niemann, H., Lösekann, T., De Beer, D., Elvert, M., Nadalig, T., Knittel, K., ... & Boetius, A. (2006). Novel microbial communities of the Haakon Mosby mud volcano and their role as a methane sink. *Nature*, *443*(7113), 854-858.

Nobu, M. K., Narihiro, T., Kuroda, K., Mei, R., & Liu, W. T. (2016). Chasing the elusive Euryarchaeota class WSA2: genomes reveal a uniquely fastidious methyl-reducing methanogen. *The ISME journal*, *10*(10), 2478-2487.

Offre, P., Spang, A., & Schleper, C. (2013). Archaea in biogeochemical cycles. *Annual review of microbiology*, *67*, 437-457.

Olajire, A. A., & Essien, J. P. (2014). Aerobic degradation of petroleum components by microbial consortia. *Journal of Petroleum & Environmental Biotechnology*, *5*(5), 1.

Orphan, V. J., House, C. H., Hinrichs, K. U., McKeegan, K. D., & DeLong, E. F. (2001). Methane-consuming archaea revealed by directly coupled isotopic and phylogenetic analysis. *science*, *293*(5529), 484-487.

Orsi, W. D., Vuillemin, A., Rodriguez, P., Coskun, Ö. K., Gomez-Saez, G. V., Lavik, G., ... & Ferdelman, T. G. (2020). Metabolic activity analyses demonstrate that Lokiarchaeon exhibits homoacetogenesis in sulfidic marine sediments. *Nature Microbiology*, *5*(2), 248-255.

Ouboter, H. T., Berben, T., Berger, S., Jetten, M. S., Sleutels, T., Ter Heijne, A., & Welte, C. U. (2022). Methane-Dependent Extracellular Electron Transfer at the Bioanode by the Anaerobic Archaeal Methanotroph "Candidatus Methanoperedens". *Frontiers in Microbiology*, 1065.

Pace, N. R., Stahl, D. A., Lane, D. J., & Olsen, G. J. (1986). The analysis of natural microbial populations by ribosomal RNA sequences. *Advances in microbial ecology*, 1-55.

Palmer, M., Venter, S. N., McTaggart, A. R., Coetzee, M. P., Van Wyk, S., Avontuur, J. R., ... & Steenkamp, E. T. (2019). The synergistic effect of concatenation in phylogenomics: the case in Pantoea. *PeerJ*, *7*, e6698.

Parks, D. H., Imelfort, M., Skennerton, C. T., Hugenholtz, P., & Tyson, G. W. (2015). CheckM: assessing the quality of microbial genomes recovered from isolates, single cells, and metagenomes. *Genome research*, *25*(7), 1043-1055.

Parks, D. H., Rinke, C., Chuvochina, M., Chaumeil, P. A., Woodcroft, B. J., Evans, P. N., ... & Tyson, G. W. (2017). Recovery of nearly 8,000 metagenome-assembled genomes substantially expands the tree of life. *Nature microbiology*, *2*(11), 1533-1542.

Parks, D. H., Chuvochina, M., Waite, D. W., Rinke, C., Skarshewski, A., Chaumeil, P. A., & Hugenholtz, P. (2018). A standardized bacterial taxonomy based on genome phylogeny substantially revises the tree of life. *Nature biotechnology*, *36*(10), 996-1004.

Parks, D. H., Chuvochina, M., Rinke, C., Mussig, A. J., Chaumeil, P. A., & Hugenholtz, P. (2022). GTDB: an ongoing census of bacterial and archaeal diversity through a phylogenetically consistent, rank normalized and complete genome-based taxonomy. *Nucleic acids research*, *50*(D1), D785-D794.

Paysan-Lafosse, T., Blum, M., Chuguransky, S., Grego, T., Pinto, B. L., Salazar, G. A., ... & Bateman, A. (2023). InterPro in 2022. *Nucleic Acids Research*, *51*(D1), D418-D427.

Pedersen, R. B., Thorseth, I. H., Nygård, T. E., Lilley, M. D., & Kelley, D. S. (2010a). Hydrothermal activity at the Arctic mid-ocean ridges. *Washington DC American Geophysical Union Geophysical Monograph Series*, *188*, 67-89.

Pedersen, R. B., Rapp, H. T., Thorseth, I. H., Lilley, M. D., Barriga, F. J., Baumberger, T., ... & Jorgensen, S. L. (2010b). Discovery of a black smoker vent field and vent fauna at the Arctic Mid-Ocean Ridge. *Nature communications*, *1*(1), 126.

Pernthaler, A., Dekas, A. E., Brown, C. T., Goffredi, S. K., Embaye, T., & Orphan, V. J. (2008). Diverse syntrophic partnerships from deep-sea methane vents revealed by direct cell capture and metagenomics. *Proceedings of the National Academy of Sciences*, *105*(19), 7052-7057.

Qi, Y. L., Evans, P. N., Li, Y. X., Rao, Y. Z., Qu, Y. N., Tan, S., ... & Li, W. J. (2021). Comparative genomics reveals thermal adaptation and a high metabolic diversity in "Candidatus Bathyarchaeia". *Msystems*, *6*(4), e00252-21.

Qin, J., Li, R., Raes, J., Arumugam, M., Burgdorf, K. S., Manichanh, C., ... & Wang, J. (2010). A human gut microbial gene catalogue established by metagenomic sequencing. *nature*, *464*(7285), 59-65.

Quast, C., Pruesse, E., Yilmaz, P., Gerken, J., Schweer, T., Yarza, P., ... & Glöckner, F. O. (2012). The SILVA ribosomal RNA gene database project: improved data processing and web-based tools. *Nucleic acids research*, *41*(D1), D590-D596.

Rabus, R., Boll, M., Heider, J., Meckenstock, R. U., Buckel, W., Einsle, O., ... & Wilkes, H. (2016). Anaerobic microbial degradation of hydrocarbons: from enzymatic reactions to the environment. *Microbial Physiology*, *26*(1-3), 5-28.

Raghoebarsing, A. A., Pol, A., Van de Pas-Schoonen, K. T., Smolders, A. J., Ettwig, K. F., Rijpstra, W. I. C., ... & Strous, M. (2006). A microbial consortium couples anaerobic methane oxidation to denitrification. *Nature*, *440*(7086), 918-921.

Redmond, M. C., & Valentine, D. L. (2012). Natural gas and temperature structured a microbial community response to the Deepwater Horizon oil spill. *Proceedings of the National Academy of Sciences*, *109*(50), 20292-20297.

Reeburgh, W. S. (1976). Methane consumption in Cariaco Trench waters and sediments. *Earth and Planetary Science Letters*, *28*(3), 337-344.

Reeburgh, W. S. (2007a). Global methane biogeochemistry. *Treatise on geochemistry*, *4*, 347.

Reeburgh, W. S. (2007b). Oceanic methane biogeochemistry. *Chemical reviews*, *107*(2), 486-513.

Richter, M., & Rosselló-Móra, R. (2009). Shifting the genomic gold standard for the prokaryotic species definition. *Proceedings of the National Academy of Sciences*, *106*(45), 19126-19131.

Rinke, C., Schwientek, P., Sczyrba, A., Ivanova, N. N., Anderson, I. J., Cheng, J. F., ... & Woyke, T. (2013). Insights into the phylogeny and coding potential of microbial dark matter. *Nature*, *499*(7459), 431-437.

Rinke, C., Chuvochina, M., Mussig, A. J., Chaumeil, P. A., Davín, A. A., Waite, D. W., ... & Hugenholtz, P. (2021). A standardized archaeal taxonomy for the Genome Taxonomy Database. *Nature Microbiology*, *6*(7), 946-959.

Roberts, H. H., & Aharon, P. (1994). Hydrocarbon-derived carbonate buildups of the northern Gulf of Mexico continental slope: a review of submersible investigations. *Geo-Marine Letters*, *14*, 135-148.

Roberts, H. H. (2001). Fluid and gas expulsion on the northern Gulf of Mexico continental slope: Mud-prone to mineral-prone responses. *Washington DC American Geophysical Union Geophysical Monograph Series*, *124*, 145-161.

Rodriguez-R, L. M., & Konstantinidis, K. T. (2014). Bypassing cultivation to identify bacterial species. *Microbe*, *9*(3), 111-118.

Rosentreter, J. A., Borges, A. V., Deemer, B. R., Holgerson, M. A., Liu, S., Song, C., ... & Eyre, B. D. (2021). Half of global methane emissions come from highly variable aquatic ecosystem sources. *Nature Geoscience*, *14*(4), 225-230.

Ruff, S. E., Arnds, J., Knittel, K., Amann, R., Wegener, G., Ramette, A., & Boetius, A. (2013). Microbial communities of deep-sea methane seeps at Hikurangi continental margin (New Zealand). *PLoS One*, *8*(9), e72627.

Ruff, S. E., Kuhfuss, H., Wegener, G., Lott, C., Ramette, A., Wiedling, J., ... & Weber, M. (2016). Methane seep in shallow-water permeable sediment harbors high diversity of anaerobic methanotrophic communities, Elba, Italy. *Frontiers in Microbiology*, *7*, 374.

Saunois, M., Stavert, A. R., Poulter, B., Bousquet, P., Canadell, J. G., Jackson, R. B., ... & Zhuang, Q. (2020). The global methane budget 2000–2017. *Earth system science data*, *12*(3), 1561-1623.

Scheller, S., Yu, H., Chadwick, G. L., McGlynn, S. E., & Orphan, V. J. (2016). Artificial electron acceptors decouple archaeal methane oxidation from sulfate reduction. *Science*, *351*(6274), 703-707.

Schmidt, T. M., DeLong, E. F., & Pace, N. R. (1991). Analysis of a marine picoplankton community by 16S rRNA gene cloning and sequencing. *Journal of bacteriology*, *173*(14), 4371-4378.

Schrenk, M. O., Brazelton, W. J., & Lang, S. Q. (2013). Serpentinization, carbon, and deep life. *Reviews in Mineralogy and Geochemistry*, *75*(1), 575-606.

Seemann, T. (2014). Prokka: rapid prokaryotic genome annotation. *Bioinformatics*, *30*(14), 2068-2069.

Seitz, K. W., Dombrowski, N., Eme, L., Spang, A., Lombard, J., Sieber, J. R., ... & Baker, B. J. (2019). Asgard archaea capable of anaerobic hydrocarbon cycling. *Nature communications*, *10*(1), 1822.

Sephton, M. A., & Hazen, R. M. (2013). On the origins of deep hydrocarbons. *Reviews in Mineralogy and Geochemistry*, *75*(1), 449-465.

Shaiber, A., Willis, A. D., Delmont, T. O., Roux, S., Chen, L. X., Schmid, A. C., ... & Eren, A. M. (2020). Functional and genetic markers of niche partitioning among enigmatic members of the human oral microbiome. *Genome biology*, *21*(1), 1-35.

Shi, L. D., Guo, T., Lv, P. L., Niu, Z. F., Zhou, Y. J., Tang, X. J., ... & Zhao, H. P. (2020). Coupled anaerobic methane oxidation and reductive arsenic mobilization in wetland soils. *Nature Geoscience*, *13*(12), 799-805.

Sieber, C. M., Probst, A. J., Sharrar, A., Thomas, B. C., Hess, M., Tringe, S. G., & Banfield, J. F. (2018). Recovery of genomes from metagenomes via a dereplication, aggregation and scoring strategy. *Nature microbiology*, *3*(7), 836-843.

Sierra-Garcia, I. N., Dellagnezze, B. M., Santos, V. P., Chaves B, M. R., Capilla, R., Santos Neto, E. V., ... & Oliveira, V. M. (2017). Microbial diversity in degraded and non-degraded petroleum samples and comparison across oil reservoirs at local and global scales. *Extremophiles*, *21*, 211-229.

Simoneit, B. R., Mazurek, M. A., Brenner, S., Crisp, P. T., & Kaplan, I. R. (1979). Organic geochemistry of recent sediments from Guaymas Basin, Gulf of California. *Deep Sea Research Part A. Oceanographic Research Papers*, *26*(8), 879-891.

Simoneit, B. R., Kawka, O. E., & Brault, M. (1988). Origin of gases and condensates in the Guaymas Basin hydrothermal system (Gulf of California). *Chemical Geology*, *71*(1-3), 169-182.

Slatko, B. E., Gardner, A. F., & Ausubel, F. M. (2018). Overview of next-generation sequencing technologies. *Current protocols in molecular biology*, *122*(1), e59.

Sorokin, D. Y., Makarova, K. S., Abbas, B., Ferrer, M., Golyshin, P. N., Galinski, E. A., ... & Koonin, E. V. (2017). Discovery of extremely halophilic, methyl-reducing euryarchaea provides insights into the evolutionary origin of methanogenesis. *Nature microbiology*, *2*(8), 1-11.

Stahl, D. A., Lane, D. J., Olsen, G. J., & Pace, N. R. (1985). Characterization of a Yellowstone hot spring microbial community by 5S rRNA sequences. *Applied and environmental microbiology*, *49*(6), 1379-1384.

Staley, J. T., & Konopka, A. (1985). Measurement of in situ activities of nonphotosynthetic microorganisms in aquatic and terrestrial habitats. *Annual review of microbiology*, *39*(1), 321-346.

Steen, I. H., Dahle, H., Stokke, R., Roalkvam, I., Daae, F. L., Rapp, H. T., ... & Thorseth, I. H. (2016). Novel barite chimneys at the Loki's castle vent field shed light on key factors shaping microbial communities and functions in hydrothermal systems. *Frontiers in microbiology*, *6*, 1510.

Stephen, J. R., McCaig, A. E., Smith, Z., Prosser, J. I., & Embley, T. M. (1996). Molecular diversity of soil and marine 16S rRNA gene sequences related to beta-subgroup ammonia-oxidizing bacteria. *Applied and Environmental Microbiology*, *62*(11), 4147-4154.

Stephenson, M., & Stickland, L. H. (1933). Hydrogenase: the bacterial formation of methane by the reduction of one-carbon compounds by molecular hydrogen. *Biochemical Journal*, *27*(5), 1517.

Stokke, R., Roalkvam, I., Lanzen, A., Haflidason, H., & Steen, I. H. (2012). Integrated metagenomic and metaproteomic analyses of an ANME-1-dominated community in marine cold seep sediments. *Environmental microbiology*, *14*(5), 1333-1346.

Stokke, R., Reeves, E. P., Dahle, H., Fedøy, A. E., Viflot, T., Lie Onstad, S., ... & Steen, I. H. (2020). Tailoring hydrothermal vent biodiversity toward improved biodiscovery using a novel in situ enrichment strategy. *Frontiers in Microbiology*, 249.

Suda, K., Aze, T., Miyairi, Y., Yokoyama, Y., Matsui, Y., Ueda, H., ... & Ono, S. (2022). The origin of methane in serpentinite-hosted hyperalkaline hot spring at Hakuba Happo, Japan: Radiocarbon, methane isotopologue and noble gas isotope approaches. *Earth and Planetary Science Letters*, *585*, 117510.

Suess, E. (2020). Marine cold seeps: background and recent advances. *Hydrocarbons, oils and lipids: Diversity, origin, chemistry and fate*, 747-767.

Sunagawa, S., Coelho, L. P., Chaffron, S., Kultima, J. R., Labadie, K., Salazar, G., ... & Velayoudon, D. (2015). Structure and function of the global ocean microbiome. *Science*, *348*(6237), 1261359.

Søndergaard, D., Pedersen, C. N., & Greening, C. (2016). HydDB: a web tool for hydrogenase classification and analysis. *Scientific reports*, *6*(1), 1-8.

Talavera, G., & Castresana, J. (2007). Improvement of phylogenies after removing divergent and ambiguously aligned blocks from protein sequence alignments. *Systematic biology*, *56*(4), 564-577.

Thauer, R. K. (1998). Biochemistry of methanogenesis: a tribute to Marjory Stephenson: 1998 Marjory Stephenson prize lecture. *Microbiology*, *144*(9), 2377-2406.

Thauer, R. K., Kaster, A. K., Seedorf, H., Buckel, W., & Hedderich, R. (2008). Methanogenic archaea: ecologically relevant differences in energy conservation. *Nature Reviews Microbiology*, *6*(8), 579-591.

Timmers, P. H., Gieteling, J., Widjaja-Greefkes, H. A., Plugge, C. M., Stams, A. J., Lens, P. N., & Meulepas, R. J. (2015). Growth of anaerobic methane-oxidizing archaea and sulfate-reducing bacteria in a high-pressure membrane capsule bioreactor. *Applied and environmental microbiology*, *81*(4), 1286-1296.

Timmers, P. H., Welte, C. U., Koehorst, J. J., Plugge, C. M., Jetten, M. S., & Stams, A. J. (2017). Reverse methanogenesis and respiration in methanotrophic archaea. *Archaea*, *2017*.

Torsvik, V., Goksøyr, J., & Daae, F. L. (1990). High diversity in DNA of soil bacteria. *Applied and environmental microbiology*, *56*(3), 782-787.

Tsai, Y. L., & Olson, B. H. (1992). Detection of low numbers of bacterial cells in soils and sediments by polymerase chain reaction. *Applied and environmental microbiology*, *58*(2), 754-757.

Tyson, G. W., Chapman, J., Hugenholtz, P., Allen, E. E., Ram, R. J., Richardson, P. M., ... & Banfield, J. F. (2004). Community structure and metabolism through reconstruction of microbial genomes from the environment. *Nature*, *428*(6978), 37-43.

The UniProt Consortium. (2023). UniProt: the Universal Protein Knowledgebase in 2023. *Nucleic Acids Research*, *51*(D1), D523–D531.

Uritskiy, G. V., DiRuggiero, J., & Taylor, J. (2018). MetaWRAP—a flexible pipeline for genome-resolved metagenomic data analysis. *Microbiome*, *6*(1), 1-13.

Vanwonterghem, I., Evans, P. N., Parks, D. H., Jensen, P. D., Woodcroft, B. J., Hugenholtz, P., & Tyson, G. W. (2016). Methylotrophic methanogenesis discovered in the archaeal phylum Verstraetearchaeota. *Nature microbiology*, *1*(12), 1-9.

Viflot, T.Ø. (2019) Evidence for extensive conductive cooling and microbial carbon transformations in diffuse hydrothermal fluids from the Loki´ s Castle Vent Field.

Wallace, R. J., Rooke, J. A., McKain, N., Duthie, C. A., Hyslop, J. J., Ross, D. W., ... & Roehe, R. (2015). The rumen microbial metagenome associated with high methane production in cattle. *BMC genomics*, *16*(1), 1-14.

Wang, F. P., Zhang, Y., Chen, Y., He, Y., Qi, J., Hinrichs, K. U., ... & Boon, N. (2014). Methanotrophic archaea possessing diverging methane-oxidizing and electron-transporting pathways. *The ISME journal*, *8*(5), 1069-1078.

Wang, Y., Feng, X., Natarajan, V. P., Xiao, X., & Wang, F. (2019). Diverse anaerobic methane-and multi-carbon alkane-metabolizing archaea coexist and show activity in Guaymas Basin hydrothermal sediment. *Environmental microbiology*, *21*(4), 1344-1355.

Wang, Y., Wegener, G., Williams, T. A., Xie, R., Hou, J., Tian, C., ... & Xiao, X. (2021). A methylotrophic origin of methanogenesis and early divergence of anaerobic multicarbon alkane metabolism. *Science advances*, *7*(27), eabj1453.

Wang, Y., Xie, R., Hou, J., Lv, Z., Li, L., Hu, Y., ... & Wang, F. (2022). The late Archaean to early Proterozoic origin and evolution of anaerobic methane-oxidizing archaea. *mLife*, *1*(1), 96-100.

Weber, H. S., Habicht, K. S., & Thamdrup, B. (2017). Anaerobic methanotrophic archaea of the ANME-2d cluster are active in a low-sulfate, iron-rich freshwater sediment. *Frontiers in Microbiology*, *8*, 619.

Wegener, G., Shovitri, M., Knittel, K., Niemann, H., Hovland, M., & Boetius, A. (2008). Biogeochemical processes and microbial diversity of the Gullfaks and Tommeliten methane seeps (Northern North Sea). *Biogeosciences*, *5*(4), 1127-1144.

Wegener, G., Krukenberg, V., Riedel, D., Tegetmeyer, H. E., & Boetius, A. (2015). Intercellular wiring enables electron transfer between methanotrophic archaea and bacteria. *Nature*, *526*(7574), 587-590.

Wegener, G., Krukenberg, V., Ruff, S. E., Kellermann, M. Y., & Knittel, K. (2016). Metabolic capabilities of microorganisms involved in and associated with the anaerobic oxidation of methane. *Frontiers in microbiology*, *7*, 46.

Wegener, G., Laso-Pérez, R., Orphan, V. J., & Boetius, A. (2022). Anaerobic degradation of alkanes by marine archaea. *Annual Review of Microbiology*, *76*, 553-577.

Welhan, J. A., & Lupton, J. E. (1987). Light hydrocarbon gases in Guaymas Basin hydrothermal fluids: thermogenic versus abiogenic origin. *AAPG bulletin*, *71*(2), 215-223.

Welte, C. U., de Graaf, R., Dalcin Martins, P., Jansen, R. S., Jetten, M. S., & Kurth, J. M. (2017). A novel methoxydotrophic metabolism discovered in the hyperthermophilic archaeon Archaeoglobus fulgidus. *Environmental Microbiology*, *23*(7), 4017-4033.

Williams, T. A., Szöllősi, G. J., Spang, A., Foster, P. G., Heaps, S. E., Boussau, B., ... & Embley, T. M. (2017). Integrative modeling of gene and genome evolution roots the archaeal tree of life. *Proceedings of the National Academy of Sciences*, *114*(23), E4602-E4611.

Winogradsky, S. (1887). Über schwefelbakterien. *Bot. Ztg*, *45*(31-37), 488-610.

Winogradsky, S. (1890). Recherches sur les organisms de la nitrification. *Ann. Inst. Pasteur*, *4*, 213-231.

Woese, C. R., & Fox, G. E. (1977). Phylogenetic structure of the prokaryotic domain: the primary kingdoms. *Proceedings of the National Academy of Sciences*, *74*(11), 5088-5090.

Woese, C. R., Magrum, L. J., & Fox, G. E. (1978). Archaebacteria. *Journal of Molecular Evolution*, *11*, 245-252.

Woese, C. R., Kandler, O., & Wheelis, M. L. (1990). Towards a natural system of organisms: proposal for the domains Archaea, Bacteria, and Eucarya. *Proceedings of the National Academy of Sciences*, *87*(12), 4576-4579.

Woodcroft, B. J., Singleton, C. M., Boyd, J. A., Evans, P. N., Emerson, J. B., Zayed, A. A., ... & Tyson, G. W. (2018). Genome-centric view of carbon processing in thawing permafrost. *Nature*, *560*(7716), 49-54.

Yu, H., Skennerton, C. T., Chadwick, G. L., Leu, A. O., Aoki, M., Tyson, G. W., & Orphan, V. J. (2022). Sulfate differentially stimulates but is not respired by diverse anaerobic methanotrophic archaea. *The ISME Journal*, *16*(1), 168-177.

Zehnle, H., Laso-Pérez, R., Lipp, J., Teske, A., & Wegener, G. (2022). Candidatus Alkanophaga archaea from heated hydrothermal vent sediment oxidize petroleum alkanes.

Zhang, X., Xia, J., Pu, J., Cai, C., Tyson, G. W., Yuan, Z., & Hu, S. (2019). Biochar-mediated anaerobic oxidation of methane. *Environmental science & technology*, *53*(12), 6660-6668.

Zhang, X., Rabiee, H., Frank, J., Cai, C., Stark, T., Virdis, B., ... & Hu, S. (2020). Enhancing methane oxidation in a bioelectrochemical membrane reactor using a soluble electron mediator. *Biotechnology for biofuels*, *13*, 1-12.

Zhou, Z., Pan, J., Wang, F., Gu, J. D., & Li, M. (2018). Bathyarchaeota: globally distributed metabolic generalists in anoxic environments. *FEMS microbiology reviews*, *42*(5), 639-655.

Zhou, Z., Zhang, C. J., Liu, P. F., Fu, L., Laso-Pérez, R., Yang, L., ... & Cheng, L. (2022). Non-syntrophic methanogenic hydrocarbon degradation by an archaeal species. *Nature*, *601*(7892), 257-262.

Publications

Paper I

FEMS Microbiology Ecology, 2022, 98, 1–11
DOI: 10.1093/femsec/fiac117
Advance access publication date: 3 October 2022
Research Article

Phylogenetic and functional diverse ANME-1 thrive in Arctic hydrothermal vents

F. Vulcano[1,*], C. J. Hahn[4], D. Roerdink[2], H. Dahle[3], E. P. Reeves[2], G. Wegener[4,5,6], I. H. Steen[1], R. Stokke[1,*]

[1]Department of Biological Sciences, Center for Deep Sea Research, University of Bergen, Bergen, Norway
[2]Department of Earth Science, Center for Deep Sea Research, University of Bergen, Bergen, Norway
[3]Computational Biological Unit, Department of Informatics, Department of Biological Sciences, Center for Deep Sea Research, University of Bergen, Bergen, Norway
[4]Max-Plank Institute for Marine Microbiology, HGF MPG Joint Research Group for Deep-Sea Ecology and Technology, Bremen, 28359, Germany
[5]MARUM, Center for Marine Environmental Sciences, University Bremen, Bremen, 28359, Germany
[6]Alfred Wegener Institute Helmholtz Center for Polar and Marine Research, Bremerhaven, 27570, Germany
*Corresponding author: Thormølens gate 53 A 5006 Bergen Postboks 7803 5020 Bergen. E-mail: Francesca.Vulcano@uib.no; E-mail: Runar.Stokke@uib.no
Editor: Lee Kerkhof

Abstract

The methane-rich areas, the Loki's Castle vent field and the Jan Mayen vent field at the Arctic Mid Ocean Ridge (AMOR), host abundant niches for anaerobic methane-oxidizers, which are predominantly filled by members of the ANME-1. In this study, we used a metagenomic-based approach that revealed the presence of phylogenetic and functional different ANME-1 subgroups at AMOR, with heterogeneous distribution. Based on a common analysis of ANME-1 genomes from AMOR and other geographic locations, we observed that AMOR subgroups clustered with a vent-specific ANME-1 group that occurs solely at vents, and with a generalist ANME-1 group, with a mixed environmental origin. Generalist ANME-1 are enriched in genes coding for stress response and defense strategies, suggesting functional diversity among AMOR subgroups. ANME-1 encode a conserved energy metabolism, indicating strong adaptation to sulfate-methane-rich sediments in marine systems, which does not however prevent global dispersion. A deep branching family named *Ca*. Veteromethanophagaceae was identified. The basal position of vent-related ANME-1 in phylogenomic trees suggests that ANME-1 originated at hydrothermal vents. The heterogeneous and variable physicochemical conditions present in diffuse venting areas of hydrothermal fields could have favored the diversification of ANME-1 into lineages that can tolerate geochemical and environmental variations.

Keywords: ANME-1, comparative genomics: thermophily, hydrothermal vents, phylogenomics

Introduction

Three major groups of anaerobic methanotrophic archaea (ANME); ANME-1, ANME-2, and ANME-3 (Boetius et al. 2000, Knittel and Boetius 2009) mediate the anaerobic oxidation of methane (AOM). They reverse the methanogenesis pathway for methane oxidation (Hallam et al. 2004). Marine ANME archaea do not code for own respiratory pathways. Instead, they transfer the electrons liberated during AOM to sulfate-reducing bacteria (SRB) (McGlynn et al. 2015, Wegener et al. 2015). ANME appear globally in sulfate methane transition zone (SMTZ) of anoxic sediments and perform AOM in a wide range of physicochemical conditions (Hinrichs et al. 1999, Orphan et al. 2001, Knittel et al. 2005, Lloyd et al. 2006, Lösekann et al. 2007, Knittel and Boetius 2009, Roalkvam et al. 2011, Maignien et al. 2013, Ruff et al. 2013, Vigneron et al. 2013, Dowell et al. 2016, Ruff et al. 2016, Dombrowski et al. 2018). Among ANMEs, ANME-1 seem to be most widely distributed in thermal environments, colonizing both marine hydrothermal vents and terrestrial hot springs (Teske et al. 2002, Holler et al. 2011, Biddle et al. 2012, McKay et al. 2012, Borrel et al. 2019).

In AOM cultures from the Guaymas Basin hydrothermal sediments ANME-1 form partnership with the deep branching sulfate reducer *Candidatus* Desulfofervidus (Holler et al. 2011, Krukenberg et al. 2016). At low temperature environments like cold-seeps, ANME-1 grow with sulfate reducers of the SEEP-SRB clades (Kleindienst et al. 2012, Krukenberg et al. 2018). The mechanism for the exchange of reducing equivalents between the partner proceeds most likely through direct interspecies electron transfer (DIET) mediated by extracellular cytochromes and nanowires (Wegener et al. 2015, Skennerton et al. 2017, Krukenberg et al. 2018).

The recent-increased availability of genomes of ANME-1 have provided deep insights of their phylogeny, evolution, and metabolic properties. In the Genome Taxonomy Database (GTDB) (Rinke et al. 2021 and https://gtdb.ecogenomic.org/), ANME-1 (*Ca*. Methanophagales) is classified as a distinct order within the phylum *Halobacteriota* and the class *Syntropharchaeia*, separated from the other ANMEs (phylum *Halobacteriota*, class *Methanosarcinia*). Currently, the ANME-1 order includes the two families: ANME-1 and B39_G2. B39_G2 is affiliated to *Ca*. Alkanophagales (Wang et al. 2021, Wang et al. 2022). The ANME-1 family comprises 8 genera and 16 candidate species, whereas B39_G2 is represented by a single uncultured candidate species (Rinke et al. 2021; https://gtdb.ecogenomic.org). Besides ANME-1, the Syntropharchaeia class includes the two cultured species that oxidize the short-chain alkanes butane and propane, *Candidatus* Syntrophoarchaeum butanivorans and *Candidatus* Syntrophoarchaeum caldarius (Laso-Pérez et al. 2016). In addition, MAGs of the linage *Ca*. Alkanophagales, with the ANME-1 GTDB family B39_G2, describe a potential C_nH_{2n+2} oxidizer. These MAGs encode a divergent

Received: February 12, 2022. Revised: September 15, 2022. Accepted: September 29, 2022

Syntropharchaeum-like alkyl–coenzyme M reductase (ACR; Dombrowski et al. 2018) and a complete beta-oxidation pathway (Dong et al. 2020, Wang et al. 2021). In *Syntropharchaeia* multi-carbon metabolism seems to precede methane metabolisms. The latter capability likely appeared after the acquisition of a methane-oxidizing methyl-coenzyme M reductase (MCR) through horizontal gene transfer from the clades *Ca*. Methanofastidiosa/*Ca*. Nuwarchaeia (Borrel et al. 2019, Wang et al. 2021).

Besides few differences in the encoded MCR, all ANME-1 genomes have an identical set of enzymes for methane oxidation, with a conserved bypass of the Methylene-H_4M(S)PT reductase (Mer) enzyme (Meyerdierks et al. 2010, Stokke et al. 2012, Krukenberg et al. 2018, Borrel et al. 2019, Wang et al. 2019). Little variability has also been observed in the redox complexes for energy conservation, with only a few genomes carrying the Na^+-coupled respiratory *Rhodobacter* nitrogen fixation (Rnf) complex, in addition to $F_{420}H_2$ dehydrogenase (Fqo), heterodisulfide reductase (Hdr), F_{420}-non-reducing hydrogenase (Mvh), formate dehydrogenase (Fdh) and DIET-supporting proteins (Borrel et al. 2019). Comparative genome analyses of ANME-1 have overall revealed a limited energy metabolism, highly specialized to catalyze AOM in SMTZs.

Efforts remain to understand how the genetic features of ANME genomes connect to the distribution of ANME in geochemically different niches. A comparative assessment of ANME-1 across their habitable environments would hence be useful to reveal their total genomic heterogeneity and possible genetic signatures for niche-specific microbial functions. In this study, MAGs of ANME-1 from focused and diffuse fluid flow sites at the Loki´s Castle vent field (LCVF) (Pedersen et al. 2010) and the Jan Mayen vent field (JMVF) (Stokke et al. 2020) at the Arctic Mid-Ocean Ridge (AMOR) were reconstructed. We identified ANME-1 lineages and studied their occurrence in various hydrothermal niches. Finally, with focus on vent taxa, we compared the functions encoded in the entire ANME-1 order.

Materials and methods

Environmental samples and DNA extraction

Genomic DNA was extracted from sediment samples collected in 2010, 2017, and 2018, from a white barite chimney section (BaCh2W), the superficial layer below a white microbial mat (BaCh4M), and a dark grey barite chimney base (BaCh3G) in the diffuse venting barite field at the Loki´s Castle vent field (Steen et al. 2016). The barite chimney samples included in this study were altogether named Loki´s Castle barite field chimneys. In 2018, a patch of sediment covered by a thick microbial mat was sampled with a blade corer, resulting in a 20 cm core. Likewise, the wall of a black smoker (Baumberger et al. 2016) was subsampled for DNA extraction. At the Jan Mayen vent field, *in situ* enrichments in the Bruse vent field sediments (Stokke et al. 2020) and F3 flange section of a white smoker from the Soria Moria vent field (Dahle et al. 2015) were sampled for DNA extraction. The samples are listed in Table 1. Total DNA was extracted using FastDNA™ SPIN Kit for Soil (MP Biomedicals, Santa Ana, CA, USA) according to manufacturer instructions and sequenced at the NSC Norwegian Sequencing Center in Oslo, except for the BaCh4M sequenced at StarSEQ in Mainz, Germany.

Geochemical analysis

For geochemical analysis, porewater from the blade corer was collected at 4°C with Rhizons (pore diameter, 0.2 μm). Alkalinity and hydrogen sulfide concentrations were measured onboard immediately after sampling, using a Metrohm 888 Titrando titrator and a Silver/Sulfide ionplus® Sure-Flow® Solid State Combination Ion Selective Electrode (ISE) (Thermo Scientific). Residual porewater was stored in 3% HNO_3 acid-washed HDPE plastic bottles and frozen at −20°C for onshore for measurement of sulfate concentration (ICP-OES) (Eickmann et al. 2014).

At the Loki's Castle barite field, sediment temperatures were measured using the ROV arm equipped with a high-temperature probe hiT (WHOI MISO) (Fornari et al. 1998).

Moreover, at the Loki's Castle barite field the rates of methane oxidation and sulfate reduction were assessed in radiotracer assays with ^{14}C-methane and ^{35}S-Sulfate as described by Wegener et al. 2008. Sediments were supplemented with anoxic medium (Laso-Pérez et al. 2018) and aliquoted in replicates in exetainer vials under anoxic conditions. The headspace was filled with gaseous hydrocarbons-equilibrated sterile medium (methane, ethane, propane, and butane). After addition of the radiotracers, the incubation was stopped after 48 h at room temperature. The radio-labelled reaction products were collected through chromium distillation (for ^{35}S-Sulfide) fraction (Kallmeyer et al. 2004), or using a Phenylethylamine trap (for^{14}C-CO_2) and the associated radioactivity measured for metabolic rates estimation.

Catalyzed reported deposition fluorescence atalyzedhybridization (CARD-FISH)

Onboard, 1 g of material from barite chimneys and surrounding sediments was resuspended in 50 ml of 1×PBS (Phosphate-Buffered Saline) and fixed overnight at 4°C in 2% formaldehyde. Samples were centrifuged 15 min at 1000 × *g* at 4°C with a swing rotor to allow sediments to settle. Aliquots of the resulting supernatant were filtered on isopore polycarbonate filters (0.2 μm pore diameter, Merck Millipore). Filters were washed twice with 1× PBS pH 7.6 and stored at −20°C.

Onshore, *in situ* hybridization of rRNA with horseradish peroxidase (HRP)-labeled oligonucleotide coupled to catalyzed reporter (tyramide) deposition (Pernthaler and Amann 2004, Amann and Fuchs 2008) was performed. Briefly, filters were coated with 0.1% (w/v) low-gelling point agarose. Permeabilization of bacterial and archaeal cell walls was performed by incubation for 60 min at 37°C in lysozyme solution (10 mg/ml lysozyme in 1×PBS pH 7.6, 0.05 M EDTA pH 8.0, 0.1 M Tris-HCl pH 8.0) and incubation for 5 min at room temperature in proteinase K solution (15 μg/ml proteinase K in 10 mM Tris-HCl pH 8.0, 1 mM EDTA pH 8.0), respectively. Endogenous peroxidases were inactivated by incubating the filters in 0.15% H_2O_2 solution in methanol for 30 min at room temperature. Hybridization of rRNA was performed by incubating the filters for 2 h at 46°C in a solution 1:300 of HRP-labelled probes (8 pmol/μl working solution) and hybridization buffer (900 mM NaCl, 20 mM Tris-HCl pH 8.0, 1×blocking reagent (Roche), 10% dextrane sulfate, 0.02% sodium dodecyl sulfate (SDS) and probe-specific formamide %) in humidified hybridization chambers. After 15 min washing at 48°C in preheated washing buffer (5 mM EDTA pH 8.0, 20 mM Tris-HCl pH 8.0, 0.01% SDS and NaCl according to formamide concentration in hybridization buffer), filters were washed again in 1×PBS pH 7.6 for 15 min. Filters were incubated at 46°C for 45 min in humidified chambers in a solution 1000:10:1 of amplification buffer (2 M NaCl, 1× PBS pH 7.6, 0.1× Blocking Reagent (Roche), 10% dextran sulfate), 0.15% H_2O_2 solution (5 μl of 30% H2O2 in 1 ml 1× PBS pH 7.6) and fluorescently-labeled tyramides (Alexa488 or Alexa594), for signal amplification. Washing in 1× PBS pH 7.6 was followed by

Table 1. Overview of samples from the Loki's Castle vent field (LCVF) and the Jan Mayen vent field (JMVF) included in this study.

Sample ID	Location	Type of sample	Description
LCBF* chimney (BaCh2W)	LCVF	Barite chimney	Middle section; white barite; ~ 20 °C**; diffuse flow
LCBF chimney (BaCh4M)	LCVF	Barite chimney	Superficial layer below a white mat; 0–~ 20 °C; diffuse flow
LCBF chimney (BaCh3G)	LCVF	Barite chimney	Chimney base; dark grey; ~ 20 °C ; diffuse flow
LCBF* sediments	LCVF	Hydrothermal sediments	Sediments covered by *Sulfurimonas* mat; 20 cmbsf, dark grey; 10 °C ; diffuse flow
JMVF sediments	JMVF	Hydrothermal sediments	Bruse Vent Field; *in situ* incubators; 0–74 °C***; diffuse flow
LCVF black smoker (wall/bulk)	LCVF	Black smoker	João; two presumably high-temperature samples rich in sulfide minerals (a wall section (wall) and bulk material from the chimney (bulk); temperature unknown; focused flow
JMVF white smoker flange	JMVF	White smoker	Soria Moria; flange; 70–72 °C****; focused flow

*LCBF: Loki's Castle barite field; **(Steen et al. 2016); ***(Stokke et al. 2020); ****(Dahle et al. 2015)

DNA staining by incubation of filters in (DAPI 4',6'- diamino-2-phenylindole) solution (1 μg/ml) for 10 min at room temperature. Finally, filters were mounted on glass slides using Citifluor Mountant Solution: VECTASHIELD® Antifade Mounting Medium (Vector Laboratories). After the first amplification step, filters for double hybridization were treated with an additional step of peroxidase inactivation in 0.15% H_2O_2 methanol solution. Filters were finally analyzed with epifluorescent microscopy using an Axiophot II imaging microscope (Zeiss; Germany). The probes used in this study are listed in Table S1.

Assembly, binning, and annotation

Metagenome assembly for all samples followed the procedure described for the Bruse vent field (Fredriksen et al. 2019). In short, filtering of raw Illumina MiSeq 300 paired-end reads, and assembly, were performed using the CLC genomics workbench (Qiagen, v.10–12) using default parameters (quality 0.05; length, minimum 40, and maximum 1000 nucleotides). In addition, one nucleotide was removed from terminal read ends. Assembly was performed using default parameters with an automatic k-mer size and bubble size. A minimum contig length was set to 1000 bases with scaffolding enabled.

Except for the Loki's Castle barite field sediments sample, MAGs were reconstructed using MetaBat (Kang et al. 2015). MAGs from Loki's Castle barite field sediments were reconstructed using a combination of MetaBat 2.15, MaxBin v.2.2.7 (Wu et al. 2016), concoct 1.1.0 (Alneberg et al. 2014), and DAS Tool (Sieber et al. 2018). For MAGs Chimney19_Bin_00 366 and Chimney19_MAG_00 329, first a co-assembly was done with MEGAHIT (Li et al. 2015), then automatic binning was performed using again concoct and MetaBat. Reference genomes were downloaded from the Assembly database at NCBI (April 2020/May 2021). Contamination and completeness of the individual MAGs and of the reference genomes in the current study were assessed on the presence of lineage-specific, conserved single-copy marker genes using CheckM v1.0.7 (Parks et al. 2015). Functional annotation of MAGs and downloaded genomes were performed within the anvi'o (v6.2 and v.7) pipeline (Eren et al. 2021). The predicted coding sequences (Prodigal v2.6.3, February 2016) (Hyatt et al. 2010) were annotated against the following HMM profiles using scripts within anvi'o: Archaea_76 (Lee 2019), Ribosomal_RNAs (Seemann T, https://github.com/tseemann/barrnap), the Pfam database v 32.0 (2018–08), the COG database (Galperin *et al.* 2015) using DIAMOND as search algorithm (v 0.9.14) (Buchfink et al. 2014), and search against the KOfam HMM database (Aramaki et al. 2020). In addition, for each contig database, amino acid sequences were exported, annotated with GhostKoala (default parameters) (Kanehisa et al. 2016), and imported back into anvi'o (Graham, https://merenlab.org/2018/01/17/importing-ghostkoala-annotations/).

Estimates of relative abundances of ANME archaea

Phylogenetic composition and abundance for each metagenome were first assessed by the assembly of SSU sequences with phyloFlash (Gruber-Vodicka et al. 2020, https://github.com/HRGV/phyloFlash). Furthermore, filtered reads were mapped against all contigs using BBMap v.Feb.2020 (Bushnell B.—sourceforge.net/projects/bbmap/) with default parameters. The relative abundance of each MAG was calculated using the -coverage and -profile commands in CheckM v1.0.7 (Parks et al. 2015) using the BBMap mapping file.

Taxonomic classification, phylogenetic and phylogenomic analysis

Classification of MAGs was performed using the GTDB toolkit (GTDB-Tk) (Chaumeil et al. 2020) and the GTDB version R06-RS202 (Parks et al. 2018, Parks et al. 2021).

Amino acid sequences from 35 selected single-copy marker genes (Table S2), identified from the HMM profile Archaea_76 (Lee 2019) in anvi'o, were extracted from the ANME-1 AMOR MAGs and 384 reference genomes publicly available at NCBI (reference genomes were selected based on Borrel et al. 2019, Hahn et al. 2020, Schwank et al. 2019). The extracted single-copy marker genes were aligned using MAFFT L-INS-i v7.397 (2018/Apr/16) (Katoh 2002), trimmed with TrimAL (TrimAL v 1.4. rev15, -gappyout) and concatenated with catfasta2phyml (https://github.com/nylander/catfasta2phyml/blob/master/catfasta2phyml.pl). A maximum-likelihood tree of the concatenated sequences was calculated with IQ-TREE multicore version 1.6.7 with LG+F+R10 model and 1000 bootstraps. The ANI of AMOR ANME-1 genomes and references was calculated using anvi'o integrated PyANI v.0. 2. 7 (Pritchard et al. 2016).

For phylogeny based on the subunit A of methyl-coenzyme M reductase (McrA), all MAGs were screened for the McrA protein sequences against the HMM profile for KEGG orthology ID K00399 available at https://data.ace.uq.edu.au/public/graftm/7/(7.27.methyl_coenzyme_reductase_alpha_subunit.mcrA.gpkg.tar.gz (09-Aug-2017)) (Boyd et al. 2018), as exemplified in anvi'o pipeline by Lee (https://merenlab.org/2016/05/21/archaeal-single-copy-genes/). Identified McrA sequences were extracted from the contig databases (https://merenlab.org/2016/05/21/archaeal-single-copy-genes/) and aligned with MAFFT v7.397 (2018/Apr/16) (Katoh *et al.*, 2002) using the G-INS-i iterative refinement method, and gaps removed using TrimAL v 1.4. rev15 with the gappyout option (Capella-Gutiérrez *et al.* 2009). Finally, the phylogenetic tree was calculated with IQ-TREE v 1.6.12 (Nguyen et al. 2015) model LG+F+R6 and 1000 bootstraps. An identical procedure was followed for phylogenetic analysis of the16S rRNA gene. When available, 16S rRNA sequences were extracted from the MAGs using anvi'o (v6) (–hmm-source Ribosomal_RNAs –gene Archaeal_16S_rRNA). A list of sequences used in the 16S rRNA phylogeny and MAGs which 16S rRNA genes were extracted is given in Table S3A and B. Reference sequences were selected based on Teske et al. 2002, Knittel et al. 2005, Lösekann et al. 2007, Biddle et al. 2012).

A complex pangenome, representing 38 genomes with >70% completeness and <10% contamination, was reconstructed using the anvi'o workflow for microbial pangenomics (https://merenlab.org/2016/11/08/pangenomics-v2/#displaying-the-pan-genome). Singletons were removed with the option '—min-occurrence 2' to simplify the pangenome visualization. Organization of the pangenome of the assembled genomes was based on presence-absence of groups of genes with homologous amino acid sequence (gene clusters) (Shaiber et al. 2020). From this, a dendrogram was re-constructed representing the hierarchical clustering based on gene cluster frequency (Delmont and Eren 2018). Functional enrichment analysis was performed using anvi'o v6 program anvi-compute-functional-enrichment. Functions were considered enriched for q-values < 0.05 based on Shaiber *et al.* 2020.

Results

Distribution and morphology of ANME-1 under different environmental settings

To resolve the genomic diversity of ANME-1 in hydrothermal vents, we performed a metagenome-based study focusing on two methane-enriched hydrothermal vents systems, the Jan Mayen vent field and the Loki's Castle vent field located on the Arctic Mid-Ocean Ridge. The analyzed samples cover a wide diversity of hydrothermal settings, including various niches in the Loki's Castle barite field. This is a low-temperature diffuse flow area, situated approximately 50 meters apart from the Loki's Castle black smoker, characterized by venting of hydrothermal fluids through sediments and barite chimneys (Steen et al. 2016) (Table 1). When 16S rRNA gene sequences were retrieved from the metagenomic dataset, ANME were detected in all samples. They remained either taxonomically unassigned or assigned to ANME-1a. Estimated relative abundances of ANME-1 varied considerably between the samples (Fig. S1A) and reflected differences in fluid flow rates and in end-member fluid concentration of methane between and within the two vent fields (Baumberger et al. 2016, Steen et al. 2016, Dahle et al. 2018, Stokke et al. 2020). In the Jan Mayen vent field, where an endmember fluid concentration of 5.4 mmol kg^{-1} of methane was measured (Dahle et al. 2018, Stokke et al. 2020), ANME-1 reach a relative abundance between 5 and 14% in diffuse venting sediments. In the flange of a white smoker the relative abundance of ANME-1 16S rRNA gene was approximately 10% (Fig. S1A).

The highest relative abundance of ANME-1 was observed in the high-temperature venting black smoker in the Loki´s Castle vent field consistent with higher endmember fluid concentration of methane of 12-13 mmol kg^{-1} methane (Baumberger et al. 2016). End-member fluids are highly diluted in the diffuse-flow barite field in the Loki´s Castle. Nevertheless, the sediments hosted an abundant population of ANME-1, indicating high flowrates of methane. Consistently, a steep temperature gradient and a shallow SMTZ were observed (2–4 cmbsf) (Fig. S1B). Moreover, methane oxidation rates of 110 nmol d^{-1} $g_{(wetweight;\ ww)}{}^{-1}$ and a methane dependent sulfate-reduction rate (SRR) of 30 nmol d^{-1} $g_{ww}{}^{-1}$ respectively, were measured (Fig. S1C). The lowest relative abundance of ANME-1 was observed in the barite chimneys at Loki's Castle barite field (Fig. S1A).

We visualized ANME-1 and their partners from different locations using CARD-FISH. In sediments, rod-shaped ANME-1 and Deltaproteobacteria form well-mixed large aggregates with diameters between 40 and 80 μm of (Fig. 1A). In the barite chimneys, the few ANME-1 appeared in short chains of 2 to 10 cells (Fig. 1B). ANME-1 rods and Deltaproteobacteria were loose within a matrix of mineral particles. Occasionally, ANME-1 cells formed filaments with a length of up to 100 μm in the external layers of the barite chimneys (Fig. 1C). This morphology resembled the chain-forming aggregates described in 50 °C enrichments of ANME-1-Guaymas/SRB (Holler et al. 2011). Notably, *Ca*. Desulfofervidus was observed in the barite field sediments at 10°C (Fig. S1A).

Taxonomy and distribution of ANME-1 archaea

In total we reconstructed 19 ANME-1 related MAGs (Table S4B). Three from the barite field sediments, seven from barite chimneys and two from the black smoker were found at Loki´s Castle vent field. From the Jan Mayen vent field, five MAGs from sediments and two from the flange were obtained (for details see Table 1). The MAGs were on average 83% complete and showed low contamination values (<2.6%, 0.65% on average) (Table S4C). Our phylogenomic analysis identified three families in the ANME-1 order (Fig. 2A). These were of the classical ANME-1 which included the clusters ANME-1a and ANME-1b (Knittel et al. 2005) (Fig. S2) and *Ca*. Alkanophagaceae (Wang et al. 2021). The third represented a novel deep branching family, that we named *Ca*. Veteromethanophagaceae. The name stands for 'old methane consumer': *vetero-*, old (Latin); *methano-*, pertaining to methane (new Latin); *phagaceae*, eating (Greek). The topology of the phylogenomic tree was overall consistent with the 16S rRNA and McrA gene phylogenies (Fig. S2 and Fig. S3).

Out of the eight identified ANME-1 genera, our reconstructed MAGs in the ANME-1 family affiliated either with the genus QEXZ01 (7) or with the genus G60ANME1 (11) (Fig. 2A and Table S4C). Among them, six species-level subgroups were defined based on pairwise average nucleotide identity (ANI) (Fig. S4 and Table S5). They were named AMOR ANME-1 (AA) subgroups (AA_1 to AA_6) where subgroups AA_1 and AA_2 were of genus QEXZ01 and subgroups AA_3 to AA_6 of genus G60ANME1(Fig. 2A and Table S5). Subgroups AVet_7 and AAlk_8 were identified within *Ca*. Veteromethanophagaceae and *Ca*. Alkanophagaceae, respectively (Fig. 2A and Table S5).

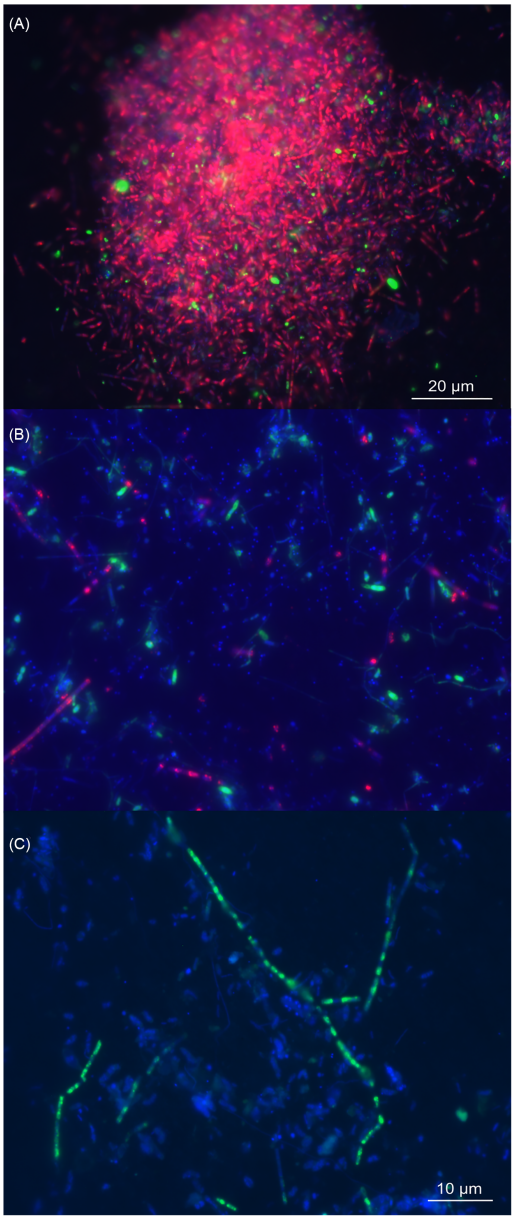

Figure 1. Micrographs of ANME-1 and partner bacteria of the Loki's Castle barite field. **(A)** Aggregates of ANME-1 (ANME-1–350 probe) and Deltaproteobacteria (Delta495 probes) in Loki's Castle barite field sediments and **(B)** barite chimneys. ANME-1 and Deltaproteobacteria are in red and green, respectively. **(C)** Filaments of ANME-1 in the upper section of a barite chimney, stained in green. Scale bars are reported for A and B-C.

ANME-1 genera showed differences in their geographic origin and distribution. Based on our analysis, the genus G60ANME1 clustered with genomes exclusively from marine hydrothermal vents. The genus G60ANME1 was originally named after a MAG assembled from a 60 °C AOM culture from the Guaymas Basin vent system (Krukenberg et al. 2018). The genus QEXZ01, from hydrothermal vents located at AMOR, also grouped with genomes from the Guaymas Basin vent system, the cold seeps in the Gulf of Mexico and from marine sediments of Aarhus Bay. Genomes, exclusively of hydrothermal origin (Guaymas Basin) were observed in genus ANME-1a. The genera WJOV01 and QENJ01 included only genomes from marine cold seeps. QENH01, JACGMN01 and ANME-1-THS included genomes with a mixed provenance. Notably, the genera ANME-1-THS and JACGMN01 contained genomes from terrestrial hot springs, marine cold seeps, and alkaline vent fluids. Altogether, most ANME-1 genera seemed to have a wide geographic distribution, which argues for their large adaptability to diverse environmental conditions. Some genera seemed, however, restricted to a specific type of environment or geographic location.

On a local scale, at the Arctic Mid Ocean Ridge, the AMOR subgroups showed heterogeneity in their abundance and distribution within and between the hydrothermal vent fields (Fig. 2B). In the Loki's Castle barite field, we found five of the six ANME-1 subgroups (AA_1–AA_5). All five were detected in barite chimneys, although in low relative abundances. The barite field sediments hosted three subgroups (AA_1, AA_3, AA_4) of which AA_1 dominated with up 40% of the total community. The high-temperature black smoker at Loki's Castle hosted only the AA_6 subgroup, but this represented up to 73% of the total microbial community. Notably, the wall and the bulk sample from the of the black smoker chimney hosted the subgroup of the *Ca*. Veteromethanophagaceae, AVet_7. At Jan Mayen vent field, only two of the six ANME-1 subgroups were observed. AA_6 occurred in the temperate sediments at approximately 25% rel. abundance. AA_1 occurred in the flange with a rel. abundance of 14%. Notably, the flange also hosted the subgroup of *Ca*. Alkanophagaceae, AAlk_8, in low abundances (0.24%.).

Comparative genomics of ANME-1

To further explain the observed phylogenetic diversity and the wide adaptability of ANME-1 to diverse environmental conditions, we analyzed their genomic content. Based on functional annotation against the KOfam HMM database, all ANME-1 MAGs from AMOR, including the new family *Ca*. Veteromethanophagaceae encode very similar metabolic pathways. This included genes of the reverse methanogenesis pathway, redox complexes, and the enzymes of the reverse acetyl-CoA pathway (Table S6A and B) (Meyerdierks et al. 2010, Stokke et al. 2012, Krukenberg et al. 2018). They all showed the potential for DIET as they coded for multiple multi-heme cytochromes of the kind that was expressed in consortia-forming ANME-1 cultures (Fig. S5) (Wegener et al. 2015, Krukenberg et al. 2018). Even the amino acid, cofactors and vitamin metabolisms were conserved (Table S7).

The AAlk_8 appeared as a multi-carbon degrader, as it encoded a divergent Syntropharchaeum-like McrA, all genes for beta-oxidation and Mer (Table S6B and Fig. S6), a complete Mvh and lacked cytochromes (Dong et al. 2020; Wang et al. 2021).

To further compare ANME-1 genomes based on their overall genome content, a pangenome analysis was performed (Fig. 3A). The pangenome consisting of 64264 genes was organized into in 6058 gene clusters (Delmont et al. 2018). The core pangenome

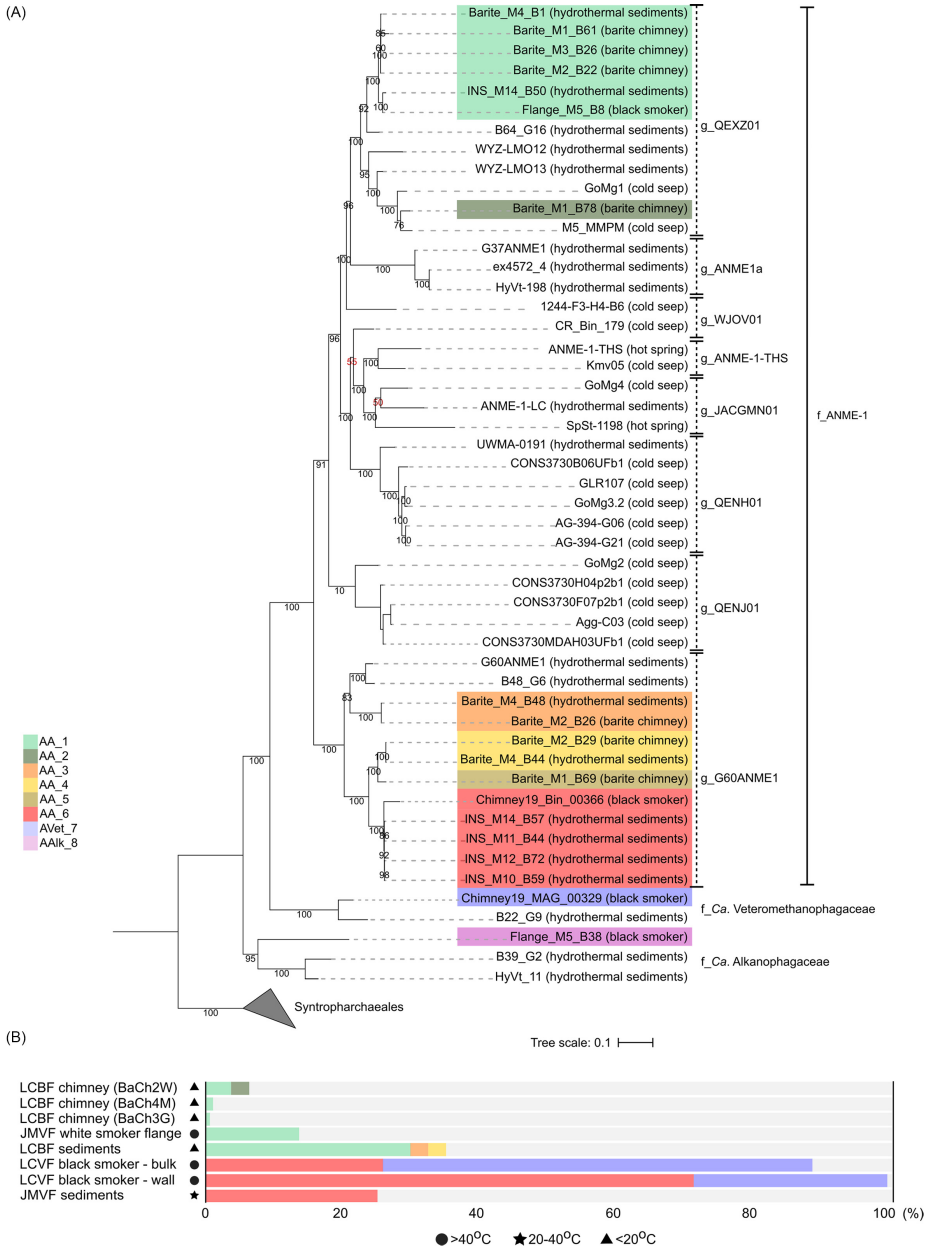

Figure 2. Phylogenomic analysis of ANME-1. **(A)** Phylogenomic tree of the ANME-1 order based on concatenated alignment of 35 marker genes. The ANI-defined AMOR subgroups are highlighted by colors as in the legend. For each genome, the environment of origin is indicated in parenthesis next to the leaf name. The genus- and family- level classification from GTDB-tk is indicated on the right (g_ for genus; f_ for family). Bootstrap values < 60 are in red. **(B)** Relative abundance of the AMOR subgroups in various samples at Loki's Castle vent field and Jan Mayen vent field. The estimated temperature at each site is indicated by symbols. 'LCBF': Loki's Castle barite field, 'JMVF': Jan Mayen vent field, 'LCVF': Loki's Castle vent field.

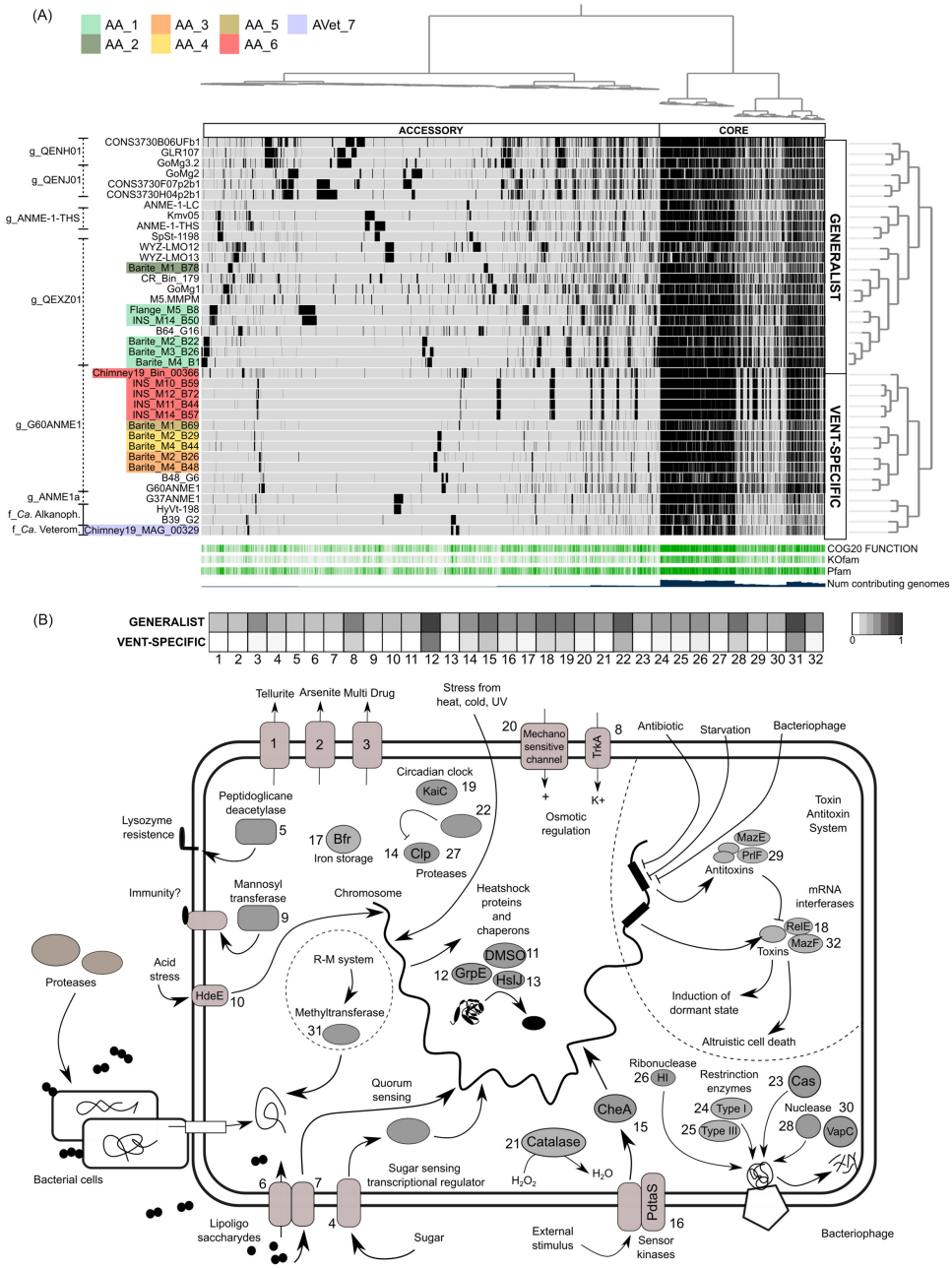

Figure 3. Gene clusters enriched in generalist ANME-1 and their cellular function. **(A)** Pangenome of the ANME-1 order. Hierarchical clustering is expressed by the dendrogram on the left of the phylogram. Genomes are thereafter divided into generalist and vent-specific. The core and the accessory pangenome are indicated. The coverage of COG, KOfam and Pfam annotations and the number of genomes contributing to each gene cluster are given below the phylogram. GTDB-tk classification is on the right. **(B)** Diagram of the cellular function of 32 genes enriched in generalist ANME-1. The occurrence of each gene in generalists and vent-specific genomes is indicated in the heatmap. More details of each cellular function are given in Table S8.

comprised 1604 gene clusters (46147 genes), while the accessory pangenome consisted of 4454 gene clusters (18117 genes).

When the ANME-1 genomes were hierarchically clustered based on their similarity in gene cluster frequency, the resulting dendrogram identified two major functional groups of genomes (Fig. 3A). Based on habitat of origin, they were defined as vent-specific and generalist ANME-1. The vent-specific group consisted of genomes reconstructed only from hydrothermal vents and included genus G60ANME1 (AA_3, AA_4, AA_5 and AA_6), genus ANME1a, and the families *Ca*. Veteromethanophagaceae, as well as the multi-carbon degrading *Ca*. Alkanophagaceae. In contrast, the generalist group consisted of genomes reconstructed from geochemically heterogeneous environments like marine cold seeps, vents, and terrestrial hot springs. It included genera QEXZ01 (AA_1 and AA_2), ANME-1-THS, JACGMN01, QENH01, QENJ01, and WJOV01.

Functional differences between the two groups were analyzed using the functional enrichment analysis of anvi'o (Shaiber et al. 2020). In the generalist group 89 genes were enriched. Of these 53 were assigned to COG categories and included inorganic ion transport and metabolism (P), posttranslational modification, protein turnover, chaperones (O), signal transduction mechanisms (T), replication, recombination, and repair (L), cell wall, membrane, and envelope biogenesis (M) and translation (J) (Table S8). Enriched genes encoded processes involved in the response to chemical gradients, pH, and hydrogen peroxide, osmotic stress regulation and detoxification of arsenic and tellurium (Fig. 3B). Moreover, they coded for transporters of nutrients, zinc, xenobiotics, and phosphate and for iron storage proteins (Fig. 3B). Finally, genes regulating the cellular physiology in response to pathogens and starvation were enriched. These included multiple mRNA interferases of the type I and II Toxin Antitoxin system (TA), typically regulating the cellular stress response (Fig. 3B). The vent-specific ANME-1 showed few enriched functions, only few that could be linked to the thermal stability of tRNA and the cellular membrane (Table S8).

Discussion

Hydrothermal vents host phylogenetically and functionally divergent ANME-1

Our comparative genomic study detailed ANME-1 genomic diversity in the Loki´s Caste vent field and Jan Mayen vent field. Eight phylogenetically distinct AMOR subgroups were defined. Besides the six that belonged to the ANME-1 family, two affiliated with deep branching lineages in the ANME-1 order, one with the *Ca*. Veteromethanophagaceae, and one with *Ca*. Alkanophagaceae, a putative multi-carbon degrader. Lineages of the ANME-1 family and *Ca*. Veteromethanophagaceae encode a set of metabolic enzymes. This indicates that despite dwelling in different geochemical setting (focused flow of black smokers and diffuse low-temperature in the barite field), ANME-1 and *Ca*. Veteromethanophagaceae systematically rely only on methane and syntrophic associations with sulfate reducers. The ANME-1 from hydrothermal vents are either vent-specific or generalists. The vent-specific ANME-1 cluster rather in the root of the ANME-1 phylogenetic tree (Wang et al. 2022). Such distribution suggests a hydrothermal and a thermophilic (Wang et al. 2022) origin of the ANME-1 order. The vent specific ANME-1 appeared limited in their encoded functional capacity. Instead, the generalists that appear also at cold-seeps and terrestrial environments encode more genes for stress response, detoxification, and defense mechanisms.

In the barite field of the methane-rich Loki's Castle vent field, the occurrence of cold seep-adapted generalist could be driven by its cold seeps-like biogeochemical environment (Pedersen et al. 2010), in close proximity to black smokers. Diluted hydrothermal fluids allow the settlement of siboglinid tube worms, typical at cold seeps (Pedersen et al. 2010). Furthermore, shallow SMTZs (Fig. S1B) are typically observed at seeps, under mats of sulfur-oxidizers (Orphan et al. 2001, de Beer et al. 2006, Lloyd et al. 2006, Roalkvam et al. 2011, Gründger et al. 2019, Carrier et al. 2020). The availability of cold seep-like niches might favor the establishment through genetic selection of generalist lineages that can colonize lower temperature environments, next to vent-specific lineages. Overall, the exposure to the high physicochemical diversity found in deep-sea hydrothermal vents like the Loki's Castle vent field could fuel such diversification of the resident ANME-1 population, on a phylogenetic and functional level. This might have happened in the later stages of ANME-1 evolution, given the likely hydrothermal origin of ANME-1. The acquisition of genetic systems for defense and stress control might have prompted their ability to disperse in cold seeps and other habitats.

ANME-1 lineages can spread and colonize distant geographic locations

According to the generally accepted theory of Beijerinck and Baas Becking (Baas-Becking 1934), microbial organisms are globally distributed, and locally selected by the environment. Recent studies have shown that Beijerinck's theory is applicable to deep-sea hydrothermal microbes (Dick 2019), and sequences belonging to members of the hydrothermal microbiome have been found in open ocean waters (Gonnella et al. 2016). It is not clear how strict anaerobes like ANME-1 could freely disperse in the water column and still be viable and able to colonize geographically distant areas. Nevertheless, phylogenetic evidence supports connectivity between geographically distant sites, such as AMOR and the Guaymas Basin vent field. The genus QENH01 appears at the Hydrate Ridge (Pacific Ocean), Hikurangi Margin (Pacific Ocean), and Gulf of Mexico (Atlantic Ocean). Such extensive biogeographic distance could be explained by the global deep ocean circulation (Talley 2013). Importantly, the deep ocean remained anoxic until well after the Great Oxygenation Event (2 Gyr) (Canfield 1998) and later experienced anoxic episodes (Jenkyns 2010), which may have promoted ANME-1 dispersal. In today's oxic ocean, ANME-1 could travel in a dormant state, as suggested for microaerophilic Campylobacterota and Aquificales (Gonnella et al. 2016), or could be transported in anoxic microniches. Connectivity likely exists between marine and terrestrial environments. *Ca*. Methanoalium (ANME-1-THS and JACGMN01) was initially defined as a 'land' clade after the reconstruction of ANME-1-THS from a Tibetan Hot Spring (Borrel et al. 2019). Chadwick's (Chadwick et al. 2022) and our study expanded this clade with additional genomes from a hot spring in California (SpSt_1198), a marine cold seep in the Gulf of Mexico (GoMg4), the Lost City alkaline vent on the Atlantic Massif (ANME-1-LC), and a terrestrial mud volcano located close to the coast of the Black Sea (Kmv05). Further genomic analysis is required to fully decipher the physiological mechanisms at the basis of ANME-1 phylogenetic/functional diversification and dispersal, such as dynamics of the horizontal gene transfer processes and genetic systems for sporulation and induction of dormancy.

Conclusions

Overall, our metagenomic approach targeting a wide spectrum of hydrothermal settings in the Loki´s Castle and the Jan Mayen vent

fields, allowed us to propose that hydrothermal vents, characterized by geochemical and thermal heterogeneity, could fuel ANME-1 phylogenetic and functional diversification, acting as evolutionary hotspots. Furthermore, they may have promoted the divergence between vent-specific and generalist ANME-1. Despite ANME-1 capacity to disperse globally, marine ANME-1 are overall characterized by metabolic homogeneity and are well adapted to SMTZs. Notably, yet the still small sample size might underestimate their distribution. Further genomic studies are required to complement ANME-1 taxonomy, to confirm the observed functional groups and to determine how selective advantage mechanisms and horizontal gene transfer have shaped ANME-1 lineages through time.

Authors contribution

FV, IHS, and RS conceived the study. GW and CH helped with geochemical analysis and microscopy. RS and HD sampled and reconstructed the genomes; ER and DR helped with geochemical analysis. FV analyzed the data. FV and IS wrote the manuscript. GW, CH, RS, and HD substantially contributed to the final content of the text.

Acknowledgments

We thank the cruise leader professor Rolf-Birger Pedersen, the ROV operators and ROV team leader Stig Vågenes, and the rest of the crew of G. O. SARS for their assistance during sampling campaigns 2010–2018. The computations associated to taxonomic classification were performed on resources provided by Sigma2–the National Infrastructure for High Performance Computing and Data Storage in Norway. We thank Dr Anita-Elin Fedøy for assistance on the DNA extraction; Linn Merethe Brekke Olsen and Hildegunn Almelid for performing the geochemical analysis; Dr Thibaut Barreyre for providing the temperature probe; Dr Achim Mall, Emily Denny, Dr Hasan Arsin and Dr Dimitri Kalenitchenko for their constructive comments. We are grateful to the authors of cited studies and to the colleagues that contribute with valuable feedback to our work. The authors declare no conflict of interest.

Supplementary data

Supplementary data are available at FEMSEC online.

Conflict of interest statement. The authors declare no conflict of interest.

Funding

This work was funded by the Research Council of Norway (RCN) through the Center for Excellence in Geobiology, the KG Jebsen Foundation, the Trond Mohn Foundation and University of Bergen through the Centre for Deep Sea research (grant # TMS2020TMT13), and the RCN funded DeepSeaQuence project (project number 315427).

References

Alneberg J, Bjarnason BS, De Bruijn I *et al.* Binning metagenomic contigs by coverage and composition. *Nat Methods* 2014;**11**:1144–6.

Amann R, Fuchs BM. Single-cell identification in microbial communities by improved fluorescence in situ hybridization techniques. *Nat Rev Microbiol* 2008;**6**:339–48.

Aramaki T, Blanc-Mathieu R, Endo H *et al.* KofamKOALA: KEGG Ortholog assignment based on profile HMM and adaptive score threshold. *Bioinformatics* 2020;**36**:2251–2.

Baas-Becking LGM. *Geobiologie of Inleiding Tot de Milieukunde*. Van Stockkum & Zoon: The Hague, 1934

Baumberger T, Früh-Green GL, Thorseth IH *et al.* Fluid composition of the sediment-influenced Loki's Castle vent field at the ultra-slow spreading arctic mid-ocean ridge. *Geochim Cosmochim Acta* 2016;**187**:156–78.

Biddle JF, Cardman Z, Mendlovitz H *et al.* Anaerobic oxidation of methane at different temperature regimes in Guaymas Basin hydrothermal sediments. *ISME J* 2012;**6**:1018–31.

Boetius A, Ravenschlag K, Schubert CJ *et al.* A marine microbial consortium apparently mediating AOM. *Nature* 2000;**407**:623–6.

Borrel G, Adam PS, McKay LJ *et al.* Wide diversity of methane and short-chain alkane metabolisms in uncultured archaea. *Nat Microbiol* 2019;**4**:603–13.

Boyd JA, Woodcroft BJ, Tyson GW. GraftM: a tool for scalable, phylogenetically informed classification of genes within metagenomes. *Nucleic Acids Res* 2018;**46**:e59.

Buchfink B, Xie C, Huson DH. Fast and sensitive protein alignment using DIAMOND. *Nat Methods* 2014;**12**:59–60.

Canfield DE. A new model for proterozoic ocean chemistry. *Nature* 1998;**396**:450–3.

Capella-Gutiérrez S, Silla-Martínez JM, Gabaldón T. trimAl: a tool for automated alignment trimming in large-scale phylogenetic analyses. *Bioinformatics* 2009;**25**:1972–3.

Carrier V, Svenning MM, Gründger F *et al.* The impact of methane on microbial communities at marine arctic gas hydrate bearing sediment. *Front Microbiol* 2020;**11**:1–20.

Chadwick GL. *et al.*"Comparative genomics reveals electron transfer and syntrophic mechanisms differentiating methanotrophic and methanogenic archaea." *PLoS Biol* 2022;**20.1**:e3001508.

Chaumeil PA, Mussig AJ, Hugenholtz P *et al.* GTDB-Tk: a toolkit to classify genomes with the genome taxonomy database. *Bioinformatics* 2020;**36**:1925–7.

Dahle H, Le Moine Bauer S, Baumberger T *et al.* Energy landscapes in hydrothermal chimneys shape distributions of primary producers. *Front Microbiol* 2018;**9**:1–12.

Dahle H, Økland I, Thorseth IH *et al.* Energy landscapes shape microbial communities in hydrothermal systems on the Arctic Mid-Ocean Ridge. *ISME J* 2015;**9**:1593–606.

De Beer D, Sauter E, Niemann H *et al.* In situ fluxes and zonation of microbial activity in surface sediments of the Håkon Mosby Mud Volcano. *Limnol Oceanogr* 2006;**51**:1315–31.

Delmont TO, Eren EM. Linking pangenomes and metagenomes: the prochlorococcus metapangenome. *PeerJ* 2018;**2018**:1–23.

Dick GJ. The microbiomes of deep-sea hydrothermal vents: distributed globally, shaped locally. *Nat Rev Microbiol* 2019;**17**: 271–83.

Dombrowski N, Teske AP, Baker BJ. Expansive microbial metabolic versatility and biodiversity in dynamic Guaymas Basin hydrothermal sediments. *Nat Commun* 2018;**9**:4999.

Dong X, Rattray JE, Campbell DC *et al.* Thermogenic hydrocarbon biodegradation by diverse depth-stratified microbial populations at a Scotian Basin cold seep. *Nat Commun* 2020;**11**:1–14.

Dowell F, Cardman Z, Dasarathy S *et al.* Microbial communities in methane- and short chain alkane-rich hydrothermal sediments of Guaymas Basin. *Front Microbiol* 2016;**7**: 17.

Eickmann B, Thorseth IH, Peters M *et al.* Barite in hydrothermal environments as a recorder of subseafloor processes: a multiple-isotope study from the Loki's Castle vent field. *Geobiology* 2014;**12**:308–21.

Eren AM, Kiefl E, Shaiber A *et al.* Community-led, integrated, reproducible multi-omics with anvi'o. *Nat Microbiol* 2021;**6**:3–6.

Fornari DJ, Shank T, Von Damm KL *et al.* Time-series temperature measurements at high-temperature hydrothermal vents, East Pacific Rise 9°49′-51′N: evidence for monitoring a crustal cracking event. *Earth Planet Sci Lett* 1998;**160**:419–31.

Fredriksen L, Stokke R, Jensen MS *et al.* Discovery of a thermostable GH10 xylanase with broad substrate specificity from the Arctic Mid-Ocean Ridge vent system. *Appl Environ Microbiol* 2019;**85**:e02970–18

Galperin MY, Makarova KS, Wolf YI *et al.* Expanded microbial genome coverage and improved protein family annotation in the COG database. *Nucleic Acids Res* 2015;**43**:D261–9.

Gonnella G, Böhnke S, Indenbirken D *et al.* Endemic hydrothermal vent species identified in the open ocean seed bank. *Nat Microbiol* 2016;**1**:1–7.

Gruber-Vodicka HR, Seah BKB, Pruesse E. phyloFlash: rapid small-subunit rRNA profiling and targeted assembly from metagenomes. *Msystems* 2020;**5**:e00920–20

Gründger F, Carrier V, Svenning MM *et al.* Methane-fuelled biofilms predominantly composed of methanotrophic ANME-1 in Arctic gas hydrate-related sediments. *Sci Rep* 2019;**9**:1–10.

Hahn CJ, Laso-Pérez R, Vulcano F *et al.* "Candidatus Ethanoperedens," a thermophilic genus of archaea mediating the anaerobic oxidation of Ethane. *MBio* 2020;**11**:e00600–20.

Hallam SJ, Putnam N, Preston CM *et al.* Reverse methanogenesis: testing the hypothesis with environmental genomics. *Science (80-)* 2004;**305**:1457–62.

Hinrichs KU, Hayes JM, Sylva SP *et al.* Methane-consuming archaebacteria in marine sediments. *Nature* 1999;**398**:802–5.

Holler T, Widdel F, Knittel K *et al.* Thermophilic anaerobic oxidation of methane by marine microbial consortia. *ISME J* 2011;**5**:1946–56.

Hyatt D, Chen GL, LoCascio PF *et al.* Prodigal: prokaryotic gene recognition and translation initiation site identification. *BMC Bioinf* 2010;**11**:119

Jenkyns HC. Geochemistry of oceanic anoxic events. *Geochem Geophys Geosyst* 2010;**11**:1–30.

Kallmeyer J, Ferdelman TG, Weber A *et al.* Jens Kallmeyer, Timothy G. Ferdelman, Andreas Weber, Henrik Fossing, and Bo Barker Jørgensen. A cold chromium distillation procedure for radiolabeled sulfide applied to sulfate reduction measurements. *Limnol Oceanogr: Methods* 2004;**2**:171–80. 2004: 171–80.

Kanehisa M, Sato Y, Morishima K. BlastKOALA and GhostKOALA: KEGG tools for functional characterization of genome and metagenome sequences. *J Mol Biol* 2016;**428**:726–31.

Kang DD, Froula J, Egan R *et al.* MetaBAT, an efficient tool for accurately reconstructing single genomes from complex microbial communities. *PeerJ* 2015;**2015**:1–15.

Katoh K. MAFFT: a novel method for rapid multiple sequence alignment based on fast Fourier transform. *Nucleic Acids Res* 2002;**30**:3059–66.

Kleindienst S, Ramette A, Amann R *et al.* Distribution and in situ abundance of sulfate-reducing bacteria in diverse marine hydrocarbon seep sediments. *Environ Microbiol* 2012;**14**:2689–710.

Knittel K, Boetius A. Anaerobic oxidation of methane: progress with an unknown process. *Annu Rev Microbiol* 2009;**63**:311–34.

Knittel K, Lösekann T, Boetius A *et al.* Diversity and distribution of methanotrophic archaea at cold seeps. *Appl Environ Microbiol* 2005;**71**:467–79.

Krukenberg V, Harding K, Richter M *et al.* Candidatus Desulfofervidus auxilii, a hydrogenotrophic sulfate-reducing bacterium involved in the thermophilic anaerobic oxidation of methane. *Environ Microbiol* 2016;**18**:3073–91.

Krukenberg V, Riedel D, Gruber-Vodicka HR *et al.* Gene expression and ultrastructure of meso- and thermophilic methanotrophic consortia. *Environ Microbiol* 2018;**20**:1651–66.

Laso-Pérez R, Krukenberg V, Musat F *et al.* Establishing anaerobic hydrocarbon-degrading enrichment cultures of microorganisms under strictly anoxic conditions. *Nat Protoc* 2018;**13**:1310–30.

Laso-Pérez R, Wegener G, Knittel K *et al.* Thermophilic archaea activate butane via alkyl-coenzyme M formation. *Nature* 2016;**539**:396–401.

Lee MD. GToTree: a user-friendly workflow for phylogenomics. *Bioinformatics* 2019;**35**:4162–4.

Li D, Liu CM, Luo R *et al.* MEGAHIT: an ultra-fast single-node solution for large and complex metagenomics assembly via succinct de Bruijn graph. *Bioinformatics* 2015;**31**:1674–6.

Lloyd KG, Lapham L, Teske A. An anaerobic methane-oxidizing community of ANME-1b archaea in hypersaline gulf of Mexico sediments. *Appl Environ Microbiol* 2006;**72**:7218–30.

Lösekann T, Knittel K, Nadalig T *et al.* Diversity and abundance of aerobic and anaerobic methane oxidizers at the Haakon Mosby Mud Volcano, Barents Sea. *Appl Environ Microbiol* 2007;**73**:3348–62.

Maignien L, Parkes RJ, Cragg B *et al.* Anaerobic oxidation of methane in hypersaline cold seep sediments. *FEMS Microbiol Ecol* 2013;**83**:214–31.

McGlynn SE, Chadwick GL, Kempes CP *et al.* Single cell activity reveals direct electron transfer in methanotrophic consortia. *Nature* 2015;**526**:531–5.

McKay LJ, MacGregor BJ, Biddle JF *et al.* Spatial heterogeneity and underlying geochemistry of phylogenetically diverse orange and white Beggiatoa mats in Guaymas Basin hydrothermal sediments. *Deep Res Part I Oceanogr Res Pap* 2012;**67**:21–31.

Meyerdierks A, Kube M, Kostadinov I *et al.* Metagenome and mRNA expression analyses of anaerobic methanotrophic archaea of the ANME-1 group. *Environ Microbiol* 2010;**12**:422–39.

Nguyen LT, Schmidt HA, Von Haeseler A *et al.* IQ-TREE: a fast and effective stochastic algorithm for estimating maximum-likelihood phylogenies. *Mol Biol Evol* 2015;**32**:268–74.

Orphan VJ, Hinrichs KU, Ussler W *et al.* Comparative analysis of methane-oxidizing archaea and sulfate-reducing bacteria in anoxic marine sediments. *Appl Environ Microbiol* 2001;**67**:1922–34.

Parks DH, Chuvochina M, Rinke C *et al.* GTDB: an ongoing census of bacterial and archaeal diversity through a phylogenetically consistent, rank normalized and complete genome-based taxonomy. *Nucleic Acids Res* 2021;**202**:1–10.

Parks DH, Chuvochina M, Waite DW *et al.* A standardized bacterial taxonomy based on genome phylogeny substantially revises the tree of life. *Nat Biotechnol* 2018;**36**:996.

Parks DH, Imelfort M, Skennerton CT *et al.* CheckM: assessing the quality of microbial genomes recovered from isolates, single cells, and metagenomes. *Genome Res* 2015;**25**:1043–55.

Pedersen RB, Rapp HT, Thorseth IH *et al.* Discovery of a black smoker vent field and vent fauna at the Arctic Mid-Ocean Ridge. *Nat Commun* 2010;**1**:126.

Pernthaler A, Amann R. Simultaneous fluorescence in situ hybridization of mRNA and rRNA in environmental bacteria. *Appl Environ Microbiol* 2004;**70**:5426–33.

Pritchard L, Glover RH, Humphris S *et al.* Genomics and taxonomy in diagnostics for food security: soft-rotting enterobacterial plant pathogens. *Anal Methods* 2016;**8**:12–24.

Rinke C, Chuvochina M, Mussig AJ *et al.* A standardized archaeal taxonomy for the Genome Taxonomy Database. *Nat Microbiol* 2021;**6**:946–59.

Roalkvam I, Jørgensen SL, Chen Y *et al.* New insight into stratification of anaerobic methanotrophs in cold seep sediments. *FEMS Microbiol Ecol* 2011;**78**:233–43.

Ruff SE, Arnds J, Knittel K *et al.* Microbial communities of deep-sea methane seeps at Hikurangi continental margin (New Zealand). *PLoS One* 2013;**8**:e72627.

Ruff SE, Kuhfuss H, Wegener G *et al.* Methane seep in shallow-water permeable sediment harbors high diversity of anaerobic methanotrophic communities, Elba, Italy. *Front Microbiol* 2016;**7**:1–20.

Schwank K, Bornemann TLV, Dombrowski N *et al.* An archaeal symbiont-host association from the deep terrestrial subsurface. *ISME J* 2019;**13**:2135–9.

Shaiber A, Willis AD, Delmont TO *et al.* Functional and genetic markers of niche partitioning among enigmatic members of the human oral microbiome. *Genome Biol* 2020;**21**:292.

Sieber CMK, Probst AJ, Sharrar A *et al.* Recovery of genomes from metagenomes via a dereplication, aggregation and scoring strategy. *Nat Microbiol* 2018;**3**:836–43.

Skennerton CT, Chourey K, Iyer R *et al.* Erratum for Skennerton *et al.*, "Methane-Fueled syntrophy through extracellular electron transfer: uncovering the genomic traits conserved within diverse bacterial partners of anaerobic methanotrophic archaea." *MBio* 2017;**8**:e00530–17

Steen IH, Dahle H, Stokke R *et al.* Novel barite chimneys at the Loki's Castle vent field shed light on key factors shaping microbial communities and functions in hydrothermal systems. *Front Microbiol* 2016;**6**:1510.

Stokke R, Reeves EP, Dahle H *et al.* Tailoring hydrothermal vent biodiversity toward improved biodiscovery using a novel in situ enrichment strategy. *Front Microbiol* 2020;**11**:249.

Stokke R, Roalkvam I, Lanzen A *et al.* Integrated metagenomic and metaproteomic analyses of an ANME-1-dominated community in marine cold seep sediments. *Environ Microbiol* 2012;**14**:1333–46.

Talley LD. Closure of the global overturning circulation through the Indian, Pacific, and southern oceans. *Oceanography* 2013;**26**:80–97.

Teske A, Hinrichs KU, Edgcomb V *et al.* Microbial diversity of hydrothermal sediments in the Guaymas Basin: evidence for anaerobic methanotrophic communities. *Appl Environ Microbiol* 2002;**68**:1994–2007.

Vigneron A, Cruaud P, Pignet P *et al.* Archaeal and anaerobic methane oxidizer communities in the Sonora Margin cold seeps, Guaymas Basin (Gulf of California). *ISME J* 2013;**7**:1595–608.

Wang Y, Wegener G, Hou J *et al.* Expanding anaerobic alkane metabolism in the domain of Archaea. *Nat Microbiol* 2019;**4**:595–602.

Wang Y, Wegener G, Williams TA *et al.* A methylotrophic origin of methanogenesis and early divergence of anaerobic multicarbon alkane metabolism. *Sci Adv* 2021;**7**:eabj1453

Wang Y, Xie R, Hou J *et al.* The late Archaean to early Proterozoic origin and evolution of anaerobic methane - oxidizing archaea. 2022;**1**:96–100.

Wegener G, Krukenberg V, Riedel D *et al.* Intercellular wiring enables electron transfer between methanotrophic archaea and bacteria. *Nature* 2015;**526**:587–90.

Wegener G, Shovitri M, Knittel K *et al.* Biogeochemical processes and microbial diversity of the Gullfaks and Tommeliten methane seeps (Northern North Sea). *Biogeosciences* 2008;**5**:1127–44.

Wu YW, Simmons BA, Singer SW. MaxBin 2.0: an automated binning algorithm to recover genomes from multiple metagenomic datasets. *Bioinformatics* 2016;**32**:605–7.

Paper II

AMERICAN SOCIETY FOR MICROBIOLOGY | mBio®

RESEARCH ARTICLE
Applied and Environmental Science

"*Candidatus* Ethanoperedens," a Thermophilic Genus of *Archaea* Mediating the Anaerobic Oxidation of Ethane

Cedric Jasper Hahn,[a] Rafael Laso-Pérez,[a,b,c] Francesca Vulcano,[d] Konstantinos-Marios Vaziourakis,[a,e] Runar Stokke,[d] Ida Helene Steen,[d] Andreas Teske,[f] Antje Boetius,[a,b,c] Manuel Liebeke,[a] Rudolf Amann,[a] Katrin Knittel,[a] Gunter Wegener[a,b,c]

[a]Max-Planck Institute for Marine Microbiology, Bremen, Germany
[b]MARUM, Center for Marine Environmental Sciences, University of Bremen, Bremen, Germany
[c]Alfred Wegener Institute Helmholtz Center for Polar and Marine Research, Bremerhaven, Germany
[d]K.G. Jebsen Centre for Deep Sea Research and Department of Biological Sciences, University of Bergen, Bergen, Norway
[e]University of Patras, Patras, Greece
[f]The University of North Carolina at Chapel Hill, Chapel Hill, North Carolina, USA

ABSTRACT Cold seeps and hydrothermal vents deliver large amounts of methane and other gaseous alkanes into marine surface sediments. Consortia of archaea and partner bacteria thrive on the oxidation of these alkanes and its coupling to sulfate reduction. The inherently slow growth of the involved organisms and the lack of pure cultures have impeded the understanding of the molecular mechanisms of archaeal alkane degradation. Here, using hydrothermal sediments of the Guaymas Basin (Gulf of California) and ethane as the substrate, we cultured microbial consortia of a novel anaerobic ethane oxidizer, "*Candidatus* Ethanoperedens thermophilum" (GoM-Arc1 clade), and its partner bacterium "*Candidatus* Desulfofervidus auxilii," previously known from methane-oxidizing consortia. The sulfate reduction activity of the culture doubled within one week, indicating a much faster growth than in any other alkane-oxidizing archaea described before. The dominance of a single archaeal phylotype in this culture allowed retrieval of a closed genome of "*Ca.* Ethanoperedens," a sister genus of the recently reported ethane oxidizer "*Candidatus* Argoarchaeum." The metagenome-assembled genome of "*Ca.* Ethanoperedens" encoded a complete methanogenesis pathway including a methyl-coenzyme M reductase (MCR) that is highly divergent from those of methanogens and methanotrophs. Combined substrate and metabolite analysis showed ethane as the sole growth substrate and production of ethyl-coenzyme M as the activation product. Stable isotope probing demonstrated that the enzymatic mechanism of ethane oxidation in "*Ca.* Ethanoperedens" is fully reversible; thus, its enzymatic machinery has potential for the biotechnological development of microbial ethane production from carbon dioxide.

IMPORTANCE In the seabed, gaseous alkanes are oxidized by syntrophic microbial consortia that thereby reduce fluxes of these compounds into the water column. Because of the immense quantities of seabed alkane fluxes, these consortia are key catalysts of the global carbon cycle. Due to their obligate syntrophic lifestyle, the physiology of alkane-degrading archaea remains poorly understood. We have now cultivated a thermophilic, relatively fast-growing ethane oxidizer in partnership with a sulfate-reducing bacterium known to aid in methane oxidation and have retrieved the first complete genome of a short-chain alkane-degrading archaeon. This will greatly enhance the understanding of nonmethane alkane activation by noncanonical methyl-coenzyme M reductase enzymes and provide insights into additional metabolic steps and the mechanisms underlying syntrophic partnerships. Ultimately, this knowledge could lead to the biotechnological development of alkanogenic microorganisms to support the carbon neutrality of industrial processes.

Citation Hahn CJ, Laso-Pérez R, Vulcano F, Vaziourakis K-M, Stokke R, Steen IH, Teske A, Boetius A, Liebeke M, Amann R, Knittel K, Wegener G. 2020. "*Candidatus* Ethanoperedens," a thermophilic genus of *Archaea* mediating the anaerobic oxidation of ethane. mBio 11:e00600-20. https://doi.org/10.1128/mBio.00600-20.

Editor Douglas G. Capone, University of Southern California

Address correspondence to Gunter Wegener, gwegener@mpi-bremen.de.

Received 13 March 2020
Accepted 23 March 2020
Published 21 April 2020

KEYWORDS alkane degradation, archaea, syntrophy, methyl-coenzyme M reductase, model organism, hydrothermal vents

In deep marine sediments, organic matter undergoes thermocatalytic decay, resulting in the formation of natural gas (methane to butane) and crude oil. If not capped, the gas fraction will rise toward the sediment surface due to buoyancy, porewater discharge, and diffusion. Most of the gas is oxidized within the sediments coupled to the reduction of the abundant electron acceptor sulfate (1, 2). Responsible for the anaerobic oxidation of alkanes are either free-living bacteria or microbial consortia of archaea and bacteria. Most free-living bacteria use alkyl succinate synthases to activate the alkane, forming succinate-bound alkyl units as primary intermediates (3). Usually, these alkanes are completely oxidized, and this process is coupled to sulfate reduction in the same cells, as has been shown, for example, in the deltaproteobacterial butane-degrading strain BuS5 (4). However, alkane oxidation in seafloor sediments is to a large extent performed by dual species consortia of archaea and bacteria (5, 6). As close relatives of methanogens, the archaea in these consortia activate alkanes as thioethers and completely oxidize the substrates to CO_2. The electrons released during alkane oxidation are consumed by the sulfate-reducing partner bacteria.

The anaerobic methane-oxidizing archaea (ANME) activate methane using methyl-coenzyme M (CoM) reductases (MCRs) that are highly similar to those of methanogens, forming methyl-coenzyme M as the primary intermediate (7). The methyl group is oxidized via a reversal of the methanogenesis pathway (8). Thermophilic archaea of the genus "*Candidatus* Syntrophoarchaeum" thrive on the oxidation of butane and propane. In contrast to ANME, they contain four highly divergent MCR variants, which generate butyl- and propyl-coenzyme M (CoM) as primary intermediates (9). Based on genomic and transcriptomic evidence, the CoM-bound alkyl units are transformed to fatty acids and oxidized further via beta-oxidation. The reactions transforming the CoM-bound alkyl units to CoA-bound fatty acids and the enzymes performing such reactions are so far unknown. The CoA-bound acetyl units are completely oxidized in the Wood-Ljungdahl pathway including the upstream part of the methanogenesis pathway. In hydrogenotrophic methanogens, the enzymes of this pathway are used to reduce CO_2-forming methyl-tetrahydromethanopterin for methanogenesis and for biomass production. In "*Ca.* Syntrophoarchaeum," this pathway is used in reverse direction for the complete oxidation of acetyl-CoA. Both the thermophilic ANME-1 and "*Ca.* Syntrophoarchaeum" form dense consortia with their sulfate-reducing partner bacterium "*Candidatus* Desulfofervidus" (HotSeep-1 clade) (10, 11). The transfer of reducing equivalents between the alkane-oxidizing archaea and their partners is likely mediated by pilus-based nanowires and cytochromes produced by the two consortial partners (12). For a critical view on electron transfer in anaerobic oxidation of methane (AOM) consortia, see reference 13.

Sulfate-dependent ethane oxidation has been described multiple times in slurries of marine sediments (4, 14, 15). The first functional description of this process was based on a cold-adapted culture derived from Gulf of Mexico sediments (5). In this culture, "*Candidatus* Argoarchaeum" (formerly known as GoM-Arc1 clade) activates ethane with the help of divergent MCRs that are phylogenetically placed on a distinct branch next to those of "*Ca.* Syntrophoarchaeum." Based on the presence of all enzymes of the Wood-Ljungdahl pathway that can be used for acetyl-CoA oxidation, it has been suggested that the CoM-bound ethyl groups are transferred to CoA-bound acetyl units. The required intermediates for this reaction mechanism are so far unknown (5). "*Ca.* Argoarchaeum" forms unstructured consortia with yet-unidentified bacterial partners and grows slowly with substrate turnover rates comparable to AOM (5). Additional metagenome-assembled genomes (MAGs) of the GoM-Arc1 clade derived from the Guaymas Basin and the Gulf of Mexico have similar gene contents, suggesting that these GoM-Arc1 archaea are ethane oxidizers (16, 17).

To date, the understanding of short-chain alkane-metabolizing archaea mainly relies

on comparison of their genomic information with those of methanogens that are well characterized with regard to their enzymes. Due to the slow growth of the alkane-oxidizing archaea and the resulting lack of sufficient biomass, specific biochemical traits remain unknown. For instance, the structural modifications of noncanonical MCRs or the proposed transformation of the CoM-bound alkyl to CoA-bound acetyl units in the short-chain alkane degraders has not been proven. Here, we describe a faster-growing, thermophilic ethane-oxidizing culture from sediments of the Guaymas Basin. Metagenomic analyses of Guaymas Basin sediments revealed a great diversity of potential alkane degraders with divergent MCR enzymes (9, 18). With ethane as sole energy source and sulfate as electron acceptor, we obtained well-growing meso- and thermophilic ethane-degrading enrichment cultures from these sediments. Their low strain diversity makes them particularly suitable for assessing the pathways of the anaerobic oxidation of ethane.

Taxonomy of "*Candidatus* Ethanoperedens thermophilum." Etymology: *ethano* (new Latin), pertaining to ethane; *peredens* (Latin), consuming, devouring; *thermophilum* (Greek), heat-loving. The name implies an organism capable of ethane oxidation at elevated temperatures. Locality: enriched from hydrothermally heated, hydrocarbon-rich marine sediment of the Guaymas Basin at 2,000-m water depth, Gulf of California, Mexico. Description: anaerobic, ethane-oxidizing archaeon, mostly coccoid, about 0.7 μm in diameter, forms large irregular cluster in large dual-species consortia with the sulfate-reducing partner bacterium "*Candidatus* Desulfofervidus auxilii."

RESULTS AND DISCUSSION

Establishment of meso- and thermophilic ethane-oxidizing enrichment cultures. Sediments were sampled from the gas- and oil-rich sediments covered by sulfur-oxidizing mats of the Guaymas Basin. From these sediments and artificial seawater medium, a slurry was produced under anoxic conditions and distributed into replicate bottles. These bottles were supplied with an ethane headspace (2 atm) and incubated at 37°C and 50°C. Additional growth experiments were performed with methane, and controls were set up with a nitrogen atmosphere. As a measure of metabolic activity, sulfide concentrations were tracked over time (for further details, see Materials and Methods). Both methane and ethane additions resulted in the formation of 15 mM sulfide within 4 months. Nitrogen controls produced only little sulfide ($<$2 mM) that likely corresponds to the degradation of alkanes and organic matter from the original sediment. Subsequent dilution (1:3) of the ethane and methane cultures and further incubation with the corresponding substrates showed faster, exponentially increasing sulfide production in the ethane culture, suggesting robust growth of the ethane-degrading community (Fig. 1A). After three consecutive dilution steps, virtually sediment-free cultures were obtained. These cultures produced approximately 10 mM sulfide in 8 weeks. All further experiments were conducted with the faster-growing 50°C culture (Ethane50). Sequencing of metagenomes, however, was done on both, the 50°C and 37°C (Ethane37) culture.

A stoichiometric growth experiment with the Ethane50 culture (Fig. 1B) showed that ethane was completely oxidized while sulfate was reduced to sulfide according to the formula $4C_2H_6 + 7SO_4^{2-} \rightarrow 8HCO_3^- + 7HS^- + 4H_2O + H^+$.

An experiment tracking the exponential development of sulfide over time suggested doubling times of only 6 days at low sulfide concentrations of $<$5 mM (Fig. 1B), which is substantially faster than estimated for thermophilic AOM consortia, with about 60 days (10), and also faster than the cold-adapted anaerobic ethane-oxidizing cultures (5). Sulfide concentrations over 5 mM seemed to suppress activity and growth of the ethane-oxidizing microorganisms (Fig. 1C). Hence, flowthrough bioreactors could be beneficial to increase biomass yields of anaerobic ethane degraders.

Microbial composition of the Ethane50 culture. Amplified archaeal and bacterial 16S rRNA genes of the original sediment and early, still sediment-containing cultures (150 days of incubation) were sequenced to track the development of microbial compositions over time (for primers, see Table S1 in the supplemental material). The

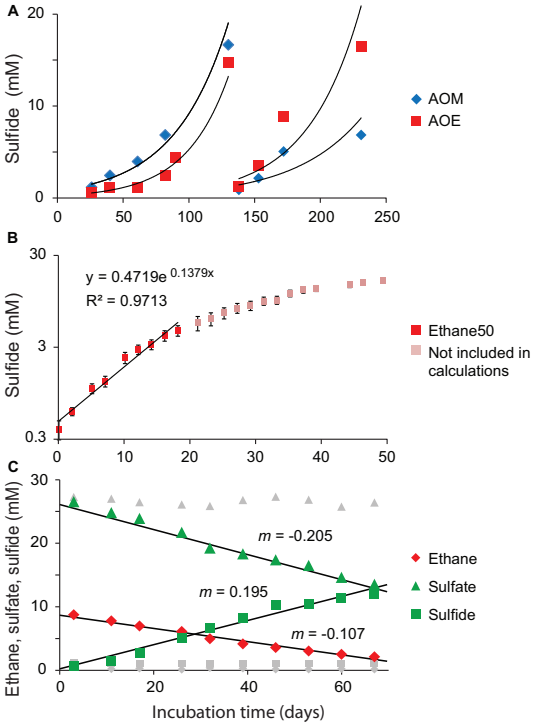

FIG 1 Cultivation and stoichiometry test of the Ethane50 culture. (A) Rates of methane-dependent (blue) and ethane-dependent (red) sulfide production in sediments of the Guaymas Basin incubated at 50°C. (B) Determination of activity doubling times in anaerobic ethane-oxidizing culture. Logarithmic *y* axis with sulfide production shows a decrease in activity at 3 mM sulfide and estimated activity doubling times in low sulfide concentrations of 6 to 7 days. (C) Development of ethane (diamonds), sulfate (triangles), and sulfide (squares) concentrations in the Ethane50 culture. Gray symbols show corresponding concentrations measured in control incubations without ethane addition (data from 1 of 3 replicate incubations; for complete data, see Table S6). The ratios of the slopes of sulfate and sulfide to ethane (1.92 and 1.82, respectively) are close to the stoichiometric ratios of sulfate reduction and ethane oxidation. The small offset may relate to biomass production and sampling artifacts.

original sediment contained large numbers of ANME-1 and the putative partner bacterium "*Ca.* Desulfofervidus." The AOM culture became further enriched in ANME-1 archaea and "*Ca.* Desulfofervidus," whereas in the Ethane50 culture the GoM-Arc1 clade increased from <0.1% in the original sediment to roughly 35% of all archaea (Fig. 2A). Notably, the relative abundance of "*Ca.* Desulfofervidus" increased also in the Ethane50 culture. This indicates that "*Ca.* Desulfofervidus" was also involved as a partner bacterium in the thermophilic ethane culture.

To visualize the cells involved in the anaerobic oxidation of ethane (AOE), oligonucleotide probes specific for the GoM-Arc1 clade and "*Ca.* Desulfofervidus" were applied on the Ethane50 culture using catalyzed reporter deposition fluorescence *in situ* hybridization (CARD-FISH; for probes, see Table S1). The Ethane50 culture contained large and tightly packed consortia with sizes of up to 40 μm in diameter formed by GoM-Arc1 and "*Ca.* Desulfofervidus" cells (Fig. 2D and E). In the consortia, archaea and bacteria grew spatially separated. These large consortia apparently develop from small but already dense consortia found in the inoculate, similar to what was found for cold-adapted AOM consortia (19). Such a separation of the partner organisms is also characteristic for consortia in the butane-degrading culture (9) and for most AOM consortia (20). In contrast, in thermophilic AOM consortia of ANME-1 and "*Ca.* Desul-

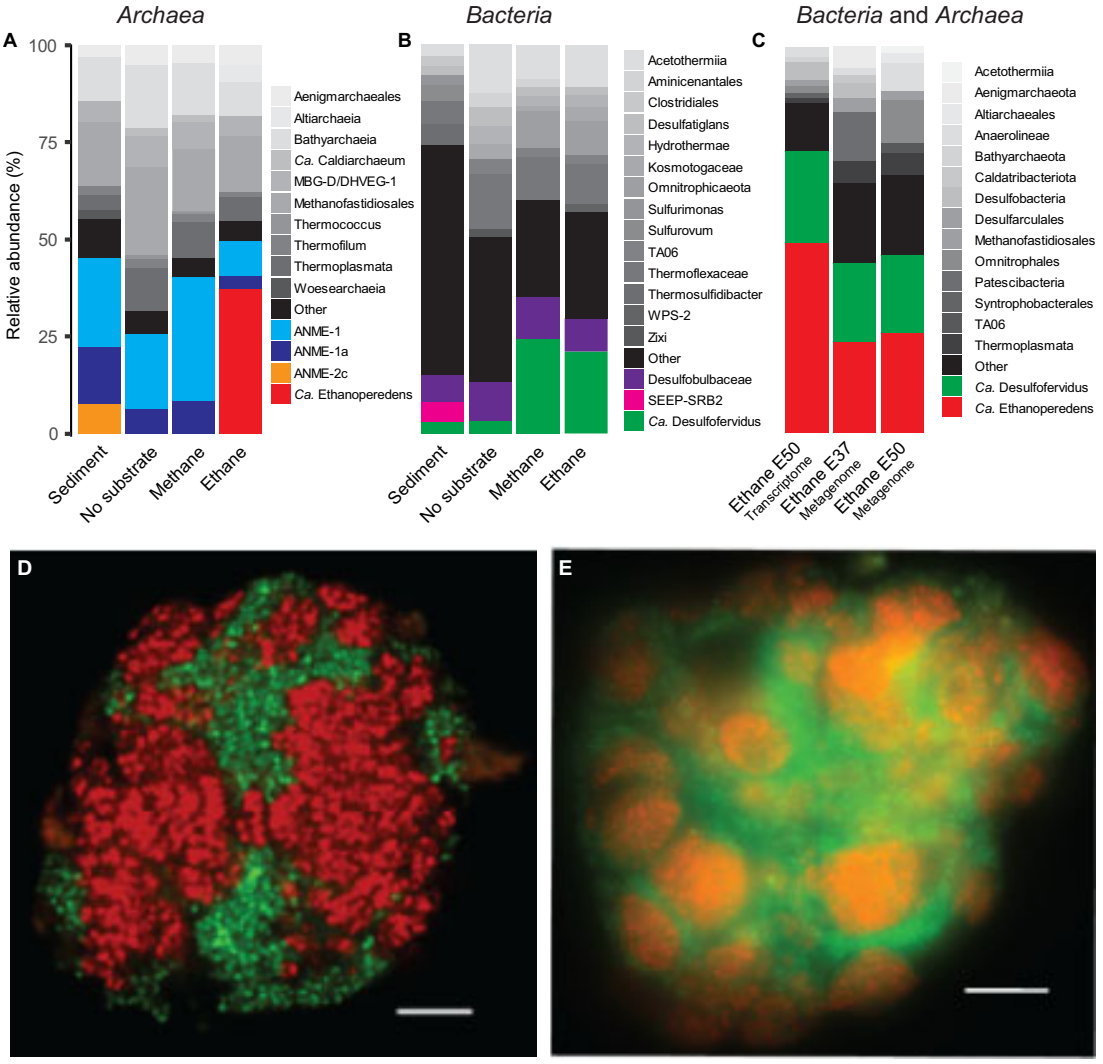

FIG 2 Microbial composition of the Ethane50 culture. (A and B) Relative abundance of phylogenetic clades of archaea (A) and bacteria (B) based on 16S rRNA gene amplicon sequencing present in the inoculated sediment, and in cultures with no substrate, with methane and ethane after 150 days of incubation. (C) Relative abundance of active microbial groups based on 16 rRNA fragments recruited from the genome of Ethane37 and Ethane50 after 2.5 years of incubation and the transcriptome of the Ethane50 culture after 1 year of incubation with ethane. (D and E) Laser-scanning micrograph (D) and epifluorescence micrograph (E) of microbial consortia stained with probes specific for the GoM-Arc1 clade (red, Alexa 594) and "*Ca.* Desulfofervidus" (green, Alexa 488) in the Ethane50 culture. Bar, 10 μm.

fofervidus," the partner cells appear well mixed (21). The Ethane50 culture differs from the cold-adapted ethane-oxidizing culture, in which "*Ca.* Argoarchaeum" forms rather loose assemblages with yet-uncharacterized bacteria (5).

To analyze the metabolic potential of the microorganisms involved in ethane degradation, Ethane37 and Ethane50 cultures were subjected to transcriptomic and genomic analysis. The 16S rRNA sequences extracted from the shotgun RNA reads of the Ethane50 culture were strongly dominated by GoM-Arc1 (50%) and "*Ca.* Desulfofervidus" (20%; Fig. 2C), supporting a crucial role of these two organisms in thermophilic

ethane degradation. Long-read DNA sequencing for the Ethane50 culture resulted in a partial genome of GoM-Arc1 with 76.2% completeness (GoM-Arc1_E50_DN), whereas by applying this approach to the Ethane37 culture, we obtained a closed genome of the GoM-Arc1 archaeon (GoM-Arc1_E37). The two GoM-Arc1 genomes share an average nucleotide identity (ANI) of 98%; hence, a complete consensus genome for Ethane50 (GoM-Arc1_E50) was obtained by mapping long reads of the Ethane50 culture on the closed GoM-Arc1_E37 genome (see Materials and Methods and Table S2). GoM-Arc1_E50 had a size of 1.92 Mb and a GC content of 46.5%. To assess the genomic diversity of archaea of the GoM-Arc1 clade, additionally a MAG of GoM-Arc1 from the Loki's Castle hydrothermal vent field (GoM-Arc1-LC), with a completeness of 68% and eight single-cell amplified genomes (SAGs) from different cold seeps and different completenesses (10% to 59%) were retrieved (Table S2). The MAG GoM-Arc1-LC and the eight single cells have an average nucleotide identity (ANI) of over 90%, suggesting that they belong to the same or closely related species. The 16S rRNA gene identity is in the range of 99.5%, supporting a definition as same species, and shows that the same species of GoM-Arc1 can be found in diverse seep sites (Table S2 and Fig. S1). Together with several MAGs of the GoM-Arc1 clade archaea from public databases (5, 17, 18) these MAGs now provide an extensive database for the genomic description of the GoM-Arc1 clade. All GoM-Arc1 clade genomes have an estimated size smaller than 2 Mb, which is in the range of the other thermophilic alkane degraders, such as "*Ca.* Syntrophoarchaeum" (1.5 to 1.7 Mb) and ANME-1 (1.4 to 1.8 Mb) (9, 22). The genome is, however, much smaller than the 3.5-Mb genome of the mesophilic sister lineage "*Candidatus* Methanoperedens." This organism thrives on methane and is able to reduce nitrate or metals without partner bacteria (23, 24).

All GoM-Arc1 genomes contain the genes encoding the enzymes of the methanogenesis pathway, including a highly similar divergent-type MCR and the Wood-Ljungdahl pathway, but no pathway for beta-oxidation of longer fatty acids. Hence, it is likely that all members of this clade are ethane oxidizers. Based on 16S rRNA gene phylogeny and a genome tree based on 32 marker genes, the GoM-Arc1 clade divides into two subclusters. According to a 16S rRNA gene identity of ~95% (Fig. S1) and an average amino acid identity (AAI) of ~63% (Fig. 3A; Table S2), these clusters should represent two different genera. One cluster contains the recently described ethane oxidizer "*Candidatus* Argoarchaeum ethanivorans" and genomes derived from cold environments including the Gulf of Mexico and the moderately heated Loki's Castle seeps (25). The second cluster includes the thermophilic GoM-Arc1 strains found in the Ethane50 and Ethane37 cultures and sequences of other MAGs from the Guaymas Basin (16, 18). Based on the substrate specificity (see results below) and its optimal growth at elevated temperatures, we propose to name the Ethane50 strain of GoM-Arc1 "*Candidatus* Ethanoperedens thermophilum" (*Ethanoperedens*, Latin for nourishing on ethane; *thermophilum*, Latin for heat loving).

Genomic and catabolic features of "*Ca.* Ethanoperedens." The main catabolic pathways of "*Ca.* Ethanoperedens" are a complete methanogenesis and a Wood-Ljungdahl pathway (Fig. 4). Its genome encodes only one MCR. The three MCR subunits $\alpha\beta\gamma$ are on a single operon. The amino acid sequence of the alpha subunit (*mcr*A) of "*Ca.* Ethanoperedens" is phylogenetically most closely related to the recently described divergent-type MCR of "*Ca.* Argoarchaeum" with an amino acid identity of 69% but also with all other *mcr*A sequences of GoM-Arc1 archaea (5, 12, 16, 18). These MCRs form a distinct cluster in comparison to other divergent MCRs and to the canonical MCRs of methanogens and methanotrophs (Fig. 3B). The similarity of GoM-Arc1 *mcr*A sequences to the described canonical and noncanonical sequences is below 43%, and changes in the amino acid sequences are also found in the highly conserved active site of the enzyme (Fig. S2). The relative expression of the *mcr* subunits compared to all reads mapping to "*Ca.* Ethanoperedens" (reads per kilobase per million mapped reads [RPKM], i.e., *mcr*A = 9,790) is at least two times higher than the expression of all other genes of the main catabolic pathway (Fig. 4; Table S3). The relative *mcr* expression of

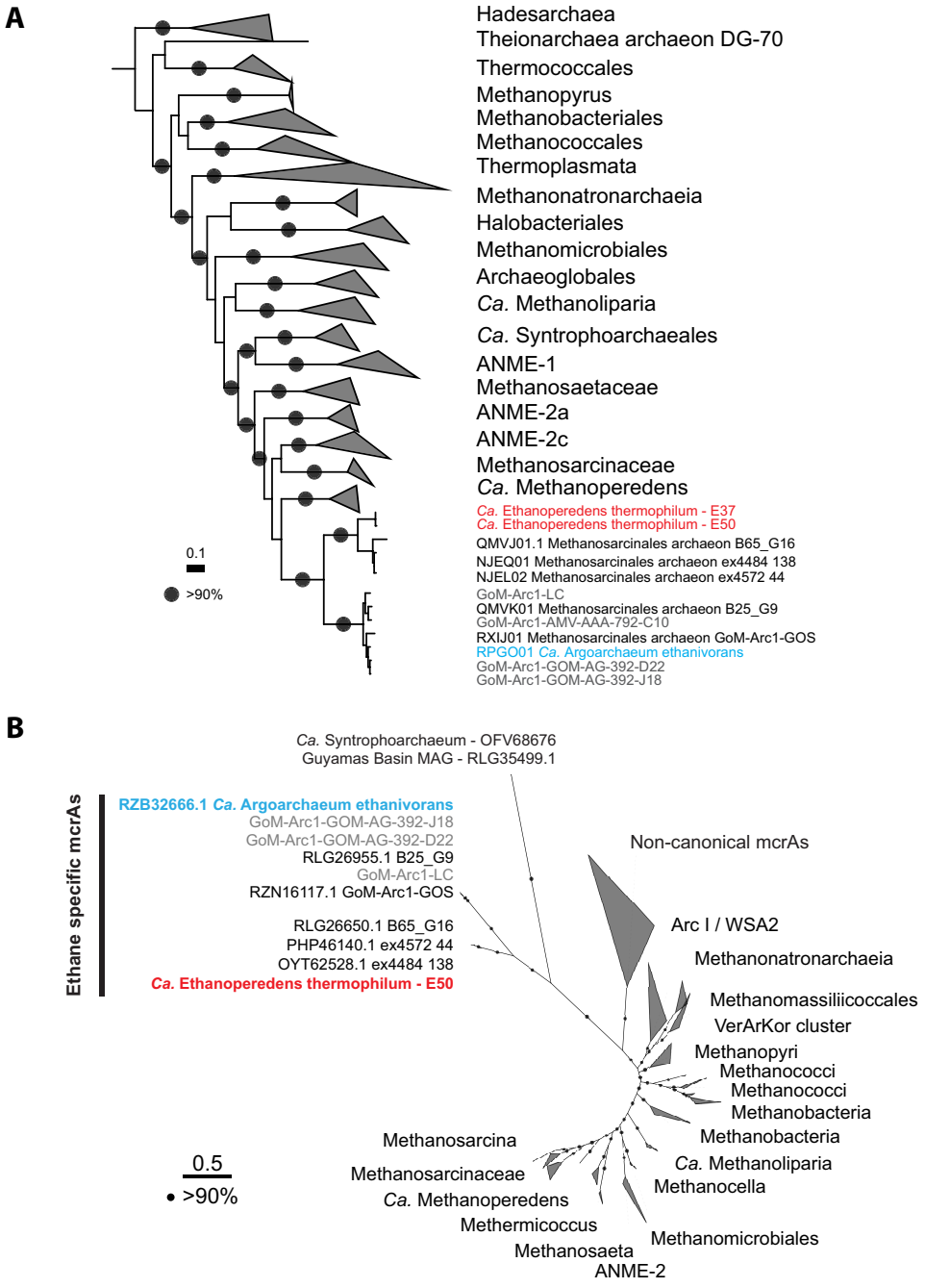

FIG 3 Phylogenetic affiliation based on 32 marker genes and *mcr*A amino acid sequences of "*Ca.* Ethanoperedens." (A) Phylogenetic affiliation of "*Ca.* Ethanoperedens" within the *Euryarchaeota* based on 32 aligned marker gene amino acid sequences; outgroup is *Thaumarchaeota*. The scale bar indicates 10% sequence divergence. (B) Phylogenetic affiliation of *mcr*A amino acid sequences. The *mcr*A sequences of GoM-Arc1 form a distinct branch within the noncanonical, potentially multicarbon alkane-activating MCRs. The *mcr*A genes of the GoM-Arc1 cluster can be further divided into those from cold-adapted organisms, including "*Ca.* Argoarchaeum ethanivorans," and

(Continued on next page)

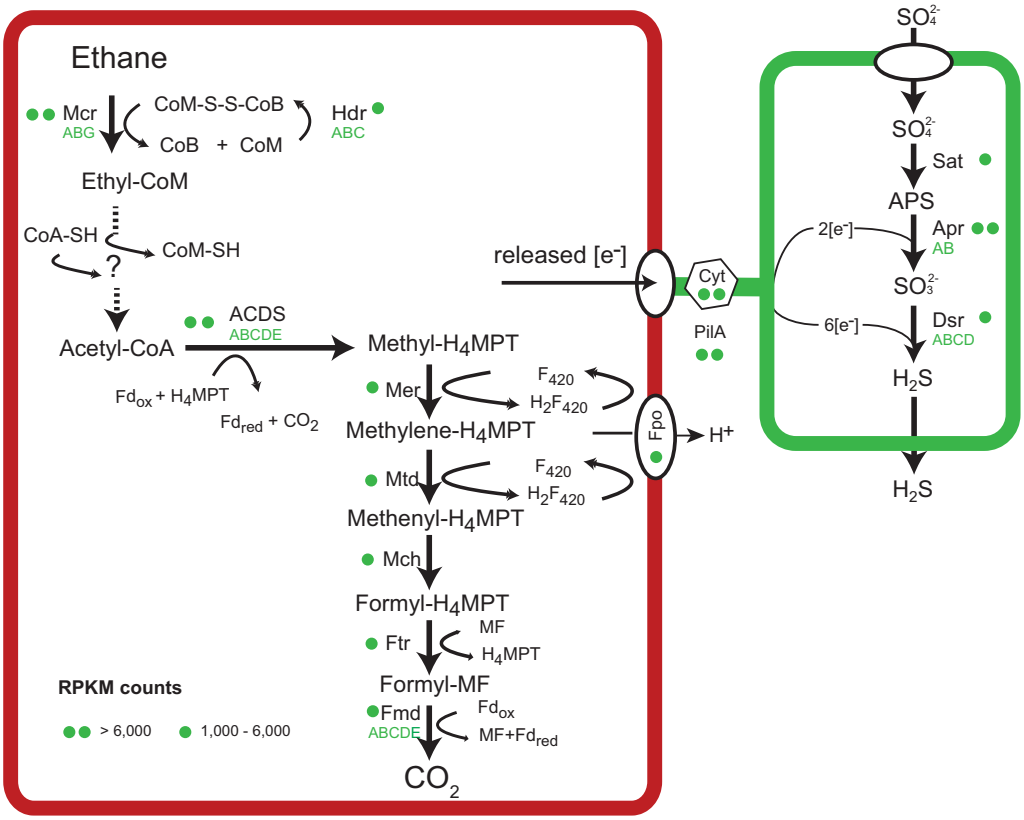

FIG 4 Metabolic model of anaerobic ethane oxidation in "*Ca.* Ethanoperedens thermophilum." Ethane is activated in the ethane-specific MCR. The produced CoM-bound ethyl groups are consecutively oxidized and transformed to CoA-bound acetyl units. Acetyl-CoA is cleaved using the ACDS of the Wood-Ljungdahl pathway. The remaining methyl groups are fully oxidized on the reversed methanogenesis pathway. Similarly to ANME archaea and **"***Ca.* Syntrophoarchaeum," "*Ca.* Ethanoperedens" does not contain a reductive pathway; hence, electrons released during ethane oxidation are transferred to the partner bacterium "*Ca.* Desulfofervidus auxilii." Therefore, in both partners, cytochromes and pili are present and expressed, similarly to what is described in thermophilic consortia performing AOM (22) (for detailed expression patterns, see Table S3).

"*Ca.* Ethanoperedens" is higher than the expression of the multiple *mcr* genes in "*Ca.* Syntrophoarchaeum" but lower than the expression of *mcr* in thermophilic ANME-1 archaea (9, 22). The relatively low expression of *mcr* in short-chain alkane-oxidizing archaea can be explained by the properties of their substrates. Short-chain alkane oxidation releases larger amounts of energy than methane oxidation. Furthermore, the cleavage of C-H bonds in multicarbon compounds requires less energy than the cleavage of C-H bonds of methane (26); hence, less MCR might be required to supply the organism with sufficient energy.

To test the substrates activated by the MCR of "*Ca.* Ethanoperedens," we supplied different alkanes to the active Ethane50 culture replicates and analyzed the extracted metabolites. Cultures supplied with ethane show the *m/z* 168.9988 of the authentic ethyl-CoM standard (Fig. 5A and B), which was not observed in the control incubation

FIG 3 Legend (Continued)
the cluster including the thermophiles of the genus "*Ca.* Ethanoperedens." Sequences from the Ethane50 enrichment are depicted in red, environmental sequences from metagenomes and single-cell genomes from this study are in gray, and "*Ca.* Argoarchaeum ethanivorans" sequences are in blue. The VerArKor cluster contains *mcr*A sequences belonging to the Verstraetearchaeota, Archaeoglobus, and Korarchaeota.

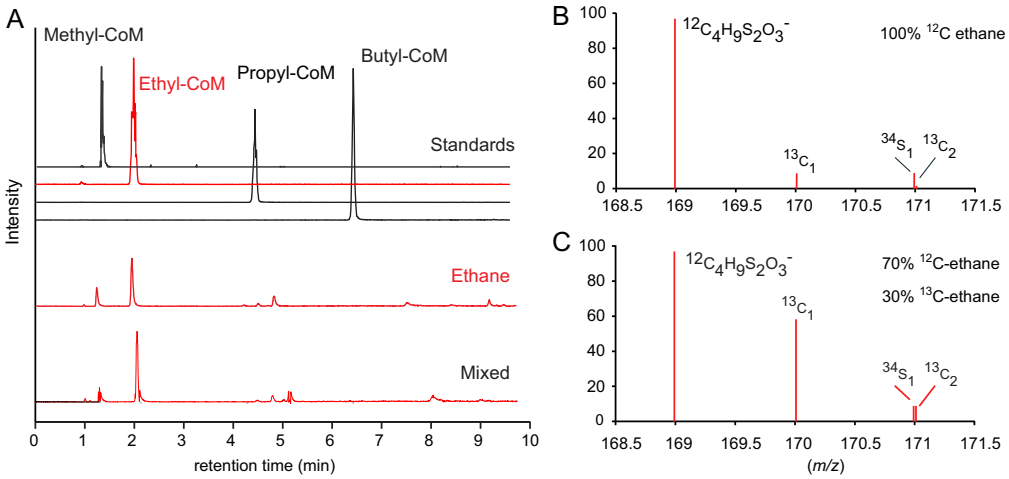

FIG 5 Detection of coenzyme M-bound intermediates in the Ethane50 culture. (A) Top four lines show total ion counts for UHPLC peaks for authentic standards of methyl-, ethyl-, propyl-, and butyl-CoM, respectively, and chromatograms for ethane and mixed alkane gases (methane to butane). (B and C) Mass spectra (*m/z* 168.5 to 171.5) for culture extracts after providing the Ethane50 culture with nonlabeled ethane (B) and 30% ^{13}C-labeled ethane (C). Diagrams show the relative intensities (*y* axes) for ethyl-CoM-H ($^{12}C_4H_9S_2O_3^-$) (calculated *m/z* 168.9988) and its isotopologues with [1-^{13}C]ethyl-CoM or [2-^{13}C]ethyl-CoM or one ^{34}S isotope.

without substrate. Moreover, addition of 30% [1-^{13}C]ethane resulted in the increase of masses expected for [1-^{13}C]ethyl-CoM and [2-^{13}C]ethyl-CoM (Fig. 5C). This confirms that "*Ca.* Ethanoperedens" produces ethyl-CoM from ethane. To test substrate specificity of "*Ca.* Ethanoperedens," we provided culture replicates with four different gaseous alkanes (methane, ethane, propane, and *n*-butane and a mix of all four substrates). Besides the ethane-amended culture, sulfide was produced only in the Ethane50 culture supplied with the substrate mix (Fig. S3). In agreement with this, no other alkyl-CoM variant apart from ethyl-CoM was detected (Fig. 5A). This shows that the MCR of "*Ca.* Ethanoperedens" and most likely all MCR enzymes of GoM-Arc1 archaea (Fig. 3B) activate ethane but no or only trace amounts of methane and other alkanes. The high substrate specificity of the MCR is crucial for GoM-Arc1 archaea, since they lack the fatty acid degradation pathway that is required to degrade butane and propane (9). "*Ca.* Ethanoperedens" contains and expresses a complete methyltransferase (*mtr*). The corresponding enzyme might cleave small amounts of methyl-CoM that might be formed as a side reaction of the MCR. The methyl unit would be directly transferred to the methylene-tetrahydromethanopterin (H_4-MPT) reductase (*mer*) and oxidized in the upstream part of the methanogenesis pathway to CO_2 (Fig. 4).

Based on the observed net reaction and the genomic information, "*Ca.* Ethanoperedens" completely oxidizes ethane to CO_2. In this pathway, coenzyme A-bound acetyl units are oxidized in the Wood-Ljungdahl pathway including the upstream part of the methanogenesis pathway (Fig. 4). Our model, however, does not explain how CoM-bound ethyl groups are oxidized to acetyl units and ligated to CoA. Similar transformations are required in the other multicarbon alkane-oxidizing archaea, such as "*Ca.* Syntrophoarchaeum" and "*Ca.* Argoarchaeum" (5, 9). Those oxidation reactions lack biochemical analogues; hence, genomic information alone allows only indirect hints on their function. In "*Ca.* Ethanoperedens," a release of ethyl units and transformation as free molecules (ethanol to acetate) is unlikely, because a formation of acetyl-CoA from acetate would require CoA ligases, which are not present in the genome. Instead, the transformation of ethyl into acetyl units could be performed by a tungstate-containing aldehyde ferredoxin oxidoreductase (AOR) that could catalyze the oxidation with cofactors such as CoM or CoA. In the archaeon *Pyrococcus furiosus*, AORs transform

aldehydes to the corresponding carboxylic acid (27). Both "*Ca*. Ethanoperedens" and "*Ca.* Argoarchaeum" genomes contain three *aor* copies, and in all cases these genes are located either in close proximity to or on operons with genes of the methanogenesis pathway. We detected a high expression of two of the three *aor* genes (RPKM *aor* = 3,805 and 7,928), indicating a viable function of the enzymes. Likewise, very high protein concentrations of these enzymes were shown for "*Ca*. Argoarchaeum" (5), supporting the hypothesis of a critical function. An *aor* gene is also present in the butane oxidizer "*Ca.* Syntrophoarchaeum," yet its expression is rather moderate (9), which puts in question its role in the catabolic pathway of this organism. In contrast, ANME archaea do not contain or overexpress *aor* genes, likely because the encoded enzymes have no central role in their metabolism. We searched the cell extracts for potential intermediates in the pathway, but based on retention time and mass, we were not able to detect potential intermediates such as ethyl-CoA. Similarly, acetyl-CoA, the substrate of the Wood-Ljungdahl pathway, was not detected. A lack of detection, however, does not exclude those compounds as intermediates. Instead, the compound turnover might be very fast, which could be required for an efficient net reaction. Additionally, a mass spectrometric detection of unknown intermediates could be hindered by compound instability or loss during the extraction. Further metabolite studies and enzyme characterizations are required to understand the role of AOR in alkane oxidation

Acetyl-CoA, the product formed by the above-proposed reactions, can be introduced into the Wood-Ljungdahl pathway. The acetyl group is decarboxylated by the highly expressed acetyl-CoA decarbonylase/synthase (ACDS), and the remaining methyl group is transferred to tetrahydromethanopterin (H_4-MPT). The formed methyl-H_4-MPT can then be further oxidized to CO_2 following the reverse methanogenesis pathway (Fig. 4). "*Ca.* Ethanoperedens" lacks genes for sulfate or nitrate reduction, similarly to other genomes of the GoM-Arc1 clade. The electrons produced in the oxidation of ethane thus need to be transferred to the sulfate-reducing partner bacterium "*Ca*. Desulfofervidus auxilii," as previously shown for the anaerobic oxidation of methane and butane. In cocultures of "*Ca.* Argoarchaeum" and their partner bacteria, Chen and coworkers (5) suggest the transfer of reducing equivalents via zero-valent sulfur between the loosely aggregated "*Ca*. Argoarchaeum" and its partner bacterium, analogous to the hypothesis of Milucka et al. (28). In the Ethane50 culture, such a mode of interaction is highly unlikely, as the partner "*Ca*. Desulfofervidus auxilii" is an obligate sulfate reducer, incapable of sulfur disproportionation (11). Based on genomic information, direct electron transfer appears to be more likely. Alkane-oxidizing archaea and their partner bacterium "*Ca.* Desulfofervidus auxilii," produce cytochromes and pilus-based nanowires when supplied with their substrate (9, 29, 30). Also, "*Ca.* Ethanoperedens" contains 11 different genes for cytochromes with expression values of up to 14,800 RPKM representing some of the highest-expressed genes in the culture (Table S3). Interestingly, "*Ca.* Ethanoperedens" also contains and expresses a type IV pilin protein with a high RPKM value of 11,246. The partner bacterium "*Ca.* Desulfofervidus" also shows a high expression of pili and cytochromes under ethane supply, showing their potential importance for the interaction of these two organisms in the syntrophic coupling of ethane oxidation to sulfate reduction.

Environmental distribution of GoM-Arc1 archaea. 16S rRNA gene sequences clustering with "*Ca.* Ethanoperedens" and "*Ca.* Argoarchaeum" have been found in hydrocarbon-rich marine environments like cold-seep and hot-vent environments, including asphalt seeps in the Gulf of Mexico and the Guaymas Basin hydrothermal vents in the Gulf of California (31–33). In some environments like oil seeps of the Gulf of Mexico and gas-rich barite chimneys of Loki's Castle, 16S rRNA gene surveys have shown that up to 30% of archaeal gene sequences belonged to the GoM-Arc1 clade (12). To estimate absolute abundances and potential partnerships of GoM-Arc1 in the environment, we performed CARD-FISH on samples from different seep and vent sites across the globe (Fig. 6). With up to 10^8 cells per ml, archaea of the GoM-Arc1 clade

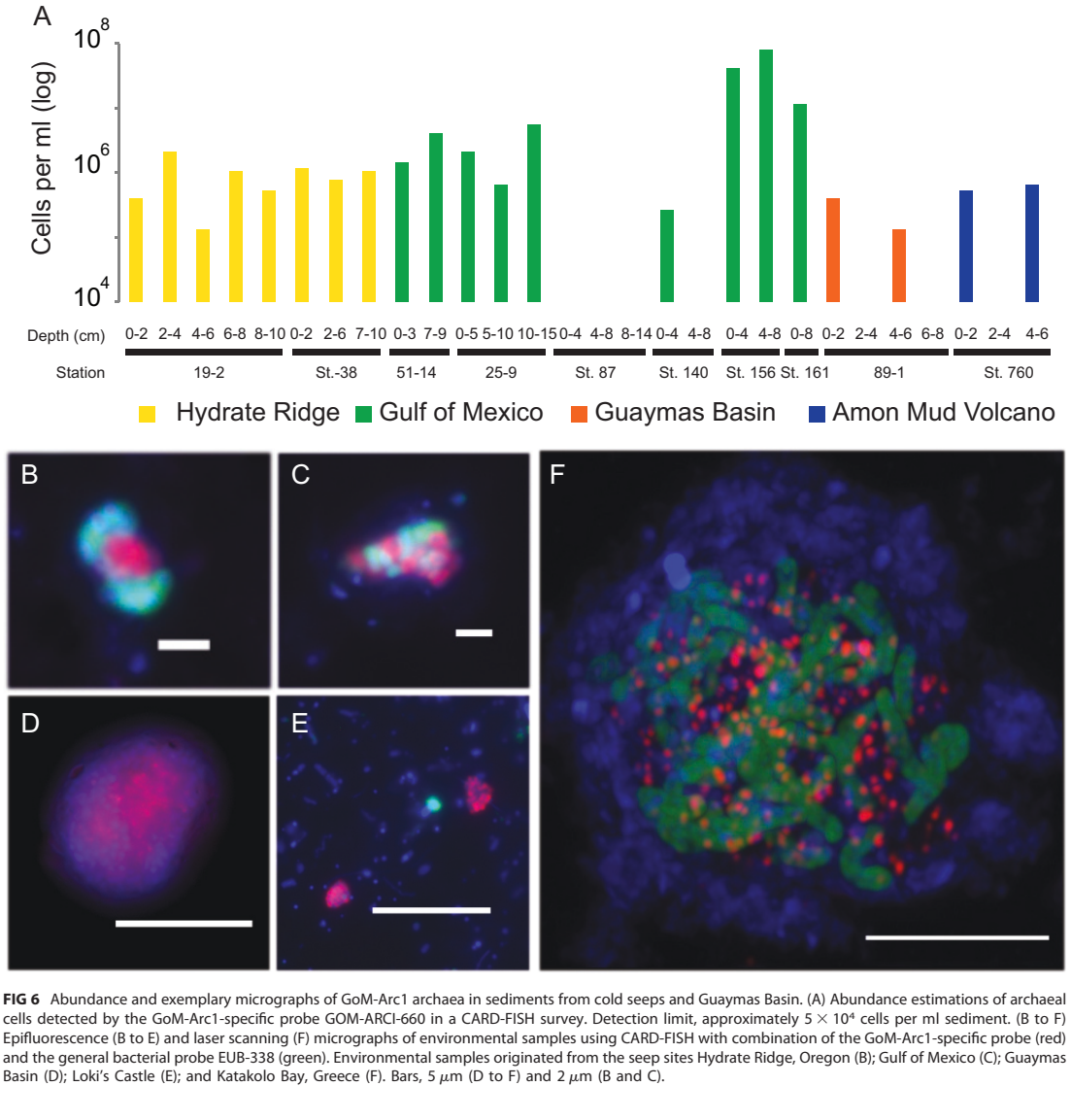

FIG 6 Abundance and exemplary micrographs of GoM-Arc1 archaea in sediments from cold seeps and Guaymas Basin. (A) Abundance estimations of archaeal cells detected by the GoM-Arc1-specific probe GOM-ARCI-660 in a CARD-FISH survey. Detection limit, approximately 5×10^4 cells per ml sediment. (B to F) Epifluorescence (B to E) and laser scanning (F) micrographs of environmental samples using CARD-FISH with combination of the GoM-Arc1-specific probe (red) and the general bacterial probe EUB-338 (green). Environmental samples originated from the seep sites Hydrate Ridge, Oregon (B); Gulf of Mexico (C); Guaymas Basin (D); Loki's Castle (E); and Katakolo Bay, Greece (F). Bars, 5 μm (D to F) and 2 μm (B and C).

were particularly abundant in cold-seep sediments in the northern Gulf of Mexico (station 156). This cold seep transports thermogenic hydrocarbon gases that are particularly enriched in short-chain alkanes (34, 35). Other cold-seep and hot-vent sediments from the Guaymas Basin, Hydrate Ridge, and Amon Mud Volcano contain between 10^5 and 10^6 GoM-Arc1 cells per ml of sediment, which represents 1 to 5% of the archaeal community (Fig. 6A). At all sites, we found that GoM-Arc1 associates with partner bacteria. At the hydrothermally heated site in the Guaymas Basin, GoM-Arc1 aggregated with "*Ca.* Desulfofervidus," the partner bacterium of the Ethane37 and Ethane50 cultures. At Loki's Castle, GoM-Arc1 and "*Ca.* Desulfofervidus" were cooccurring in barite chimneys based on sequence information, yet they were not found to form the same tight consortia as at other sites. At the temperate site Katakolo Bay in

Greece, GoM-Arc1 archaea formed consortia with very large, yet unidentified vibrioform bacteria (Fig. 6B to F). These cells hybridized with a probe for *Deltaproteobacteria* but not with probes for known partner bacteria (for probes, see Table S1). At the cold-seep sites, the associated cells could not be stained with probes for the known partner bacteria of cold-adapted ANME, including SEEP-SRB1 and SEEP-SRB2, and also not with that for "*Ca.* Desulfofervidus." It remains an important question as to how the archaea can select only a few specific types of bacteria as partners in the anaerobic alkane oxidation and for which specific traits they are selected. Based on their global presence in hydrocarbon-rich environments, GoM-Arc1 archaea could be considered key players in the anaerobic oxidation of ethane in marine sediments. Their role would be similar to the role of ANME archaea in AOM.

Future possible applications of "*Ca.* Ethanoperedens." Archaea of the GoM-Arc1 cluster are likely the dominant, if not the only, organisms capable of anaerobic oxidation of ethane on the global seafloor. An important further task is to assess deep oil and gas reservoirs for their diversity of ethane oxidizers. The rapid growth of "*Ca.* Ethanoperedens" and the streamlined genome make it a model organism for the study of anaerobic ethanotrophy in archaea. The biochemistry of short-chain alkane-oxidizing archaea will be of high interest for future biotechnological applications. An organism using the metabolism of "*Ca*. Ethanoperedens" in the reverse direction should be able to produce ethane, similarly to methane production by methanogens. Yet, there is scarce isotopic evidence for the existence of ethanogenic organisms in nature (36). Furthermore, under common environmental conditions thermodynamics favor the production of methane from inorganic carbon over the production of ethane. To test the general reversibility of the ethane oxidation pathway, we incubated the active Ethane50 culture with ^{13}C-labeled inorganic carbon and traced the label transfer into ethane. Within 18 days, [δ-^{13}C]ethane values increased from −3‰ to +120‰, whereas isotopic compositions in the nonlabeled culture remained stable (Fig. S4). Considering the forward rate and ethane stock, the back reaction amounts to 1.5‰ to 3% of the forward reaction, which is in the range for back fluxes of carbon measured in AOM (21, 37). This experiment shows that the ethane oxidation pathway is fully reversible. To test the net ethane formation in the Ethane50 culture, we removed sulfate from culture aliquots and added hydrogen as electron donor. These cultures formed between 1 and 17 μmol liter^{-1} ethane within 27 days (Table S6). The ethane production was, however, a very small fraction (0.08%) of the ethane oxidation rate in replicate incubations with ethane and sulfate. No ethane was formed in the presence of hydrogen and sulfate. We interpret the ethane formation in the culture as enzymatic effect in the ethane-oxidizing consortia. Bacterial hydrogenases will fuel reducing equivalents into the pathway, which may ultimately lead to the reduction of carbon dioxide to ethane. A growing culture could not be established under these conditions, however, the experiments suggest that related or genetically modified methanogenic archaea could thrive as ethanogens. A complete understanding of the pathway and enzymes of GoM-Arc1 archaea, however, is required to develop the biotechnological potential of an ethanogenic organism. To allow energy-conserving electron flows in this organism, a genetically modified methanogen should be used as host organism. For a targeted modification of such archaea, the pathway of ethane oxidation must be completely understood, and research should focus especially on the transformation of coenzyme M-bound ethyl units to coenzyme A-bound acetyl units.

MATERIALS AND METHODS

Inoculum and establishment of alkane-oxidizing cultures. This study is based on samples collected during R/V *Atlantis* cruise AT37-06 with submersible *Alvin* to the Guaymas Basin vent area in December 2016 (for locations, see Table S4 in the supplemental material). A sediment sample was collected by push coring within a hydrothermal area marked by conspicuous orange-type *Beggiatoa* mats (dive 4869, core 26, 27′0.4505′N 111°24.5389′W, 2,001-m water depth, 20 December 2016). The sampling site was located in the hydrothermal area where, during a previous *Alvin* visit, sediment cores containing locally ^{13}C-enriched ethane had indicated ethane-oxidizing microbial activity (33). *In situ* temperature measurements using the *Alvin* heat flow probe revealed a steep temperature gradient reaching 80°C at 30- to 40-cm sediment depth. The retrieved samples contained large amounts of natural

gas as observed by bubble formation. Soon after recovery, the overlying *Beggiatoa* mat was removed, and the top 10 cm of the sediment was filled into 250-ml Duran bottles, which were gastight sealed with butyl rubber stoppers. In the home laboratory, sediments were transferred into an anoxic chamber. There, a sediment slurry (20% sediment and 80% medium) was produced with synthetic sulfate reducer (SR) medium (pH 7.0) (38, 39) and distributed into replicate bottles (sediment dry weight per bottle, 1.45 g). These bottles were amended with methane or ethane (0.2 MPa) or kept with an N_2 atmosphere without alkane substrate. These samples were incubated at 37°C, 50°C, and 70°C. To determine substrate-dependent sulfide production rates, sulfide concentrations were measured every 2 to 4 weeks using a copper sulfate assay (40). Ethane-dependent sulfide production was observed at 37°C and 50°C but not at 70°C. When the sulfide concentration exceeded 15 mM, the cultures were diluted (1:3) in SR medium and resupplied with ethane. Repeated dilutions led to virtually sediment-free, highly active cultures within 18 months. A slight decrease of the initial pH value to 6.5 led to increased ethane oxidation activity and faster growth in the culture.

Quantitative substrate turnover experiment. The Ethane50 culture was equally distributed in six 150-ml serum flasks using 20 ml inoculum and 80 ml medium. Three replicate cultures were amended with 0.05-MPa ethane in 0.1-MPa N_2-CO_2, while 3 negative controls were amended with 0.15-MPa N_2-CO_2. Both treatments were incubated at 50°C. Weekly, 0.5-ml headspace gas samples were analyzed for ethane content using an Agilent 6890 gas chromatograph in splitless mode equipped with a packed column (Supelco Porapak Q, 6 ft by 1/8 ft by 2.1-mm stainless steel column, oven temperature 80°C). The carrier gas was helium (20 ml per minute), and hydrocarbons were detected by flame ionization detection. Each sample was analyzed in triplicates and quantified against ethane standards of 5, 10, and 100%. Derived concentrations were converted into molar amounts by taking the headspace size, pressure, and temperature into account. Results were corrected for sampled volumes. Sulfide concentrations were measured as described above. To determine sulfate concentrations, 1 ml of sample was fixed in 0.5 ml zinc acetate. Samples were diluted 1:50 with deionized water (MilliQ grade; >18.5 MΩ), and samples were measured using nonsuppressed ion chromatography (Metrohm 930 Compact IC Metrosep A PCC HC/4.0 preconcentration and Metrosep A Supp 5-150/4.0 chromatography column).

DNA extraction, 16S rRNA gene amplification, and tag sequencing. DNA was extracted from the different cultures and the original sediment with the Mo Bio Power soil DNA extraction kit (Mo Bio Laboratories Inc., Carlsbad, CA, USA) using a modified protocol. Twenty milliliters of the culture was pelleted via centrifugation (5,000 × *g*; 10 min). The pellet was resuspended in phosphate-buffered saline (PBS) and transferred to the PowerBeat tube (Mo Bio Power soil DNA extraction kit; Mo Bio Laboratories Inc., Carlsbad, CA, USA). The cells were lysed by three cycles of freezing in liquid nitrogen (20 s) and thawing (5 min at 60°C). After cooling down to room temperature, 10 μl of proteinase K (20 mg ml^{-1}) was added and incubated for 30 min at 55°C. Subsequently, 60 μl of solution C1 (contains SDS) was added, and the tubes were briefly centrifuged. The samples were homogenized 2 times for 30 s at 6.0 m/s using a FastPrep-24 instrument (MP Biomedicals, Eschwege, Germany). In between the runs, the samples were kept on ice for 5 min. After these steps, the protocol was followed further according to the manufacturer's recommendations. DNA concentrations were measured using a Qubit 2.0 instrument (Invitrogen, Carlsbad, CA, USA). Two nanograms of DNA was used for amplicon PCR, and the product was used for 16S rRNA gene amplicon library preparation according to the 16S metagenomic sequencing library preparation guide provided by Illumina. The Arch349F-Arch915R primer pair was used to amplify the archaeal V3-V5 region, and the Bact341F-Bact785R primer pair was used for the bacterial V3-V4 region (see Table S1 in the supplemental material). Amplicon libraries for both *Archaea* and *Bacteria* were sequenced on an Illumina MiSeq instrument (2- by 300-bp paired-end run, v3 chemistry) at CeBiTec (Bielefeld, Germany). After analysis, adapters and primer sequences were clipped from the retrieved sequences using cutadapt (41) (v1.16) with 0.16 (−e) as maximum allowed error rate and no indels allowed. Resulting reads were analyzed using the SILVAngs pipeline using the default parameters (https://ngs.arb-silva.de/silvangs/) (42–44).

Extraction of high-quality DNA, library preparation, and sequencing of gDNA. Biomass from 200 ml of the Ethane50 and Ethane37 cultures was pelleted by centrifugation and resuspended in 450 μl of extraction buffer. Genomic DNA was retrieved based on a modified version of the protocol described in reference 45, including three extraction steps. Resuspended pellet was frozen in liquid N_2 and thawed in a water bath at 65°C. Another 1,350 μl of extraction buffer was added. Cells were digested enzymatically by proteinase K (addition of 60 μl of 20 mg/ml, incubation at 37°C for 1.5 h under constant shaking at 225 rpm) and chemically lysed (addition of 300 μl 20% SDS for 2 h at 65°C). Samples were centrifuged (20 min, 13,000 × *g*), and the clear supernatant was transferred to a new tube. Two milliliters of chloroform-isoamyl alcohol (16:1, vol/vol) was added to the extract, mixed by inverting, and centrifuged for 20 min at 13,000 × *g*. The aqueous phase was transferred to a new tube, mixed with 0.6 volumes of isopropanol, and stored overnight at −20°C for DNA precipitation. The DNA was redissolved in water at 65°C for 5 min and then centrifuged for 40 min at 13,000 × *g*. The supernatant was removed, and the pellet was washed with ice-cold ethanol (80%) and subjected to centrifugation for 10 min at 13,000 × *g*. The ethanol was removed, and the dried pellet was resuspended in PCR-grade water. This procedure yielded 114 μg and 145 μg high-quality genomic DNA (gDNA) from the Ethane37 and the Ethane50 cultures, respectively. Samples were sequenced with Pacific Biosciences Sequel as a long amplicon (4 to 10 kb) and long-read gDNA library at the Max Planck-Genome-Centre (Cologne, Germany). To evaluate the microbial community, we extracted 16S rRNA gene reads using Metaxa2 (46) and taxonomically classified them using the SILVA ACT online service (47). For assembly, either HGAP4 (implemented in the SMRTlink software by PacBio) or Canu (https://github.com/marbl/canu) was used. The closed GoM-Arc1 genome from the Ethane37 culture was prepared manually by the combination of assemblies from the

two above-mentioned tools. The final genome was polished using the resequencing tool included in the SMRTLink software by PacBio. For noncircularized *de novo* genomes, the resulting contigs were mapped via minimap2 (https://github.com/lh3/minimap2; parameter: '-x asm10') to a reference genome. The reference consensus genomes were prepared using the resequencing tool implemented in the SMRTLink software of PacBio using either the circular GoM-Arc1 *de novo* genome from this study or the publicly available "*Ca.* Desulfofervidus" genome (accession no. NZ_CP013015.1) as reference. Final genomes were automatically annotated using Prokka (48), and the annotation was refined manually using the NCBI BLAST interface (49). Average nucleotide and amino acid identities were calculated using Enveomics tools (50).

Single-cell genomics. Anoxic sediment aliquots were shipped to the Bigelow Laboratory Single Cell Genomics Center (SCGC; https://scgc.bigelow.org). Cells were separated, sorted, and lysed, and total DNA was amplified by multiple displacement amplification. Single-cell DNA was characterized by 16S rRNA gene tag sequences (12, 51). The single-cell amplified DNA from Gulf of Mexico samples was analyzed and sequenced as described before in reference 12. Single-cell amplified DNA from Amon Mud Volcano AAA-792_C10 was sequenced with HiSeq 3000 and MiSeq technology, and reads were assembled using SPAdes (52) with the single-cell mode. Assembled reads were binned based on tetranucleotides, coverage, and taxonomy using MetaWatt (53). The final SAG was evaluated for completeness and contamination using CheckM (54). Genome annotation was performed as described above.

Extraction of RNA, reverse transcription, sequencing, and read processing. Extraction and sequencing of total RNA was performed in triplicates. RNA was extracted from 150-ml active Ethane50 culture grown in separate bottles at 50°C. Total RNA was extracted and purified as described in reference 9 using the Quick-RNA miniprep kit (Zymo Research, Irvine, CA, USA) and RNeasy MinElute cleanup kit (Qiagen, Hilden, Germany). Per sample, at least 150 ng of high-quality RNA was obtained. The RNA library was prepared with the TruSeq stranded total RNA kit (Illumina). An rRNA depletion step was omitted. The samples were sequenced on an Illumina NextSeq with v2 chemistry and 1- by 150-bp read length. The sequencing produced ~50-Gb reads per sample. Adapters and contaminant sequences were removed, and reads were quality trimmed to Q10 using bbduk v36.49 from the BBMAP package. For phylogenetic analysis of the active community, 16S rRNA reads were recruited and classified based on SSU SILVA release 132 (47) using phyloFlash (55). Trimmed reads were mapped to the closed genomes of "*Candidatus* Ethanoperedens thermophilum" and "*Ca.* Desulfofervidus" using Geneious Prime 2019.2.1 (Biomatters, Ltd., Auckland, New Zealand) with a minimum mapping quality of 30%. The expression level of each gene was quantified by counting the number of unambiguously mapped reads per gene using Geneious. To consider gene length, read counts were converted to reads per kilobase per million mapped reads (RPKM).

Phylogenetic analysis of 16S rRNA genes, marker genes, and *mcr*A amino acid sequences. A 16S rRNA gene-based phylogenetic tree was calculated using publicly available 16S rRNA sequences from the SSU Ref NR 128 SILVA database (42). The tree was constructed using ARB (56) and the FastTree 2 package (57) using a 50% similarity filter. Sequence length for all 16S rRNA genes was at least 1,100 bp. After tree calculation, partial sequences retrieved from single cells were included into the tree. ARB (56) was used for visualization of the final tree. The marker gene tree was calculated using 126 publicly available genomes and genomes presented in this study. The tree was calculated based on aligned amino acid sequences of 32 marker genes picked from known archaeal marker genes (Table S5) (58). For the preparation of the aligned marker gene amino acid sequences, we used the phylogenomic workflow of Anvi'o 5.5 (59). The marker gene phylogeny was calculated using RAxML version 8.2.10 (60) with the PROTGAMMAAUTO model and LG likelihood amino acid substitution. One thousand fast bootstraps were calculated to find the optimal tree according to RAxML convergence criteria. The software iTOL v3 was used for tree visualization (61). The *mcr*A amino acid phylogenetic tree was calculated using 358 sequences that are publicly available or presented in this study. The sequences were manually aligned using the Geneious Prime 2019.2.1 (Biomatters, Ltd., Auckland, New Zealand) interface, and 1,060 amino acid positions were considered. The aligned sequences were masked using Zorro (https://sourceforge.net/projects/probmask/), and a phylogenetic tree was calculated using RAxML version 8.2.10 (60) using the PROTGAMMAAUTO model and LG likelihood amino acid substitution. One thousand fast bootstraps were calculated. The tree was visualized with iTOL v3 (61).

Catalyzed reported deposition fluorescence *in situ* hybridization (CARD-FISH). Aliquots of the Ethane50 culture and environmental samples were fixed for 1 h in 2% formaldehyde, washed three times in PBS (pH 7.4)-ethanol (1:1), and stored in this solution. Aliquots were sonicated (30 s; 20% power; 20% cycle; Sonoplus HD70; Bandelin) and filtered on GTTP polycarbonate filters (0.2-μm pore size; Millipore, Darmstadt, Germany). CARD-FISH was performed according to reference 62 including the following modifications. Cells were permeabilized with a lysozyme solution (PBS [pH 7.4], 0.005 M EDTA [pH 8.0], 0.02 M Tris-HCl [pH 8.0], 10 mg ml^{-1} lysozyme; Sigma-Aldrich) at 37°C for 60 min followed by proteinase K solution treatment (7.5 μg ml^{-1} proteinase K [Merck, Darmstadt, Germany] in PBS [pH 7.4], 0.005 M EDTA [pH 8.0], 0.02 M Tris-HCl [pH 8.0]) at room temperature for 5 min. Endogenous peroxidases were inactivated by incubation in a solution of 0.15% H_2O_2 in methanol for 30 min at room temperature. Horseradish peroxidase (HRP)-labeled probes were purchased from Biomers.net (Ulm, Germany). Tyramides were labeled with Alexa Fluor 594 or Alexa Fluor 488. All probes were applied as listed in Table S1. For double hybridization, the peroxidases from the first hybridization were inactivated in 0.15% H_2O_2 in methanol for 30 min at room temperature. Finally, the filters were counterstained with DAPI (4′,6′-diamino-2-phenylindole) and analyzed by epifluorescence microscopy (Axiophot II imaging; Zeiss, Germany). Selected filters were analyzed by confocal laser scanning microscopy (LSM 780; Zeiss, Germany) including the Airyscan technology.

Synthesis of authentic standards for metabolites. To produce alkyl-CoM standards, 1 g of coenzyme M was dissolved in 40 ml 30% (vol/vol) ammonium hydroxide solution, and to this solution 1.8 to 2 g of bromoethane, bromopropane, or bromobutane was added. The mixture was incubated for 5 h at room temperature under vigorous shaking and then acidified to pH 1 with HCl. The produced standard had a concentration of approximately 25 mg ml^{-1}, which for mass spectrometry measurements was diluted to 10 μg ml^{-1}.

Extraction of metabolites from the Ethane50 culture. In the anoxic chamber, 20 ml of Ethane50 culture was harvested into 50-ml centrifuge tubes. Tubes were centrifuged at 3,000 relative centrifugal force (rcf) for 10 min, and the supernatant was removed. The pellet was resuspended in 1 ml acetonitrile-methanol-water (4:4:2, vol/vol/vol) mixture in lysing matrix tubes (MP Biomedicals, Eschwege, Germany) with glass beads. Afterward, the tubes were removed from the anoxic chamber and the samples were mechanically lysed in a FastPrep homogenizer (MP Bio) with 5 cycles with 6 M/s for 50 s and cooling on ice for 5 min between the homogenization steps. Finally, the samples were centrifuged for 5 min at 13,000 $\times$ *g*, and the supernatant was transferred to a new tube and stored at −20°C.

Solvents for LC-MS/MS. All organic solvents were liquid chromatography-mass spectrometry (LC-MS) grade, using acetonitrile (ACN; BioSolve, Valkenswaard, The Netherlands), isopropanol (IPA; BioSolve, Valkenswaard, The Netherlands), and formic acid (FA; BioSolve, Valkenswaard, The Netherlands). Water was deionized by using the Astacus MembraPure system (MembraPure GmbH, Berlin, Germany).

High-resolution LC-MS/MS. The analysis was performed using a QExactive Plus Orbitrap (Thermo Fisher Scientific) equipped with a heated electrospray ionization (HESI) probe and a Vanquish Horizon ultra-high-performance liquid chromatography (UHPLC) system (Thermo Fisher Scientific). The metabolites from cell extracts were separated on an Accucore C_{30} column (150 by 2.1 mm, 2.6 μm; Thermo Fisher Scientific), at 40°C, using a solvent gradient created from the mixture of buffer A (5% acetonitrile in water, 0.1% formic acid) and buffer B (90/10 IPA-ACN, 0.1% formic acid). The solvent gradient was the following: fraction B of 0, 0, 16, 45, 52, 58, 66, 70, 75, 97, 97.15, and 0%, at −2 min (prerun equilibration) and 0, 2, 5.5, 9, 12, 14, 16, 18, 22, 25, 32.5, 33, 34.4, and 36 min of each run, and a constant flow rate of 350 μl min^{-1}. The sample injection volume was 10 μl. The MS measurements were acquired in negative mode for a mass detection range of 70 to 1,000 Da. In alternation, a full MS and MS/MS scans of the eight most abundant precursor ions were acquired in negative mode. Dynamic exclusion was enabled for 30 s. The settings for full-range MS1 were mass resolution of 70,000 at 200 *m/z*, automatic gain control (AGC) target of 5×10^5, and injection time of 65 ms. Each MS1 was followed by MS2 scans with the following settings: mass resolution of 35,000 at 200 *m/z*, AGC target of 1×10^6, injection time of 75 ms, loop count of 8, isolation window of 1 Da, and collision energy set to 30 eV.

Determination of carbon back flux into the ethane pool. Aliquots of active AOM culture (50 ml) were transferred into 70-ml serum bottles with N_2:CO_2 headspace. In the stable-isotope probing (SIP) experiment, addition of 99% ^{13}C-labeled dissolved inorganic carbon (DIC) (1 ml, 350 mM) led to δ-^{13}C-DIC values of +25,000‰ as measured by cavity ringdown spectrometry. Ethane (2 atm = 1.8 mM) was added to both experiments, and cultures were stored at 50°C. To determine the overall ethane oxidation activity, sulfide concentrations were measured every few days as described above and converted to ethane oxidation rates using ratios in the chemical formula in Results and Discussion. To measure the development of ethane δ-^{13}C values, 1 ml of the gas phase was sampled every few days and stored in 10-ml Exetainer vials with 2 ml NaOH, and ethane isotopic composition was measured using gas chromatography coupled via a combustion interface to isotope ratio mass spectrometry (Trace GC Ultra with Carboxene-1006 Plot column, 40°C oven temp., carrier gas He with flow rate 3 ml min^{-1}; coupled via GC IsoLink to Delta V isotope ratio MS).

Net ethane production test. To test for net ethane production, in 156-ml serum flasks replicate incubations with about 0.5 g (wet weight) active Ethane50 culture in 100 ml of sulfate-free medium was prepared. Four different conditions were tested in three biological replicates with the addition of (i) 1.5 atm H_2; (ii) conditions replicating the first but with only 0.05 g biomass; (iii) 1.5 atm H_2 plus 28 mM sulfate; and (iv) an activity control with addition of sulfate and 1.5 atm ethane. Cultures were incubated over 27 days at 50°C, and sulfate and ethane concentrations were monitored as described above.

Data availability. All sequence data are archived in the ENA database under the INSDC accession numbers PRJEB36446 and PRJEB36096. Sequence data from Loki's Castle are archived under NCBI BioSample number SAMN13220465. The 16S rRNA gene amplicon reads have been submitted to the NCBI Sequence Read Archive (SRA) database under the accession number SRR8089822. All sequence information has been submitted using the data brokerage service of the German Federation for Biological Data (GFBio) (63), in compliance with the Minimal Information about any (X) Sequence (MIxS) standard (64), but some data are still under ENA embargo.

SUPPLEMENTAL MATERIAL

Supplemental material is available online only.

FIG S1, EPS file, 1 MB.

FIG S2, EPS file, 1.2 MB.

FIG S3, EPS file, 0.4 MB.

FIG S4, EPS file, 0.5 MB.

TABLE S1, XLSX file, 0.01 MB.

TABLE S2, XLSX file, 0.03 MB.

TABLE S3, XLSX file, 0.4 MB.

TABLE S4, XLSX file, 0.02 MB.
TABLE S5, XLSX file, 0.01 MB.
TABLE S6, XLSX file, 0.02 MB.

ACKNOWLEDGMENTS

We thank Susanne Menger for her contribution in culturing the target organisms, Janine Beckmann for metabolite analysis, and Heidi Taubner, Jenny Wendt, and Xavier Prieto Mollar (Hinrichs Lab, MARUM, University of Bremen) for performing isotope analyses. We are indebted to Andreas Ellrott for assisting in confocal microscopy and Gabriele Klockgether for her kind help with gas chromatography. We thank Matthew Schechter for analyzing the community compositions in a lab rotation. We also thank Tristan Wagner for vivid discussions on the metabolism of Ethanoperedens. We thank Bigelow SCGC for their work in sequencing single-cell genomes used in this study. We are enormously grateful to I. Kostadinov and the GFBIO for support and help during data submission. We are indebted to the crew and science party of R/V *Atlantis* and HOV *Alvin* expedition AT37-06.

This study was funded by the Max Planck Society and the DFG Clusters of Excellence 'The Ocean in the Earth System' and 'The Ocean Floor—Earth's Uncharted Interface' at MARUM, University of Bremen. Additional funds came from the ERC ABYSS (grant agreement no. 294757) to A.B. R/V *Atlantis* and HOV *Alvin* expedition AT37-6 was funded by NSF grant 1357238 to A. Teske.

C.J.H., K.K., and G.W. designed the research. A.T. and G.W. retrieved the original Guaymas Basin sediment sample. F.V., K.-M.V., R.S., I.H.S., and A.B. retrieved additional samples. C.J.H. and G.W. performed the cultivation, physiology, and isotope experiments. C.J.H., F.V., K.-M.V., and K.K. performed fluorescence microscopy. C.J.H., M.L., and G.W. performed metabolite analysis. C.J.H., R.L.-P., R.A., K.K., and G.W. performed metagenomic and phylogenetic analyses and developed the metabolic model, C.J.H. and G.W. wrote the manuscript with contributions from all coauthors.

REFERENCES

1. Hinrichs KU, Boetius A. 2002. The anaerobic oxidation of methane: new insights in microbial ecology and biogeochemistry, p 457–477. *In* Wefer G, Billet D, Hebbeln D, Jorgensen BB, Schlüter M, Weering TCEV (ed), Ocean margin systems. Springer-Verlag, Berlin, Germany.
2. Reeburgh WS. 2007. Oceanic methane biogeochemistry. Chem Rev 107:486–513. https://doi.org/10.1021/cr050362v.
3. Rabus R, Wilkes H, Behrends A, Armstroff A, Fischer T, Pierik AJ, Widdel F. 2001. Anaerobic initial reaction of n-alkanes in a denitrifying bacterium: evidence for (1-methylpentyl)succinate as initial product and for involvement of an organic radical in n-hexane metabolism. J Bacteriol 183:1707–1715. https://doi.org/10.1128/JB.183.5.1707-1715.2001.
4. Kniemeyer O, Musat F, Sievert SM, Knittel K, Wilkes H, Blumenberg M, Michaelis W, Classen A, Bolm C, Joye SB, Widdel F. 2007. Anaerobic oxidation of short-chain hydrocarbons by marine sulphate-reducing bacteria. Nature 449:898–910. https://doi.org/10.1038/nature06200.
5. Chen S-C, Musat N, Lechtenfeld OJ, Paschke H, Schmidt M, Said N, Popp D, Calabrese F, Stryhanyuk H, Jaekel U, Zhu Y-G, Joye SB, Richnow H-H, Widdel F, Musat F. 2019. Anaerobic oxidation of ethane by archaea from a marine hydrocarbon seep. Nature 568:108–111. https://doi.org/10.1038/s41586-019-1063-0.
6. Boetius A, Ravenschlag K, Schubert CJ, Rickert D, Widdel F, Gieseke A, Amann R, Jørgensen BB, Witte U, Pfannkuche O. 2000. A marine microbial consortium apparently mediating anaerobic oxidation of methane. Nature 407:623–626. https://doi.org/10.1038/35036572.
7. Shima S, Krueger M, Weinert T, Demmer U, Kahnt J, Thauer RK, Ermler U. 2011. Structure of a methyl-coenzyme M reductase from Black Sea mats that oxidize methane anaerobically. Nature 481:98–101. https://doi.org/10.1038/nature10663.
8. Hallam SJ. 2004. Reverse methanogenesis: testing the hypothesis with environmental genomics. Science 305:1457–1462. https://doi.org/10.1126/science.1100025.
9. Laso-Pérez R, Wegener G, Knittel K, Widdel F, Harding KJ, Krukenberg V, Meier DV, Richter M, Tegetmeyer HE, Riedel D, Richnow H-H, Adrian L, Reemtsma T, Lechtenfeld OJ, Musat F. 2016. Thermophilic archaea activate butane via alkyl-coenzyme M formation. Nature 539:396–401. https://doi.org/10.1038/nature20152.
10. Holler T, Widdel F, Knittel K, Amann R, Kellermann MY, Hinrichs K-U, Teske A, Boetius A, Wegener G. 2011. Thermophilic anaerobic oxidation of methane by marine microbial consortia. ISME J 5:1946–1956. https://doi.org/10.1038/ismej.2011.77.
11. Krukenberg V, Harding K, Richter M, Glöckner FO, Gruber-Vodicka HR, Adam B, Berg JS, Knittel K, Tegetmeyer HE, Boetius A, Wegener G. 2016. Candidatus Desulfofervidus auxilii, a hydrogenotrophic sulfate-reducing bacterium involved in the thermophilic anaerobic oxidation of methane. Environ Microbiol 18:3073–3091. https://doi.org/10.1111/1462-2920.13283.
12. Laso-Perez R, Hahn C, van Vliet DM, Tegetmeyer HE, Schubotz F, Smit NT, Pape T, Sahling H, Bohrmann G, Boetius A, Knittel K, Wegener G. 2019. Anaerobic degradation of nonmethane alkanes by "*Candidatus* Methanoliparia" in hydrocarbon seeps of the Gulf of Mexico. mBio 10:e01814-19. https://doi.org/10.1128/mBio.01814-19.
13. Walker DJ, Adhikari RY, Holmes DE, Ward JE, Woodard TL, Nevin KP, Lovley DR. 2018. Electrically conductive pili from pilin genes of phylogenetically diverse microorganisms. ISME J 12:48–58. https://doi.org/10.1038/ismej.2017.141.
14. Adams MM, Hoarfrost AL, Bose A, Joye SB, Girguis PR. 2013. Anaerobic oxidation of short-chain alkanes in hydrothermal sediments: potential influences on sulfur cycling and microbial diversity. Front Microbiol 4:110. https://doi.org/10.3389/fmicb.2013.00110.
15. Bose A, Rogers DR, Adams MM, Joye SB, Girguis PR. 2013. Geomicrobiological linkages between short-chain alkane consumption and sulfate reduction rates in seep sediments. Front Microbiol 4:386. https://doi.org/10.3389/fmicb.2013.00386.
16. Dombrowski N, Seitz KW, Teske AP, Baker BJ. 2017. Genomic insights into potential interdependencies in microbial hydrocarbon and nutrient

cycling in hydrothermal sediments. Microbiome 5:106. https://doi.org/10.1186/s40168-017-0322-2.
17. Borrel G, Adam PS, McKay LJ, Chen L-X, Sierra-García IN, Sieber CMK, Letourneur Q, Ghozlane A, Andersen GL, Li W-J, Hallam SJ, Muyzer G, de Oliveira VM, Inskeep WP, Banfield JF, Gribaldo S. 2019. Wide diversity of methane and short-chain alkane metabolisms in uncultured archaea. Nat Microbiol 4:603–613. https://doi.org/10.1038/s41564-019-0363-3.
18. Dombrowski N, Teske AP, Baker BJ. 2018. Expansive microbial metabolic versatility and biodiversity in dynamic Guaymas Basin hydrothermal sediments. Nat Commun 9:4999. https://doi.org/10.1038/s41467-018-07418-0.
19. Nauhaus K, Albrecht M, Elvert M, Boetius A, Widdel F. 2007. In vitro cell growth of marine archaeal-bacterial consortia during anaerobic oxidation of methane with sulfate. Environ Microbiol 9:187–196. https://doi.org/10.1111/j.1462-2920.2006.01127.x.
20. Knittel K, Boetius A. 2009. Anaerobic oxidation of methane: progress with an unknown process. Annu Rev Microbiol 63:311–334. https://doi.org/10.1146/annurev.micro.61.080706.093130.
21. Wegener G, Krukenberg V, Ruff SE, Kellermann MY, Knittel K. 2016. Metabolic capabilities of microorganisms involved in and associated with the anaerobic oxidation of methane. Front Microbiol 7:46. https://doi.org/10.3389/fmicb.2016.00046.
22. Krukenberg V, Riedel D, Gruber-Vodicka HR, Buttigieg PL, Tegetmeyer HE, Boetius A, Wegener G. 2018. Gene expression and ultrastructure of meso- and thermophilic methanotrophic consortia. Environ Microbiol 20:1651–1666. https://doi.org/10.1111/1462-2920.14077.
23. Haroon MF, Hu S, Shi Y, Imelfort M, Keller J, Hugenholtz P, Yuan Z, Tyson GW. 2013. Anaerobic oxidation of methane coupled to nitrate reduction in a novel archaeal lineage. Nature 500:567–570. https://doi.org/10.1038/nature12375.
24. Cai C, Leu AO, Xie G-J, Guo J, Feng Y, Zhao J-X, Tyson GW, Yuan Z, Hu S. 2018. A methanotrophic archaeon couples anaerobic oxidation of methane to Fe(III) reduction. ISME J 12:1929–1939. https://doi.org/10.1038/s41396-018-0109-x.
25. Steen IH, Dahle H, Stokke R, Roalkvam I, Daae F-L, Rapp HT, Pedersen RB, Thorseth IH. 2016. Novel barite chimneys at the Loki's Castle Vent Field shed light on key factors shaping microbial communities and functions in hydrothermal systems. Front Microbiol 6:1510. https://doi.org/10.3389/fmicb.2015.01510.
26. Ruscic B. 2015. Active thermochemical tables: sequential bond dissociation enthalpies of methane, ethane, and methanol and the related thermochemistry. J Phys Chem A 119:7810–7837. https://doi.org/10.1021/acs.jpca.5b01346.
27. Heider J, Ma K, Adams MW. 1995. Purification, characterization, and metabolic function of tungsten-containing aldehyde ferredoxin oxidoreductase from the hyperthermophilic and proteolytic archaeon *Thermococcus* strain ES-1. J Bacteriol 177:4757–4764. https://doi.org/10.1128/JB.177.16.4757-4764.1995.
28. Milucka J, Ferdelman TG, Polerecky L, Franzke D, Wegener G, Schmid M, Lieberwirth I, Wagner M, Widdel F, Kuypers MMM. 2012. Zero-valent sulphur is a key intermediate in marine methane oxidation. Nature 491:541–546. https://doi.org/10.1038/nature11656.
29. Wegener G, Krukenberg V, Riedel D, Tegetmeyer HE, Boetius A. 2015. Intercellular wiring enables electron transfer between methanotrophic archaea and bacteria. Nature 526:587–590. https://doi.org/10.1038/nature15733.
30. McGlynn SE, Chadwick GL, Kempes CP, Orphan VJ. 2015. Single cell activity reveals direct electron transfer in methanotrophic consortia. Nature 526:531–U146. https://doi.org/10.1038/nature15512.
31. Orcutt BN, Joye SB, Kleindienst S, Knittel K, Ramette A, Reitz A, Samarkin V, Treude T, Boetius A. 2010. Impact of natural oil and higher hydrocarbons on microbial diversity, distribution, and activity in Gulf of Mexico cold-seep sediments. Deep Sea Res Part 2 Top Stud Oceanogr 57:2008–2021. https://doi.org/10.1016/j.dsr2.2010.05.014.
32. Lloyd KG, Lapham L, Teske A. 2006. An anaerobic methane-oxidizing community of ANME-1b archaea in hypersaline Gulf of Mexico sediments. Appl Environ Microbiol 72:7218–7230. https://doi.org/10.1128/AEM.00886-06.
33. Dowell F, Cardman Z, Dasarathy S, Kellermann MY, Lipp JS, Ruff SE, Biddle JF, McKay LJ, MacGregor BJ, Lloyd KG, Albert DB, Mendlovitz H, Hinrichs K-U, Teske A. 2016. Microbial communities in methane- and short chain alkane-rich hydrothermal sediments of Guaymas Basin. Front Microbiol 7:17. https://doi.org/10.3389/fmicb.2016.00017.
34. Bohrmann G, Spiess V, Böckel B, Boetius A, Boles M, Brüning M, Buhmann S, Cruz Melo C, Dalthorp-Moorhouse M, Dehning K, Ding F, Escobar-Briones E, Enneking K, Felden J, Fekete N, Freidank T, Gassner A, Gaytan A, Geersen J, Hinrichs K-U, Hohnberg J, Kasten S, Keil H, Klar S, Klaucke I, Kuhlmann J, MacDonald I, Meinecke G, Mortera C, Naehr T, Nowald N, Ott C, Pacheco Muñoz J, Pelaez JR, Ratmeyer V, Renken J, Reuter M, Sackmann V, Sahling H, Schubotz F, Schewe F, Stephan S, Thal J, Trampe A, Truscheit T, Viehweger M, Wilhelm T, Wegner G, Wenzhöfer F, Zabel M. 2008. Report and preliminary results of R/V Meteor Cruise M67/2a and 2b, Balboa—Tampico—Bridgetown, 15 March–24 April, 2006. Fluid seepage in the Gulf of Mexico. Berichte aus dem Fachbereich Geowissenschaften der Universität Bremen, no. 263. Department of Geosciences, Bremen University, Bremen, Germany.
35. Brüning M, Sahling H, MacDonald IR, Ding F, Bohrmann G. 2010. Origin, distribution, and alteration of asphalts at Chapopote Knoll, Southern Gulf of Mexico. Mar Pet Geol 27:1093–1106. https://doi.org/10.1016/j.marpetgeo.2009.09.005.
36. Hinrichs K-U, Hayes JM, Bach W, Spivack AJ, Hmelo LR, Holm NG, Johnson CG, Sylva SP. 2006. *Biological formation of ethane and propane in the deep marine subsurface*. Proc Natl Acad Sci U S A 103:14684–14689. https://doi.org/10.1073/pnas.0606535103.
37. Holler T, Wegener G, Niemann H, Deusner C, Ferdelman TG, Boetius A, Brunner B, Widdel F. 2011. Carbon and sulfur back flux during anaerobic microbial oxidation of methane and coupled sulfate reduction. Proc Natl Acad Sci U S A 108:E1484–E1490. https://doi.org/10.1073/pnas.1106032108.
38. Widdel F, Bak F. 1992. Gram-negative mesophilic sulfate-reducing bacteria, p 3352–3378. *In* Balows A, Trüper HG, Dworkin M, Harder W, Schleifer K-H (ed), The prokaryotes. Springer-Verlag. New York, NY.
39. Laso-Perez R, Krukenberg V, Musat F, Wegener G. 2018. Establishing anaerobic hydrocarbon-degrading enrichment cultures of microorganisms under strictly anoxic conditions. Nat Protoc 13:1310–1330. https://doi.org/10.1038/nprot.2018.030.
40. Cord-Ruwisch R. 1985. A quick method for the determination of dissolved and precipitated sulfides in cultures of sulfate-reducing bacteria. J Microbiol Methods 4:33–36. https://doi.org/10.1016/0167-7012(85)90005-3.
41. Martin M. 2011. Cutadapt removes adapter sequences from high-throughput sequencing reads. EMBnet J 17:10–12. https://doi.org/10.14806/ej.17.1.200.
42. Quast C, Pruesse E, Yilmaz P, Gerken J, Schweer T, Yarza P, Peplies J, Glöckner FO. 2012. The SILVA ribosomal RNA gene database project: improved data processing and web-based tools. Nucleic Acids Res 41:D590–D596. https://doi.org/10.1093/nar/gks1219.
43. Yilmaz P, Parfrey LW, Yarza P, Gerken J, Pruesse E, Quast C, Schweer T, Peplies J, Ludwig W, Glöckner FO. 2014. The SILVA and "All-species Living Tree Project (LTP)" taxonomic frameworks. Nucleic Acids Res 42:D643–D648. https://doi.org/10.1093/nar/gkt1209.
44. Glockner FO, Yilmaz P, Quast C, Gerken J, Beccati A, Ciuprina A, Bruns G, Yarza P, Peplies J, Westram R, Ludwig W. 2017. 25 years of serving the community with ribosomal RNA gene reference databases and tools. J Biotechnol 261:169–176. https://doi.org/10.1016/j.jbiotec.2017.06.1198.
45. Zhou J, Bruns MA, Tiedje JM. 1996. DNA recovery from soils of diverse composition. Appl Environ Microbiol 62:316–322. https://doi.org/10.1128/AEM.62.2.316-322.1996.
46. Bengtsson-Palme J, Hartmann M, Eriksson KM, Pal C, Thorell K, Larsson DGJ, Nilsson RH. 2015. METAXA2: improved identification and taxonomic classification of small and large subunit rRNA in metagenomic data. Mol Ecol Resour 15:1403–1414. https://doi.org/10.1111/1755-0998.12399.
47. Pruesse E, Peplies J, Glockner FO. 2012. SINA: accurate high-throughput multiple sequence alignment of ribosomal RNA genes. Bioinformatics 28:1823–1829. https://doi.org/10.1093/bioinformatics/bts252.
48. Seemann T. 2014. Prokka: rapid prokaryotic genome annotation. Bioinformatics 30:2068–2069. https://doi.org/10.1093/bioinformatics/btu153.
49. Johnson M, Zaretskaya I, Raytselis Y, Merezhuk Y, McGinnis S, Madden TL. 2008. *NCBI BLAST: a better web interface*. Nucleic Acids Res 36:W5–9. https://doi.org/10.1093/nar/gkn201.
50. Rodriguez-R LM, Konstantinidis K. 2016. The enveomics collection: a toolbox for specialized analyses of microbial genomes and metagenomes. PeerJ Preprints 4:e1900v1.
51. Stepanauskas R, Fergusson EA, Brown J, Poulton NJ, Tupper B, Labonté JM, Becraft ED, Brown JM, Pachiadaki MG, Povilaitis T, Thompson BP, Mascena CJ, Bellows WK, Lubys A. 2017. Improved genome recovery and integrated cell-size analyses of individual uncultured microbial cells and viral particles. Nat Commun 8:84. https://doi.org/10.1038/s41467-017-00128-z.
52. Nurk S, Bankevich A, Antipov D, Gurevich AA, Korobeynikov A, Lapidus

A, Prjibelski AD, Pyshkin A, Sirotkin A, Sirotkin Y, Stepanauskas R, Clingenpeel SR, Woyke T, Mclean JS, Lasken R, Tesler G, Alekseyev MA, Pevzner PA. 2013. Assembling single-cell genomes and mini-metagenomes from chimeric MDA products. J Comput Biol 20:714–737. https://doi.org/10.1089/cmb.2013.0084.

53. Strous M, Kraft B, Bisdorf R, Tegetmeyer HE. 2012. The binning of metagenomic contigs for physiology of mixed cultures. Front Microbiol 3:410. https://doi.org/10.3389/fmicb.2012.00410.
54. Parks DH, Imelfort M, Skennerton CT, Hugenholtz P, Tyson GW. 2015. CheckM: assessing the quality of microbial genomes recovered from isolates, single cells, and metagenomes. Genome Res 25:1043–1055. https://doi.org/10.1101/gr.186072.114.
55. Gruber-Vodicka HR, Seah BK, Pruesse E. 2019. phyloFlash—rapid SSU rRNA profiling and targeted assembly from metagenomes. bioRxiv 521922.
56. Ludwig W. 2004. ARB: a software environment for sequence data. Nucleic Acids Res 32:1363–1371. https://doi.org/10.1093/nar/gkh293.
57. Price MN, Dehal PS, Arkin AP. 2010. FastTree 2—Approximately Maximum-Likelihood Trees for Large Alignments. PLoS One 5:e9490. https://doi.org/10.1371/journal.pone.0009490.
58. Rinke C, Schwientek P, Sczyrba A, Ivanova NN, Anderson IJ, Cheng J-F, Darling A, Malfatti S, Swan BK, Gies EA, Dodsworth JA, Hedlund BP, Tsiamis G, Sievert SM, Liu W-T, Eisen JA, Hallam SJ, Kyrpides NC, Stepanauskas R, Rubin EM, Hugenholtz P, Woyke T. 2013. Insights into the phylogeny and coding potential of microbial dark matter. Nature 499:431–437. https://doi.org/10.1038/nature12352.
59. Eren AM, Esen ÖC, Quince C, Vineis JH, Morrison HG, Sogin ML, Delmont TO. 2015. Anvi'o: an advanced analysis and visualization platform for 'omics data. PeerJ 3:e1319. https://doi.org/10.7717/peerj.1319.
60. Stamatakis A. 2014. RAxML version 8: a tool for phylogenetic analysis and post-analysis of large phylogenies. Bioinformatics 30:1312–1313. https://doi.org/10.1093/bioinformatics/btu033.
61. Letunic I, Bork P. 2016. Interactive tree of life (iTOL) v3: an online tool for the display and annotation of phylogenetic and other trees. Nucleic Acids Res 44:W242–W245. https://doi.org/10.1093/nar/gkw290.
62. Pernthaler A, Pernthaler J, Amann R. 2002. Fluorescence in situ hybridization and catalyzed reporter deposition for the identification of marine bacteria. Appl Environ Microbiol 68:3094–3101. https://doi.org/10.1128/AEM.68.6.3094-3101.2002.
63. Diepenbroek M, Glöckner FO, Grobe P, Güntsch A, Huber R, König-Ries B, Kostadinov I, Nieschulze J, Seeger B, Tolksdorf R, Triebel D. 2014. Towards an integrated biodiversity and ecological research data management and archiving platform: the German federation for the curation of biological data (GFBio), p 1711–1721. *In* Plödereder E, Grunske L, Schneider E, Ull D (ed), Informatik 2014. Gesellschaft für Informatik e.V., Bonn, Germany.
64. Yilmaz P, Kottmann R, Field D, Knight R, Cole JR, Amaral-Zettler L, Gilbert JA, Karsch-Mizrachi I, Johnston A, Cochrane G, Vaughan R, Hunter C, Park J, Morrison N, Rocca-Serra P, Sterk P, Arumugam M, Bailey M, Baumgartner L, Birren BW, Blaser MJ, Bonazzi V, Booth T, Bork P, Bushman FD, Buttigieg PL, Chain PSG, Charlson E, Costello EK, Huot-Creasy H, Dawyndt P, DeSantis T, Fierer N, Fuhrman JA, Gallery RE, Gevers D, Gibbs RA, Gil IS, Gonzalez A, Gordon JI, Guralnick R, Hankeln W, Highlander S, Hugenholtz P, Jansson J, Kau AL, Kelley ST, Kennedy J, Knights D, Koren O, Kuczynski J, Kyrpides N, Larsen R, Lauber CL, Legg T, Ley RE, Lozupone CA, Ludwig W, Lyons D, Maguire E, Methé BA, Meyer F, Muegge B, Nakielny S, Nelson KE, Nemergut D, Neufeld JD, Newbold LK, Oliver AE, Pace NR, Palanisamy G, Peplies J, Petrosino J, Proctor L, Pruesse E, Quast C, Raes J, Ratnasingham S, Ravel J, Relman DA, Assunta-Sansone S, Schloss PD, Schriml L, Sinha R, Smith MI, Sodergren E, Spor A, Stombaugh J, Tiedje JM, Ward DV, Weinstock GM, Wendel D, White O, Whiteley A, Wilke A, Wortman JR, Yatsunenko T, Glöckner FO. 2011. Minimum information about a marker gene sequence (MIMARKS) and minimum information about any (x) sequence (MIxS) specifications. Nat Biotechnol 29:415–420. https://doi.org/10.1038/nbt.1823.

Graphic design: Communication Division, UiB / Print: Skipnes Kommunikasjon AS

uib.no

ISBN: 9788230840177 (print)
9788230851302 (PDF)